Pathological study on liver homeostasis and hepatotoxicity based on macrophage functions and autophagy in rats

大阪府立大学博士（獣医学）学位論文

Pathological study on liver homeostasis and hepatotoxicity based on macrophage functions and autophagy in rats

（マクロファージ機能とオートファジーに基づいたラットの肝恒常性と肝毒性に関する病理学的研究）

Munmun Pervin

2018 年

Contents

Preface

Liver is a crucial organ in the body for nutrition metabolism and host defense mechanisms. Particularly, liver is exposed to circulating antigens and endotoxins from the gut microbiota, which may trigger systemic immune responses. Liver comprised histologically of parenchymal hepatocytes and non-parenchymal cells (such as Kupffer cells, hepatic stellate cells, endothelial cells and cholangiocytes). The relationship between these parenchymal and non-parenchymal hepatic cells is important for maintenance of liver functions and homeostasis. Hepatic macrophages mainly including Kupffer cells exist 10-20% of liver-constituting cells (Godoy et al., 2013); they are capable of presenting antigens to immune cells, and of producing cytokine and chemokines. Therefore, hepatic macrophages are considered a key player in initiating and shaping of immune responses in liver. On the other hand, hepatocytes have basal level of autophagy, which plays an important role in cell physiology and cell survival (Komatsu et al., 2005). Therefore, appropriate immune activation to challenge by pathogens or damaged tissues may result in resolution of inflammation, whereas failure to regulate appropriately activated immune mechanisms or clear pathogenic stimuli could lead to abnormal pathological inflammation and disrupted tissue homeostasis (Robinson et al., 2016). Therefore, functions of hepatic macrophages and autophagy in hepatocytes contribute not only to liver homeostasis but also to liver pathology. There is increasing evidence suggesting that hepatic macrophages and autophagic activity play a central role in maintaining liver homeostasis and in the pathogenesis of liver injury, making them attractive therapeutic target for liver diseases (Ju and Tacke, 2016; Cursio et al., 2015).

Macrophages are the ancient cells in metazoan phylogeny, belonging to the mononuclear phagocyte system. In mammals, they are found in all tissues and display great functional diversity, depending on localization and microenvironments. Macrophages are heterogeneous cell population; they are generally divided into three types, namely exudative macrophages, resident macrophages and antigen presenting cells (Golbar et al., 2012; Mosser and Edwards, 2008). Particularly, liver has Kupffer cells (a kind of tissue macrophages) which constitute 80-90% of tissue macrophages present in the body; in other

term, Kupffer cells may have a central role of in systemic and regional defense. It is also indicated that macrophage polarization is a major determinant of macrophage functions in pathological lesions (Patel et al., 2012). On the basis of the type 1 or type 2 helper T-cell polarization, macrophages appearing in pathological settings are classified into M1 macrophages (classically activated macrophages) and M2 macrophages (alternatively activated macrophages). Interestingly, M1 and M2 macrophages may be interchangeable (Wijesundera et al., 2014a; Sporrer et al., 2009); depending on microenvironmental conditions, M1 macrophages could switch into M2 phenotypes or vice versa (Bouhlel et al., 2007). Therefore, it is interesting to investigate which type of macrophages may contribute to physiological and pathophysiological adaptations in liver.

Selective depletion of macrophages *in vivo* is widely used to investigate the involvements of macrophages in normal and pathological conditions (Bautista et al., 2013; Cullen et al., 2013; Sturm et al., 2005). Macrophage depletion can be achieved by using a single intravenous injection of liposome-encapsulated dichloromethylene diphosphonate clodronate (CLD) (Van Rooijen and Sanders, 1994). CLD belongs to the family of bisphosphonate, a potent inhibitor of osteoclasts (Davison et al., 2014; Hayden et al., 2014). Acting as an anti-macrophage agent, CLD needs to be encapsulated with liposome that is readily digested by macrophages. After phagocytosis by macrophages, CLD causes damage to macrophages via apoptosis, resulting in their depletion (Van Rooijen and Sandar, 1994). Hepatic macrophages show central position not only in maintaining homeostasis of liver but also in the pathogenesis of liver injury. Thus, further studies are required to better understand these cells to guide the development of macrophage-based therapeutic interventions.

Autophagy is an intracellular degradation process, by which cells digest their damaged organelles, protein aggregates, and invading microbes through the action of lysosomes. The autophagy is characterized by the formation of double-membrane vesicles termed autophagosomes (Mizushima et al., 2010; Ohsumi, 2001). Microtubule-associated protein 1 light chain 3 beta (LC3B) is an essential component of autophagosomes. LC3B is a classic marker used for autophagy study. Most of the cells have basal level of autophagy.

Autophagy is first identified in the liver. Autophagy in hepatocytes and non-parenchymal liver cells is essential for their survival and function (Ueno and Komatsu, 2017; Zhang et al., 2012). In addition, autophagy is activated in a variety of liver diseases (including viral hepatitis, hepatocellular carcinoma, bacterial toxins, and hepatotoxicity by chemicals and drugs) (Ueno and Komatsu, 2017; Ni et al., 2012). It has been considered that autophagic activities play a vital role during the homeostatic adaptation of liver and liver injury, making it an attractive therapeutic target for liver diseases.

Lipopolysaccharide (LPS) is a predominant, integral component of gram-negative bacterial cell wall. LPS activates host immune response and exerts a wide variety of pathophysiological effects in humans and animals. Exposure to a large dose of LPS causes extensive damage to the liver and other organs (Hewett and Roth, 1993), whereas exposure to a low dose of LPS may result in a modest, non-injurious inflammatory response (Ganey and Roth, 2001). In mammals, the liver is continuously exposed to LPS, which may occur by the supply from intestinal lumen via the portal venous blood. It is reported that LPS acts as a potent activator not only for hepatic macrophages but also for autophagy. However, the effect of low dose of LPS on hepatic macrophages and autophagy remains to be investigated in terms of liver homeostasis and hepatotoxicity.

Liver injury resulting from exposure to chemicals and drugs is a major health problem. To resolve this issue or to elicit the exact mechanism, various hepatotoxicants have been used for the studies of liver injury model *in vivo*. Thioacetamide (TAA) is a popular hepatotoxicant and conventionally used for induction of both acute and chronic liver injury (Yovchev et al., 2014). TAA causes hepatocellular necrosis after biotransformation to an active metabolite via the flavine adenine dinucleotide monooxygenase pathway resulting in the formation of TAA-S-oxide. TAA-related toxic metabolite also induces the release of electrophiles and free radicals leading to lipid peroxidation and destruction of cells (Chen et al., 2005). A strong relationship of LPS and liver injury is reported in acute hepatotoxicity; LPS acts as biphasic-factors for liver injury, which can elevate or alleviate liver injury (Liu et al., 2000; Roth et al., 1997). The precise roles of hepatic macrophages and autophagy are not clear in hepatotoxicity. Therefore, it is

interesting to analyze the potential pathophysiological relevance of activated-hepatic macrophages and induced-autophagy in TAA-induced acute liver injury model.

In this thesis, a series of studies were conducted to explore underling mechanisms of liver homeostasis and hepatotoxicity, with particular references to macrophages functions and autophagy. In Chapter 1, to characterize the hepatic macrophages participating in liver homeostasis, the author used macrophage depletion condition in rat liver by a single intravenous injection of liposome-encapsulated CLD. Firstly, in Section I of Chapter 1, the author demonstrated the transient effects of empty liposomes on hepatic macrophages in rats. In Section II of Chapter 1, the author conducted immunophenotypical characterization of depleting and repopulating hepatic macrophages using macrophage-specific antibodies and analyzed the related microenvironmental conditions. In Chapter 2, to demonstrate the role of hepatic macrophages and autophagy in liver, the author used low dose of LPS in normal and hepatic macrophage-depleted rats. In Section I of Chapter 2, effects of low dose of LPS on hepatic macrophages were analyzed by single or double immunohistochemical staining and mRNA profiling for regulatory inflammatory factors. Additionally, cell specific autophagy in liver with special emphasis on hepatocyte and macrophage autophagy was analyzed immunohistochemically and autophagy-related genes were analyzed in Section II of Chapter 2. In Chapter 3, to find out the cytoprotective roles of LPS in acute hepatotoxicity with special emphasis on hepatic macrophages and autophagic functions, the author adopted LPS-pretreated TAA-induced acute liver injury model. The author investigated possible protective mechanisms of LPS in a time dependent manner in Section I of Chapter 3. Subsequently, in Section II of Chapter 3, the author illustrated cytoprotective roles of hepatic macrophages and autophagy in TAA-induced acute liver injury under LPS treatment.

In conclusion, the present studies demonstrate that heterogeneous macrophage populations and autophagy actively participate in liver homeostasis and liver pathology. Therefore, the present findings would provide a significant insight into the pathogenesis of liver injury and would be helpful in formulating therapeutic strategies by targeting macrophages and autophagy.

Chapter 1

Characterization of rat hepatic macrophages participating in liver homeostasis

Section I

Effects of empty liposomes on hepatic macrophage populations in rats

Introduction

Liposomes, which are prepared from lipids and lipid mixtures with phospholipids, represent one of the most efficacious and promising drug-carrier vehicles for intracellular delivery (Hofheinz et al., 2005). Injected liposomes are rapidly phagocytized by macrophages in the liver and spleen (Van Rooijen and Hendrikx, 2010). For this reason, liposomes have been chosen as a suitable vehicle for manipulation of macrophage functions by encapsulating toxins and chemicals (Cullen et al., 2013; Sturm et al., 2005). Hepatic macrophages can express a variety of immunophenotypes in normal and pathological conditions (Wijesundera et al., 2014a; Golbar et al., 2012). However, the detailed effects of empty liposomes, particularly on different macrophage populations, have not yet been decided. The present study was undertaken to investigate the immunophenotypes of hepatic macrophages in rats after injection of empty liposomes, in relation to hepatic homeostasis. The results revealed that injection of empty liposomes increased the number of hepatic macrophages with different immunophenotypes and influenced hepatic homeostasis, presumably through enhanced hepatic macrophage functions.

Materials and methods

Animals and diet

Eight 6-week-old male F344 rats were purchased from Charles River Laboratories Japan (Hino, Shiga, Japan). Rats were maintained in a room at 21±3°C with a 12 h light-

dark cycle. Food and water were provided *ad libitum*. Four rats were given a single intravenous injection of liposomes (http://www.clodronateliposomes.org) at a dose of 10 ml/kg body weight via the tail. The used liposomes were multilamellar, large and of various dimensions between 150 nanometers and 3 microns. They were prepared from one single phospholipid, e.g., phosphatidylcholine (egg lecithin) and cholesterol. The remaining four rats were used as untreated controls. One day after injection, all animals were euthanized under deep isoflurane anesthesia.

One hour before euthanasia, they received an intraperitoneal injection of bromo-2-deoxyuridine (BrdU; Sigma-Aldrich Co., Louis, MO, USA) at a dose of 50 mg/kg body weight. Serum samples were analyzed for aspartate transaminase (AST), alanine transaminase (ALT) and alkaline phosphatase (ALP). The animal experiments were conducted under the institutional guidelines approved by the ethical committee of Osaka Prefecture University for animal care.

Histopathology and immunohistochemistry

Liver tissues were fixed in 10% neutral buffered formalin (NBF), Zamboni's solution (0.21% picric acid and 2% paraformaldehyde in 130 mM phosphate buffer, pH 7.4) and periodate-lysine-paraformaldehyde (PLP) solution processed by the PLP-AMeX (acetone, methyl benzoate and xylene) method (Pervin et al., 2016). NBF-fixed tissue sections cut at a thickness of 3-4 μm were stained with hematoxylin and eosin (HE). Tissue sections fixed in NBF, Zamboni's solution or PLP were used for immunohistochemistry with CD163, CD68, Iba-1, Galectin-3 (Gal-3), MHC class II, CD204 and BrdU staining (Table 1). After pretreatment, tissue sections were stained with Histostainer (Nichirei Biosciences Inc., Tokyo, Japan). Briefly, sections were treated with 5% skimmed milk for 10 min and allowed to react with primary antibodies for 1 h at room temperature (RT). After incubation in 3% H_2O_2 for 15 min, a horseradish peroxidase-conjugated secondary antibody (Histofine Simple Stain MAX PO®, Nichirei Biosciences Inc., Tokyo, Japan) was applied for 30 min at RT. The sections were then incubated with 3, 3′- diaminobenzidine (Nichirei Biosciences Inc., Tokyo, Japan) and counterstained with hematoxylin. The

number of immunopositive cells with clear nuclei was counted per 40X field in five randomly selected areas in the perivenular (PV), periportal (PP) or Glisson's sheath (GS) areas including interlobular connective tissues and the portal triad. The number of BrdU-positive hepatocytes was also counted per 40X field and compared with the total number of hepatocytes.

Real time reverse transcriptase-polymerase chain reaction (RT-PCR) and microarray

Liver tissues were immersed in RNAlater® reagent (Qiagen, Hilden, Germany), kept overnight at 4°C and stored at −80°C until use. Total RNA was extracted with an SV total RNA isolation system (Promega, Fitchburg, WI, USA). RNA was reverse-transcribed to cDNA with SuperScript VILO reverse transcriptase (Life technologies, Carlsbad, CA, USA). Real time PCR was performed using TaqMan gene expression assays (Life Technologies) in a PikoReal Real-Time 96 PCR System (Thermo Fisher Scientific, CA, Massachusetts, USA). The TaqMan probes specific for the cytokines used were as follows (Assay IDs): monocyte chemoattractant protein-1 (MCP-1), Rn00580555_m1; interleukin-1β (IL-1β), Rn00580432_m1; transforming growth factor-β1 (TGF-β1), Rn00572010_m1; colony stimulating factor-1 (for macrophages) (CSF-1), Rn00696122_m1; interferon-γ (IFN-γ), Rn00594078_m1; tumor necrosis factor-α (TNF-α), Rn01525859_g1; interleukin-4 (IL-4), Rn01456866_m1; interleukin-6 (IL-6), Rn01410330_m1; interleukin-10 (IL-10), Rn00563409_m1; and β-actin, Rn00667869_m1. The mRNA expression was normalized against the expression of β-actin mRNA as the internal controller gene. The data were analyzed using the comparative C_t method ($^{\Delta\Delta}C_t$ method). Expression profiles of mRNAs were analyzed with a SurePrint G3 Rat GE8x60K Microarray (Agilent Technologies, Santa Clara, CA, USA).

Statistical evaluation

Obtained data were expressed as mean ± standard deviation (SD). Statistical analysis was performed using Student's *t*-test. $P< 0.05$ was considered significant.

Results

Histopathology and serum biochemistry

In liposome-treated rats, the AST and ALT levels were significantly decreased (Fig. 1A, B) and the ALP level was significantly increased (Fig. 1C) in comparison with the control rats. There were no significant differences in histopathology of livers between control and liposome-treated rats (Fig. 2A, B). However, BrdU-positive hepatocytes were diffusely distributed in the liver parenchyma, which significantly increased in the liposome-treated rats (Fig. 2C-E), indicating increased proliferation activity of hepatocytes.

Expression of hepatic macrophages

Macrophages expressing different immunophenotypes in the PV, PP and GS areas of livers were evaluated by using different antibodies such as CD163, CD68, Iba-1, MHC class II, Gal-3 and CD204 (Fig. 3A-F). In the PV and PP areas, the numbers of macrophages reacting to CD163, CD68, Iba-1, MHC class II, Gal-3 and CD204 were significantly increased in liposome-treated rats (Fig. 3A-F). In addition, $CD163^+$ macrophages were also increased significantly in number in the GS area (Fig. 3A). There were no macrophages positive for Gal-3 (Fig. 3E) and CD204 (Fig. 3F) in the GS area. Among macrophages expressing different antigens, $CD163^+$ and $CD68^+$ macrophages showed the greatest increase in number after liposome injection. Interestingly, macrophages reacting to all antibodies in liposome-treated rats showed a larger cytoplasm than in control rats; in particular, the morphological change was most prominent in $CD163^+$ hepatic macrophages in liposome-treated rats (Fig. 4A-D).

Expression of mRNAs

MCP-1, IL-1β and TGF-β1 mRNAs were significantly increased in liposome-treated rats (Fig. 5A-C). Other cytokines (CSF-1, CSF-2, TNF-α, INF-γ, IL-4, IL-6 and IL-10) examined did not show any significant change following liposome treatment.

A total of 721 genes were upregulated (more than 2-fold) and 703 genes were downregulated (less than 0.5-fold) in response to liposome treatment. These gene profiles were grouped into distinct, differentially-expressed functional groups (mainly, cell cycle, cytokine-cytokine interaction, and apoptosis groups) (Table 2) based on the gene ontogeny classification system (Zheng et al., 2014). In the cell cycle-related functional gene group, five genes showed upregulation, and there were no downregulated genes. Such genes relating to the cell cycle might be corresponding to increased number of BrdU-positive hepatocytes. In the cytokine-cytokine interaction gene group, a total of seven genes showed upregulation and five genes were downregulated. Apoptosis-related genes were small in number, and in fact, few apoptotic cells, demonstrable with the TUNEL method, were detected.

Discussion

Liposomes are prepared as a nontoxic, nondegradable and nonimmunogenic vehicle. The administration of empty liposomes may activate macrophages by a phagocytic stimulus (Allison, 1978); however, detailed characterization of the activated macrophages has not been reported. The present study showed that empty liposome treatment increased the number of hepatic macrophages with different immunophenotypes for all antibodies (CD163, CD68, Iba-1, MHC class II, Gal-3 and CD204) examined immediately (one day later) after injection; furthermore, it was found that $CD163^+$ and $CD68^+$ macrophages located in the PV and PP areas were most sensitive, showing an elongated/swollen, larger cytoplasm. The CD163 antibody is used to detect resident macrophages (Kupffer cells in the liver) (Polfliet et al., 2006), and CD68 expression implies phagocytic activity of macrophages (Golbar et al., 2012). CD204 is a scavenger receptor for lipid metabolism, and its expression may be also related to phagocytosis (Tomokiyo et al., 2002). The findings for these antibodies indicated that the liposome treatment might activate resident macrophages with enhanced phagocytosis. Iba-1 expression may indicate cell migration of macrophages (Sasaki et al., 2001), and Gal-3 expression may be related to fibrosis after tissue injury (Wijesundera et al., 2014a). MHC class II-expressing macrophages are

regarded as antigen-presenting cells (Ide et al., 2005). In addition to activated phagocytosis, liposome treatment could influence macrophage functions as shown in the immunohistochemistry for Iba-1, Gal-3 and MHC class II.

In contrast to the increased number of macrophages with different immunophenotypes, there was no significant change in histopathology of HE-stained sections between control and liposome-treated rats, indicating that liposomes are not toxic to hepatocytes. However, interestingly, the number of BrdU-positive hepatocytes was significantly increased following liposome treatment; this increased proliferating activity was supported by the upregulation of the cell cycle-related functional gene group in the microarray analysis. Activation of hepatic macrophages due to phagocytosis of liposomes might give rise to an imbalance in the relationship between Kupffer cells and hepatocytes, presumably resulting in proliferation of hepatocytes. Presumably, the increased ALP in liposome-treated rats may reflect the slight effect of the biliary system due to the imbalance, as the bile canaliculi are located between hepatocytes.

On the other hand, it is interesting to note that the liposome treatment in this study decreased significantly AST and ALT values. It is reported that hepatic macrophages may play a role in the clearance of such hepatic deviation enzymes; in fact, AST and ALT levels in serum were increased under hepatic macrophage depletion (Pervin et al., 2016; Radi et al., 2011). The opposite phenomenon (decreased levels) observed for AST and ALT in the present study might have been related to the increased number of activated hepatic macrophages.

During inflammation, activated macrophages produce various inflammatory factors, which can induce cell injury in the early stages or reparative fibrosis in the late stages. The increased mRNA expression of IL-1β, TGF-β1 and MCP-1 following liposome treatment also indicated the activation of hepatic macrophages. The influence of cytokine-cytokine interaction on gene profiles might be related to changes in such inflammatory factors.

In conclusion, the author showed that empty liposomes can activate hepatic macrophages with different immunophenotypes, presumably resulting in decreased AST

and ALT levels and increased expression of inflammatory factors (IL-1β, TGF-β1 and MCP-1), as well as increased hepatocyte proliferation. Recently, liposomes have been widely used as a vehicle by encapsulating drugs or toxins. In particular, in order to determine the functions of hepatic macrophages, a lioposome-encapsulated clodronate capable of eliminating hepatic macrophages was utilized in chemically-induced hepatic lesions (Cullen et al., 2013). The present study was conducted by using liver samples obtained one day after liposome injection, because the author wanted to determine the transient influence of liposomes on rat hepatic macrophages. Further studies are needed to determine the dynamic influences of liposomes on hepatic macrophages over a longer term. Toxicologic pathologists should take these liposome effects on hepatic macrophages into consideration when using liposomes as a vehicle.

Summary

Liposomes have been used as a vehicle for encapsulating chemicals or toxins in toxicological studies. The author investigated the transient effects of empty liposomes on hepatic macrophages by applying a single intravenous injection at a dose of 10 ml/kg body weight in 6-week-old male F344 rats. One day after injection, the numbers of hepatic macrophages reacting to CD163, CD68, Iba-1, MHC class II, Gal-3 and CD204 were significantly increased in liposome-treated rats. $CD163^+$ Kupffer cells and $CD68^+$ exudative macrophages with increased phagocytic activity in hepatic lobules were most sensitive. The histological architecture of the liver was not changed following liposome injection; however, hepatocytes showed increased proliferating activity, demonstrable with proliferation marker immunostaining and by an increase in gene profiles relating to the cell cycle. In liposome-treated rats, AST and ALT values were significantly decreased, and MCP-1, IL-1β and TGF-β1 mRNAs were significantly increased. Collectively, the present study showed that hepatic macrophages activated by liposomes can influence liver homeostasis. This information would be useful for background studies on liposomes.

Table 1. Details of antibodies used for the immunohistochemistry.

Antibody	Type	Fixative	Dilution	Pretreatment	Source
CD163 (ED2)	Mouse monoclonal	PLP	1/300	100µg/ml Proteinase K, 10 min	AbD Serotec, Oxford, UK
CD68 (ED1)	Mouse monoclonal	PLP	1/500	MW in citrate buffer, 20 min	AbD Serotec, Oxford, UK
Iba-1	Rabbit polyclonal	Zamboni's solution	1/1000	MW in citrate buffer, 20 min	Wako Pure Chemical Industries, Osaka, Japan
MHC class II (OX6)	Mouse monoclonal	PLP	1/1000	MW in citrate buffer, 20 min	AbD Serotec, Oxford, UK
Galectin-3 (Gal-3)	Rabbit polyclonal	Zamboni's solution	1/500	MW in citrate buffer, 20 min	Santa Cruz Biotechnology, Santa Cruz, CA, USA
CD204 (SRA-E5)	Mouse monoclonal	Zamboni's solution	1/1000	MW in citrate buffer, 20 min	Transgenic Inc., Kumamoto, Japan
BrdU	Mouse monoclonal	NBF	1/500	4N HCl, 30 min and 100µg/ml Proteinase K, 10 min	Dako Corp, Glostrup, Denmark

PLP: periodate-lysine-paraformaldehyde; MW: microwave; BrdU: bromo-2-deoxyuridine; NBF: neutral buffered formalin.

Table 2. Up-regulated (more than 2-fold) and down-regulated (less than 0.5-fold) genes in the liver of liposome-treated versus control rats.

Functional category	Gene symbol	Gene description	Fold change
Up-regulated genes			
Cell cycle	Anapc1	Rattus norvegicus anaphase promoting complex subunit 1 (Anapc1), mRNA [NM_001107771]	3.55
	Tgfb1	Rattus norvegicus transforming growth factor, beta 1 (Tgfb1), mRNA [NM_021578]	2.67
	Tgfb3	Rattus norvegicus transforming growth factor, beta 3 (Tgfb3), mRNA [NM_013174]	2.63
	Pkmyt1	Rattus norvegicus protein kinase, membrane associated tyrosine/threonine 1 (Pkmyt1), mRNA [NM_001105766]	2.54
	Gadd45a	Rattus norvegicus growth arrest and DNA-damage-inducible, alpha (Gadd45a), mRNA [NM_024127]	2.07
Cytokine-cytokine interaction	Cxcl9	Rattus norvegicus chemokine (C-X-C motif) ligand 9 (Cxcl9), mRNA [NM_145672]	11.83
	Ccl2	Rattus norvegicus chemokine (C-C motif) ligand 2 (Ccl2), mRNA [NM_031530]	7.88
	Il18r1	Rattus norvegicus interleukin 18 receptor 1 (Il18r1), mRNA [NM_001106905]	3.84
	Il1b	Rattus norvegicus interleukin 1 beta (Il1b), mRNA [NM_031512]	3.42
	Epor	Rattus norvegicus erythropoietin receptor (Epor), mRNA [NM_017002]	2.86
	Tnfrsf21	Rattus norvegicus tumor necrosis factor receptor superfamily, member 21 (Tnfrsf21), mRNA [NM_001108207]	2.81
	Flt4	Rattus norvegicus fms-related tyrosine kinase 4 (Flt4), mRNA [NM_053652]	2.68
Down-regulated genes			
Cytokine-cytokine interaction	Acvr2b	Rattus norvegicus activin A receptor, type IIB (Acvr2b), mRNA [NM_031554]	0.49
	Acvr2a	Rattus norvegicus activin A receptor, type IIA (Acvr2a), mRNA [NM_031571]	0.41
	Bmpr2	Rattus norvegicus bone morphogenetic protein receptor, type II (serine/threonine kinase) (Bmpr2), mRNA [NM_080407]	0.35
	Il1rap	Rattus norvegicus interleukin 1 receptor accessory protein (Il1rap), transcript variant 1, mRNA [NM_012968]	0.32
	Amh	Rattus norvegicus anti-Mullerian hormone (Amh), mRNA [NM_012902]	0.18
Apoptosis	Ntrk1	Rattus norvegicus neurotrophic tyrosine kinase, receptor, type 1 (Ntrk1), mRNA [NM_021589]	0.32

Figure legends

Fig. 1. A-C: Blood biochemical analyses in control and liposome-treated rats. Aspartate transaminase (AST) (A), alanine transaminase (ALT) (B) and alkaline phosphatase (ALP) (C). Student's *t*-test. *, $P<0.05$, significantly different from control rats.

Fig. 2. A-B: Histopathology of the liver in control and liposome-treated rats. The hepatic architecture is normal in rats of both groups. C-D: BrdU-positive hepatocytes are seen in livers of control (C) and liposome-treated rats (D). E. The kinetic of BrdU-positive hepatocytes in the liver. The number of positive hepatocytes was significantly increased in liposome-treated rats. Student's *t*-test. *, $P<0.05$, significantly different from control rats. CV: central vein, BrdU: bromo-2-deoxyuridine. Bar = 50 μm.

Fig. 3. The kinetics of macrophages reacting to CD163 (A), CD68 (B), Iba-1 (C), MHC class II (D), Gal-3 (E) and CD204 (F) in the perivenular (PV) (■), periportal (PP) (□) and Glisson's sheath (GS) (▨) areas of the liver in control and liposome-treated rats. Student's *t*-test. *, $P<0.05$, significantly different from control rats.

Fig. 4. Immunohistochemistry with CD163 in control and liposome-treated rats in the perivenular (PV) and periportal (PP) areas of the liver. Macrophages reacting to CD163 are seen in the control rats in the PV (A) and PP (C) areas; the positive cells have a round shape with processes (inset). Increased numbers of macrophages are seen in the PV (B) and PP (D) areas in liposome-treated rats; $CD163^+$ cells appear more swollen and enlarged in size, with fewer processes (inset). CV: central vein, GS: Glisson's sheath. Bar = 50 μm.

Fig. 5. Levels of mRNA expression of inflammatory cytokines MCP-1 (A), IL-1β (B) and TGF-β1 (C) in control and liposome-treated rats. Expression levels are normalized to the β-actin mRNA level. Student's *t*-test. *, $P<0.05$, significantly different from control rats.

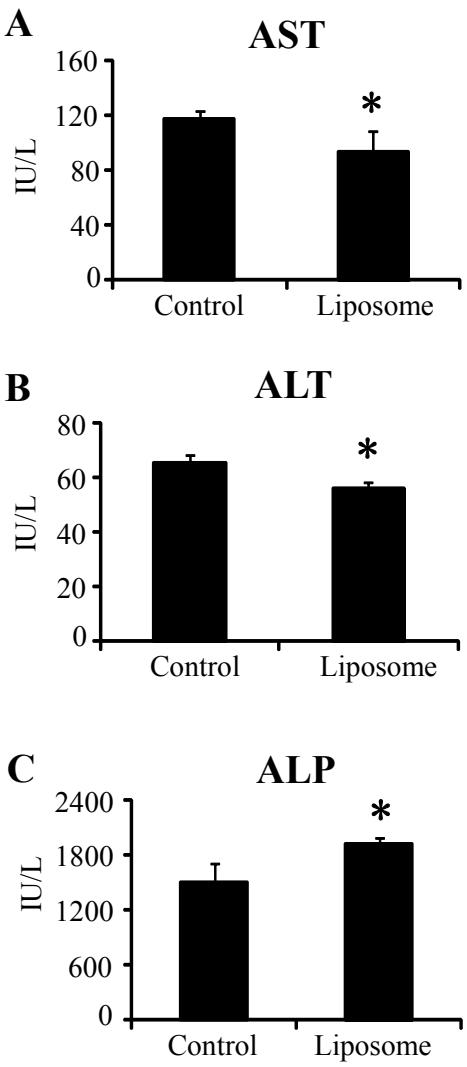
A
AST
160
120
80
40
0
IU/L
*
Control
Liposome
B
ALT
80
60
40
20
0
IU/L
*
Control
Liposome
C
ALP
2400
1800
1200
600
0
IU/L
*
Control
Liposome

Fig. 1

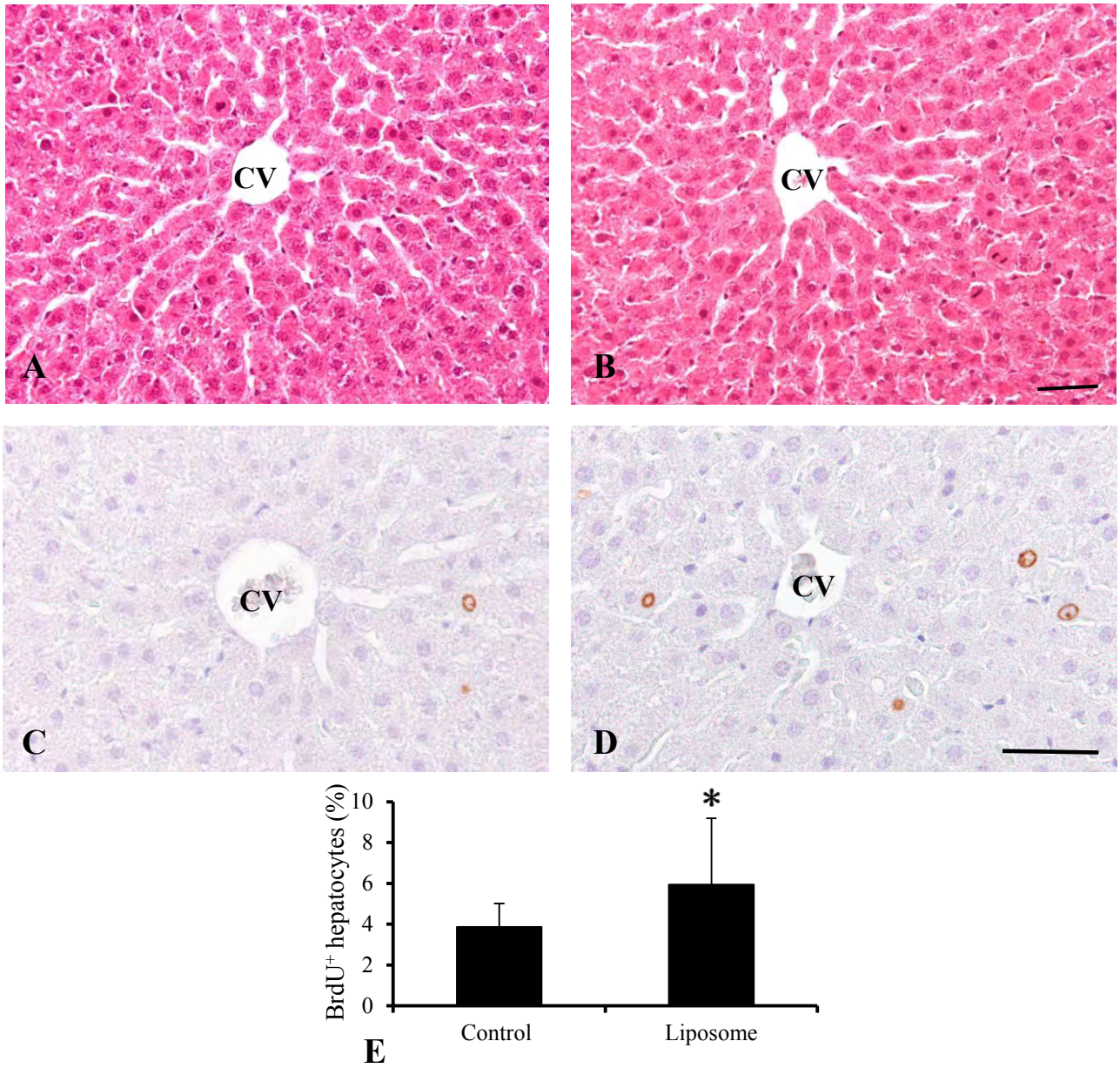
CV
A
CV
B
CV
C
CV
D
BrdU+ hepatocytes (%)
10
8
6
4
2
0
*
Control
Liposome
E

Fig. 2

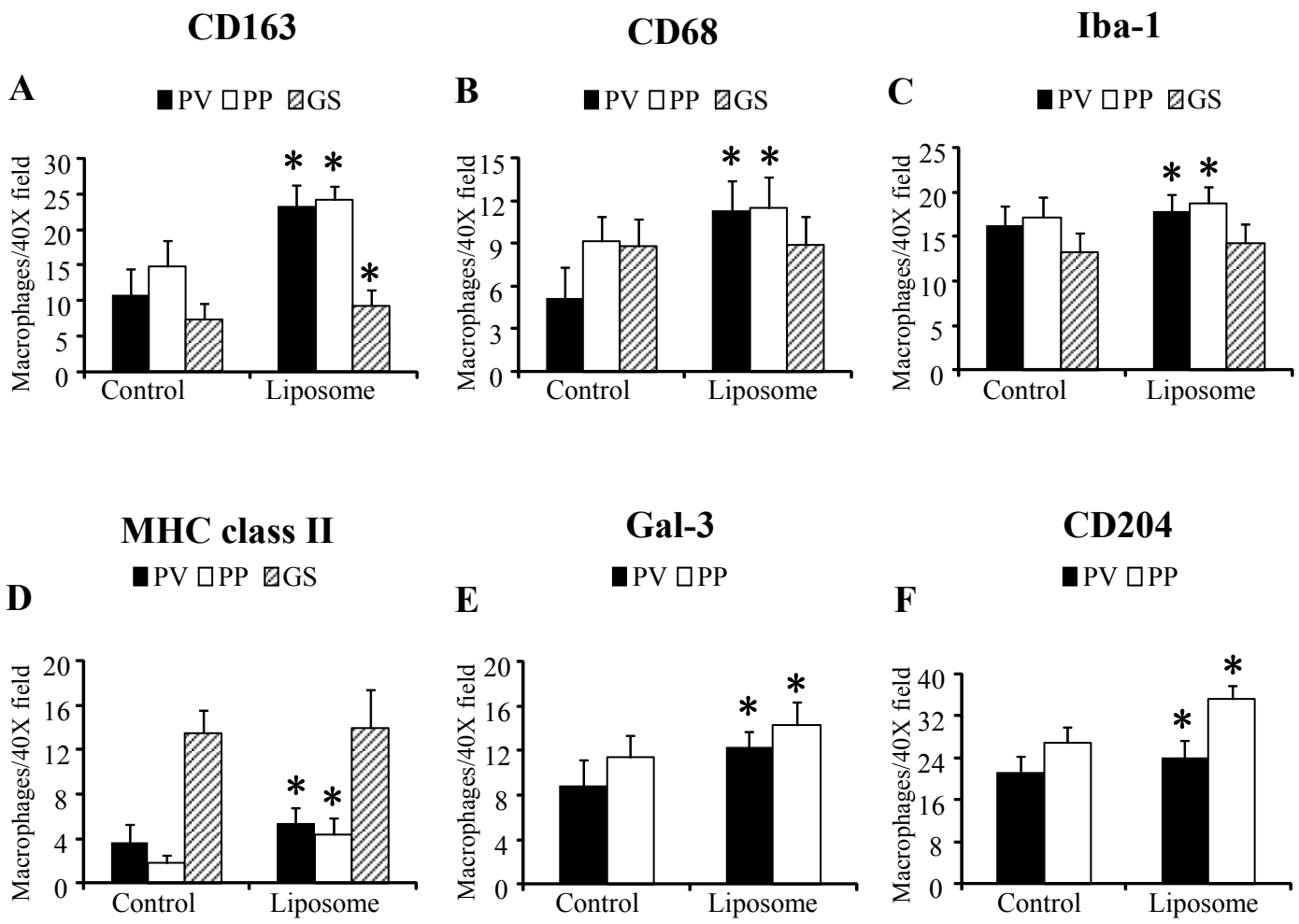
CD163
A
PV PP GS
Macrophages/40X field
30
25
20
15
10
5
0
Control
Liposome
CD68
B
PV PP GS
Macrophages/40X field
15
12
9
6
3
0
Control
Liposome
Iba-1
C
PV PP GS
Macrophages/40X field
25
20
15
10
5
0
Control
Liposome
MHC class II
D
PV PP GS
Macrophages/40X field
20
16
12
8
4
0
Control
Liposome
Gal-3
E
PV PP
Macrophages/40X field
20
16
12
8
4
0
Control
Liposome
CD204
F
PV PP
Macrophages/40X field
40
32
24
16
8
0
Control
Liposome

Fig. 3

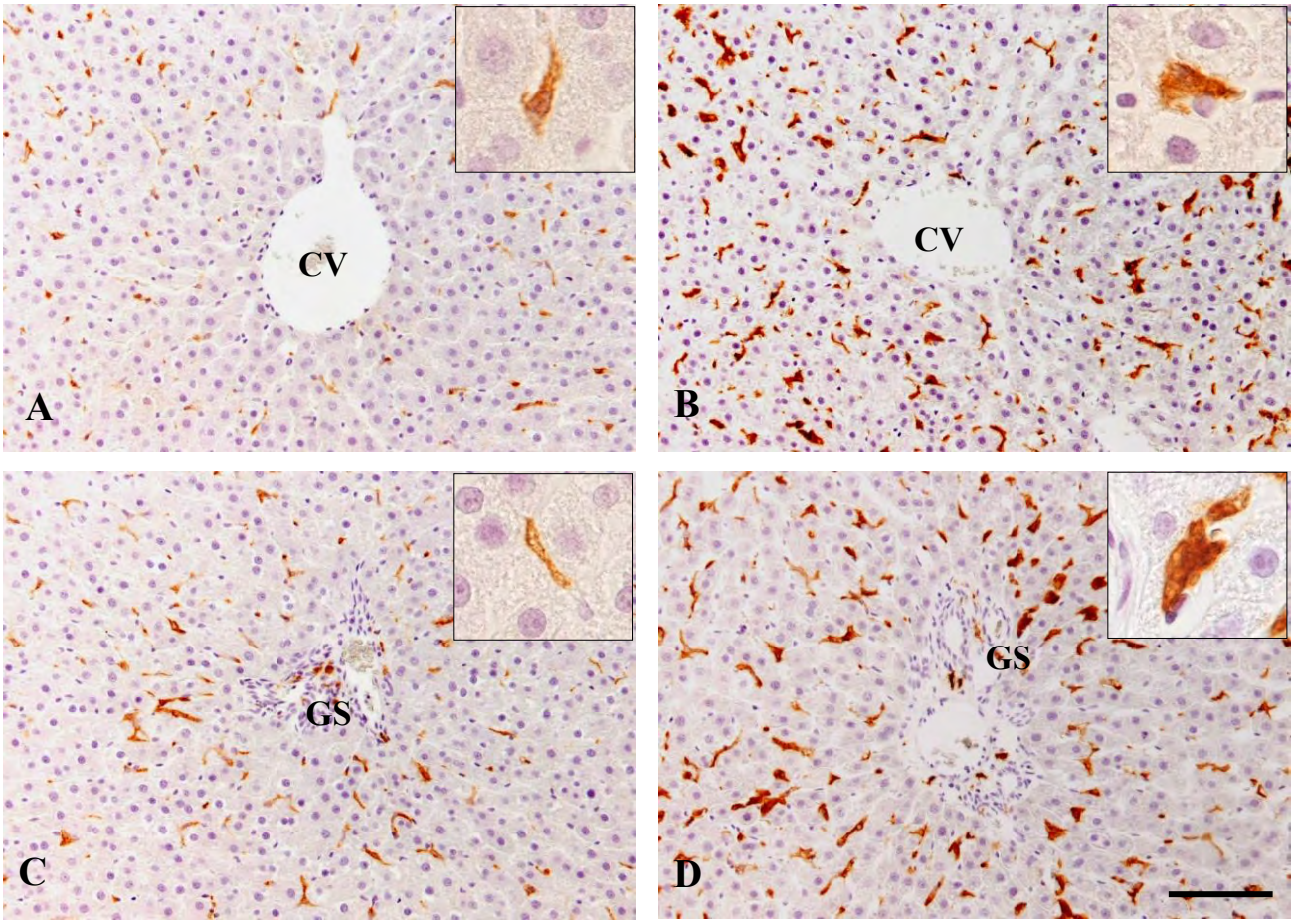

Fig. 4

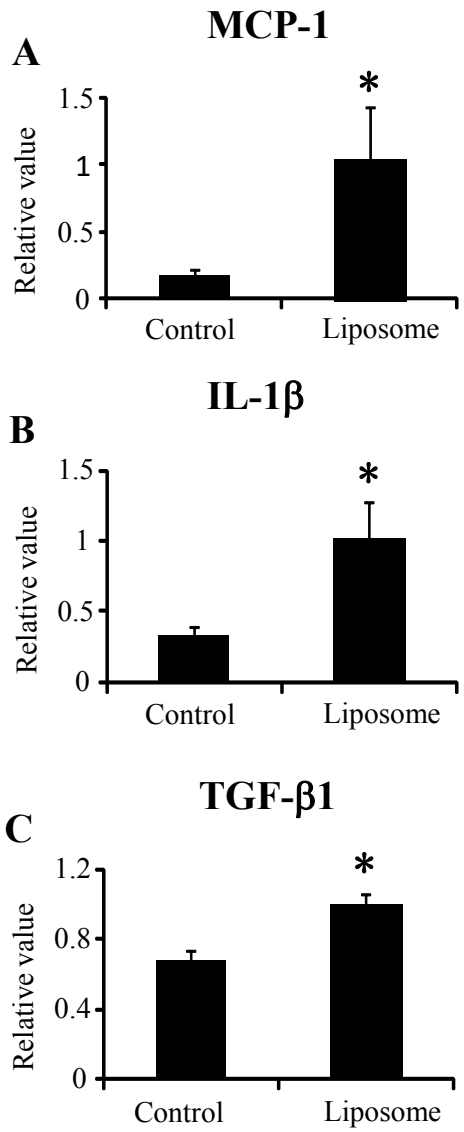
MCP-1
A
Relative value
1.5
1
0.5
0
*
Control
Liposome
IL-1β
B
Relative value
1.5
1
0.5
0
*
Control
Liposome
TGF-β1
C
Relative value
1.2
0.8
0.4
0
*
Control
Liposome

Fig. 5

Section II

Immunophenotypes of depleting and repopulating hepatic macrophages in rats treated with clodronate

Introduction

Showing high plasticity and functional diversity depending on microenvironments, macrophages exist as the resident type in the whole body, and appear as the exudative type in pathological lesions. Liver anchorages the most abundant pool of macrophages in the body of mammals. The representative hepatic macrophages are Kupffer cells (Golbar et al., 2012); additionally, MHC class II-expressing macrophages (as interstitial dendritic cells) are present in the Glisson's sheath in rats (Mori et al., 2009). Hepatic macrophages play a crucial role in the homeostasis and pathogenesis of liver diseases after hepatocytes injury mediated by chemicals. Activated hepatic macrophages after liver injury produce inflammatory/cytotoxic mediators, and anti-inflammatory factors produced by macrophages lead to healing after injury (Wijesundera et al., 2014a; Laskin, 1990), indicating biphasic functions of hepatic macrophages. Therefore, recently, macrophages are divided mainly as classically activated inflammatory macrophages (M1) and alternatively activated reparative macrophages (M2) (M1/M2 macrophage polarization) in rats and mice (Martinez et al., 2008; Duffield et al., 2005; Stein et al., 1992).

To know the functional aspects of macrophages, macrophage depletion has been widely used in normal and pathological conditions (Bautista et al., 2013; Cullen et al., 2013; Sturm et al., 2005). Macrophages can be depleted by injection of liposome-encapsulated dichloromethylene diphosphonate clodronate (CLD) (Van Rooijen and Sanders, 1994). CLD belongs to the family bisphosphonate used for treating osteolytic bone diseases and osteoporosis (Fleisch, 1989). Acting as an anti-macrophage agent, CLD

needs to be encapsulated with liposome that is readily digested. Once ingested by macrophages, CLD causes damage to macrophages via apoptosis, resulting in their depletion (Van Rooijen and Sandar, 1994). In the present study, the author carried out the detailed immunophenotypical analyses of depleting and repopulating macrophages after CLD injection in rats, using different antibodies specific for rat macrophages. Furthermore, microenvironmental conditions, which may be changed in the absence of hepatic macrophages, were investigated, focusing on hepatic enzymes by biochemical analyses, inflammatory/anti-inflammatory cytokines at mRNA levels and genes relating to homeostasis by comprehensive gene analysis. The data shown in the present study would provide useful information when chemicals with possible hepatotoxicity via hepatic macrophage alterations are evaluated.

Materials and methods

Animals and experimental procedures

Twenty-eight 6-week-old male F344 rats were purchased from Charles River Laboratories Japan (Hino, Shiga, Japan), and used after one-week acclimatization. They were housed in an animal room at 21±3°C with a 12 h light-dark cycle, and fed a standard diet for rats (DC-8, CLEA Japan, Tokyo, Japan) and supplied with tap water *ad libitum*. Twenty-four rats were given a single injection of liposomal CLD suspension (5 mg/ml in sterile phosphate buffer saline (PBS)) (http://www.clodronateliposomes.org, last accessed on June 17, 2015) at 50 mg/kg body weight intravenously via tail vein; the CLD dose, capable of inducing almost complete depletion of hepatic macrophages after a single injection, was determined based on the preliminary experiment. Along with hepatic macrophages, although the CLD can deplete macrophages in the spleen and bone marrow (Van Rooijen et al., 1990), the author focused on immunohistochemical characteristics of hepatic macrophages. Four rats were euthanized by exsanguination under isoflurane anesthesia on each time point of post-injection (PI) days 1, 3, 5, 7, 9 and 12. The remaining four rats were injected an equivalent volume of liposome suspension in PBS, which served as controls and were euthanized on PI day 1. One hour before euthanasia, all rats received

intra-peritoneal injection of bromo-2-deoxyuridine (BrdU; Sigma-Aldrich Co., Louis, MO, USA) dissolved in physiological saline at 50 mg/kg body weight. The animal experiments were conducted under the institutional guidelines approved by the ethical committee of Osaka Prefecture University for animal care.

Blood biochemistry

At necropsy, blood was collected from the abdominal aorta, and serum samples were analyzed for aspartate transaminase (AST), alanine transaminase (ALT), alkaline phosphatase (ALP) and γ-glutamyl transferase (γ-GTP) and total bilirubin (T. Bil) by SRL Inc. (Tokyo, Japan).

Histopathology and Immunohistochemistry

Liver tissues from the left lateral lobe were collected and immediately fixed in 10% neutral buffered formalin (NBF), in Zamboni's (0.21% picric acid and 2% paraformaldehyde in 130 mM phosphate buffer, pH 7.4) and in periodate-lysine-paraformaldehyde (PLP) solution processed by PLP-AMeX (Acetone, methyl benzoate and xylene) method (Golbar et al., 2011). NBF-fixed tissues were dehydrated and embedded in paraffin and sectioned at 3-4 μm in thickness. The deparaffinized sections were stained with hematoxylin and eosin (HE) for histopathological examination.

Tissue sections fixed in NBF, Zamboni's solution, or PLP were used for the immunohistochemistry. Deparaffinized tissue sections were used for CD163, CD68, Iba-1, Galectin-3 (Gal-3), MHC class II, CD204 and BrdU staining (Table 1). After pretreatments, tissue sections were stained by the Histostainer (Histofine, Nichirei Bioscience Inc., Tokyo, Japan). Briefly, sections were incubated with 5% skimmed milk in PBS for 10 min, followed by 1 h incubation with primary antibodies. After treatment with 3% H_2O_2 in PBS for 15 min, application of horseradish peroxidase-conjugated secondary antibody (Histofine simple stain MAX PO®; Nichirei Inc., Tokyo, Japan) for 30 min was done. Then, they were incubated with 3, 3'-diaminobenzidine (DAB) (Nichirei Inc., Tokyo, Japan) for 5 min. Sections were counterstained with hematoxylin for 1 min. For negative controls,

tissue sections were treated with mouse or rabbit non-immunized serum instead of the primary antibody. Cells expressing CD163, CD68, Iba-1, Gal-3, MHC class II and CD204 were counted per 40X field in randomly selected five areas in the perivenular (PV), periportal (PP) or Glisson's sheath (GS) areas. The number of BrdU-positive hepatocytes was also counted per 40X field and compared with the total number of hepatocytes.

Double immunofluorescence staining

Fresh frozen liver sections (10 μm in thickness) from control and CLD-treated rats on PI days 1 and 12 were used. Double immunofluorescence was carried out using CD163 in combination with CD68, Gal-3, MHC class II and CD204. Briefly, after fixation in cold acetone:methanol (1:1) for 10 min at 4^{o}C, the sections were incubated with 10% normal goat serum for 15 min. The sections were reacted with the primary antibody overnight at 4^{o}C. After rinsing with PBS, the sections were incubated for 45 min with the secondary antibody goat anti-mouse IgG-conjugated with Alexa 488 or Alexa 568 (Invitrogen, Carlsbad, CA, USA) for CD68; and goat anti-rabbit IgG-conjugated with Alexa 568 (Invitrogen, Carlsbad, CA, USA) for Gal-3. The sections were then incubated with the primary antibody labeled with fluorescent dye conjugated secondary antibody: Alexa 488-labeled CD163 (AbD Serotec, Oxford, UK) for CD163/CD68; Alexa 488-labeled MHC class II (AbD Serotec, Oxford, UK) for CD163/ MHC class II; Alexa 488-labeled CD163 (AbD Serotec, Oxford, UK) for CD163/CD204. The sections were visualized with Vectashield^{TM} mounting medium containing 4′, 6-diamidino-2-phenylindole (DAPI) (Vector Laboratories Inc., Burlingame, CA, USA) for nuclear staining, and analyzed by a virtual slide scanner (VS-120, Olympus, Tokyo, Japan).

Real time reverse transcriptase-polymerase chain reaction (RT-PCR) and microarray

Liver samples from the left median lobe were immediately immersed in RNAlater$^{®}$ (Qiagen GmbH, Hilden, Germany) overnight at 4^{o}C and stored at −80^{o}C until use. Total RNA was extracted from liver tissues by using an SV total RNA isolation system Kit^{TM} (Promega, Madison, WI, USA) according to the manufacturer's instructions. The extracted RNA was reverse-transcribed by using SuperScript VILO (Invitrogen, Carlsbad, CA,

USA). Real time PCR was performed using TaqMan gene expression assays (Life Technologies, Carlsbad, CA, USA) in a PikoReal Real-time 96 PCR System (Thermo Scientific, Massachusetts, CA, USA). The TaqMan probes specific for the cytokines used were as follows (Assay IDs): monocyte chemoattractant protein-1 (MCP-1), Rn00580555_m1; interleukin-1β (IL-1β), Rn00580432_m1; transforming growth factor-β1 (TGF-β1), Rn00572010_m1; colony stimulating factor-1 (for macrophages) (CSF-1), Rn00696122_m1; interleukin-4 (IL-4), Rn01456866_m1; interleukin-6 (IL-6), Rn01410330_m1; interleukin-10 (IL-10), Rn00563409_m1; and β-actin, Rn00667869_m1. The mRNA expression was normalized against the expression of β-actin mRNA as the internal control. The data were analyzed using the comparative C_t method ($^{\Delta\Delta}C_t$ method). Expression profiles of mRNAs were analyzed by SurePrint G3 Rat GE8x60K Microarray Kit (Agilent Technologies, Santa Clara, CA, USA).

Statistical evaluation

Obtained data were expressed as mean ± standard deviation (SD). Statistical analysis was performed using Dunnett's multiple comparison test. Significance was considered at $P < 0.05$.

Results

Blood biochemistry

The values of AST, ALP and γ-GTP on PI days 1 to 3, ALT on PI days 1 to 9 and T. Bil on PI day 1 in CLD-treated rats showed a significant increase, and then returned to control levels until PI day 12 (Fig. 1A-E).

Histopathology and BrdU immunohistochemistry

In HE-stained sections, similar to control rats (Fig. 2A), there were no marked changes of livers histopathologically in CLD-treated rats at each examination point (Fig. 2B). Interestingly, the number of BrdU-positive hepatocytes was significantly increased on

day 1 (Fig. 2D, E), indicating increased proliferative activity in comparison with control rats (Fig. 2C).

Immunohistochemistry for hepatic macrophages

The kinetics of macrophages reacting to CD163, CD68, Iba-1, Gal-3, MHC class II and CD204 is shown in Fig. 3A-F, respectively, and representative findings are presented in Fig. 4A-R for the PV areas and Fig. 5A-R for the PP and GS areas.

CD163 immunostaining

In control rats, $CD163^+$ cells were present mainly along the sinusoids in the PV and PP areas (Figs. 4A and 5A), indicating Kupffer cells; additionally, there were cells reacting to CD163 in the GS area (Fig. 5A), which are regarded as resident (tissue) macrophages.

In CLD-injected rats, the numbers of $CD163^+$ cells were drastically decreased in all areas of the liver on PI days 1-7, with almost complete depletion (particularly on PI days 5 and 7) (Figs. 3A, 4B and 5B). On PI days 9 and 12, the number of $CD163^+$ cells continued to be decreased in the GS area (Figs. 3A, 4C and 5C).

CD68, Iba-1 and Gal-3 immunostaining

In control rats, macrophages reacting to CD68 and Iba-1 were evenly distributed throughout the hepatic lobule in the PV, PP and GS areas, being smaller in number in contrast to $CD163^+$ cell number (Figs. 4D, G and 5D, G). On the other hand, Gal-3^+ cells were not seen in the GS area, although a small number of the positive cells were diffusely distributed in the PV and PP areas (Figs. 4J and 5J). Cells reacting to CD68, Iba-1 and Gal-3 in the PV and PP areas were regarded as Kupffer cells, because they were also located along the sinusoid and co-expressed CD163 in double immunofluorescence, as mentioned below.

In CLD-treated rats, the kinetic of hepatic macrophages reacting to CD68, Iba-1 and Gal-3 showed similar pattern to each other in each area (except for Gal-3^+ cells in the GS area); after drastic reduction on PI day 1, they were gradually repopulated on PI days

3-12. Although their levels continued to be significantly decreased compared to control rats by PI day 12 (Fig. 3B-D). Interestingly, in contrast to $CD163^+$ cells, cells reacting to CD68 and Iba-1 were not completely depleted during the observation period (Figs. 4E, F, H, I and 5E, F, H, I). The repopulation of $Gal\text{-}3^+$ cells seen in the PV and PP areas after depletion on PI day 1 appeared to be slower, as compared with that of $CD68^+$ and $Iba\text{-}1^+$ cells (Figs. 3D, 4K, L and 5K, L).

MHC class II and CD204 immunostaining

In control rats, MHC class II^+ cells were rarely seen in the PV and PP areas, while they were present mainly in the GS area, indicative of the antigen-presenting dendritic cells (Figs. 4M and 5M) (Mori et al., 2009). On the other hand, $CD204^+$ cells were evenly distributed in the PV and PP areas and were completely absent in the GS area (Figs. 4P and 5P). MHC class II^+ and $CD204^+$ cells present along the sinusoids were regarded as Kupffer cells, because they co-expressed CD163 in double immunofluorescence, as mentioned below.

Injection of CLD significantly reduced the number of cells reacting to MHC class II and CD204 in each area (except for $CD204^+$ cells in the GS area) with approximately half to control levels and the reduced levels were almost consistent on PI days 1-12 (Figs. 3E, F, 4N, O, Q, R and 5N, O, Q, R).

Immunophenotypes of $CD163^+$ Kupffer cells

To investigate the properties of $CD163^+$ Kupffer cells, double immunofluorescence for $CD163^+$ cells with antibodies against CD68, Gal-3, MHC class II and CD204 were conducted in the PV area of livers in control and CLD-treated rats on PI days 1 and 12 (Fig. 6A-L).

All (100%) of $CD68^+$ (Fig. 6A-C) and $CD204^+$ cells (Fig. 6D-F) reacted simultaneously to CD163 in control and CLD-treated rats on PI days 1 and 12 (Fig. 7A, B). Although many $Gal\text{-}3^+$ cells (72%) in control rats showed a positive reaction to CD163, the $CD163^+Gal\text{-}3^+$cell number was decreased (9%) on PI day 1, and then increased (57%) on

PI day 12 (Figs. 6G-I and 7C). In control rats, some of MHC class II^+ cells (14%) showed a positive reaction to CD163; in CLD-treated rats, the percentage of MHC class II^+CD163^+ cells were increased on PI days 1 (24%) and 12 (44%) (Figs. 6J-L and 7D).

The findings of double immunofluorescence labeling indicated that in control rats, $CD163^+$ Kupffer cells expressed simultaneously CD68, Gal-3, MHC class II and CD204. However, the number of cells reacting to CD68, Gal-3, MHC class II and CD204 was smaller than that of $CD163^+$ cells, indicating that all Kupffer cells do not always express antigens of CD68, Gal-3, MHC class II or CD204; there are various hepatic macrophages different from Kupffer cells, because the kinetic of cells reacting to CD68, Gal-3, MHC class II and CD204 after CLD injection was different from that of $CD163^+$ Kupffer cells. Additionally, $CD163^+Gal\text{-}3^+$ and $CD163^+$MHC class II^+ double positive Kupffer cells might be more sensitive immunophenotypes to CLD treatment, because $Gal\text{-}3^+$ and MHC class II^+ macrophages were reduced in numbers on PI day 1.

mRNA expressions of cytokines

The mRNA expression level for macrophage growth factors and inflammatory cytokines showed unique sequential change (Fig. 8A-G). mRNAs of cytokines relating to macrophage induction and activation (such as MCP-1, CSF-1, IL-6 and IL-4) were significantly increased exclusively on PI day 1 (Fig. 8A-D); among them, MCP-1 mRNA was significantly decreased on PI days 5-12 (Fig. 8A). On the contrary, besides IL-1β (pro-inflammatory factor) on PI days 1-12, mRNAs of IL-10 on PI days 1-9 and TGF-β1 on PI days 3-12 (both, anti-inflammatory factors) were significantly decreased (Fig. 8E-G).

These findings indicated that increases in macrophage induction and activation factors (such as MCP-1, CSF-1, IL-6 and IL-4) at the early stages after CLD injection might be a reactive phenomenon to the depletion of hepatic macrophages to re-constitute liver structure; decreases in pro-inflammatory (IL-1β) and anti-inflammatory (IL-10 and TGF-β1) factors during repopulation of hepatic macrophages might imply that

repopulating macrophages are not inflammatory cells, but constitutive cells necessary for homeostasis.

Gene expression profile of macrophage-depleted rat livers by microarray analysis

A number of genes were up-regulated (more than 2-fold) or down-regulated (less than 0.5-fold) in response to CLD treatment on PI day 1, in comparison with control rats (Tables 2 and 3). These gene profiles could be grouped into distinct, differentially-expressed functional groups based on the gene ontogeny classification system (Zheng et al., 2014). The up-regulated genes included those that are associated with "cell proliferation", "hepatic secretory protein", "cell surface and structural protein", "signal transduction and transcription factor" and "apoptosis" (Table 2). In contrast, the down-regulated genes involved those that are associated with "cell proliferation", "growth factors and their receptors", "signal transduction and transcription factor" and "apoptosis" (Table 3). Out of them with up- or down-regulated gene profiles, the number of genes relating to "cell proliferation" was the greatest, which might be corresponding to increased number of BrdU-positive hepatocytes.

Discussion

Liver is the most essential target organ for chemicals, because many chemicals are metabolized in liver. Besides hepatocytes as the parenchymal cells, hepatic macrophages exist as a non-parenchymal cell type at 10-20 % of liver-constituting cells (Godoy et al., 2013). Recently, macrophages appearing in experimentally-induced pathological conditions in rats have been detected by immunohistochemistry with different antibodies specific for macrophages in order to investigate the pathogenesis through macrophage functions (Golbar et al., 2013, 2011). Macrophages involved in hepatotoxicity may be functionally evaluated by M1/M2 macrophage polarization (Wijesundera et al., 2014a, b). In the present study, therefore, the author attempted to immunophenotypically characterize the depleting and repopulating hepatic macrophages in CLD-treated rats by using different

antibodies for rat macrophage detection, in order to establish the base-line data of hepatic macrophage-depletion conditions.

Immunophenotypical characterization of depleting and repopulating hepatic macrophages after CLD injection

$CD163^+$ Kupffer cells

CD163 is the protein of the hemoglobin-haptoglobin complex receptor, and the antigen is expressed generally in the resident macrophages (such as Kupffer cells) in normal rat tissues (Ide et al., 2005). $CD163^+$ Kupffer cells along the sinusoid were drastically decreased on PI day 1 after CLD injection and the almost complete absence continued until PI day 12. CLD injection could reduce Kupffer cells in rats and mice, and the effect was maintained for one week (Yamamoto et al., 1996; Van Rooijen et al., 1990). Additionally, the present study showed that $CD163^+$ resident macrophages in the GS area were also completely depleted by CLD injection through the observation period. From these findings it is suggested that CLD could be very effective for depletion of Kupffer cells.

Macrophages expressing CD68, Iba-1, Gal-3, MHC class II and CD204

CD68 antigen is located on the lysosomal membrane of macrophages, and $CD68^+$ cells have been reported to increase in number in injured areas as the most common infiltrating cells with activated phagocytosis and production of cytotoxic factors (Golbar et al., 2011; Suda et al., 1998; Damoiseaux et al., 1994). Iba-1 has actin-cross linking activity which may act in membrane ruffling and phagocytosis of activated macrophages (Sasaki et al., 2001; Ohsawa et al., 2000). Gal-3, a protein involved in the galectin family of mammalian proteins, was originally described as Mac-2 antigen expressed on the surface of activated macrophages (Dong and Hughes, 1997). The MHC class II molecule is expressed in activated macrophages and dendritic cells, implying antigen-presenting capacity (Zhao et al., 2006; Ide et al., 2005). CD204 antibody was generated by immunizing scavenger receptor knockout mice with recombinant human type I scavenger

receptor protein (Tomokiyo et al., 2002), and its expression is related to activated lipid metabolism in macrophages via the scavenger receptor (Greaves et al., 1998).

Double immunofluorescence using control rat livers indicated that there were $CD163^+$ cells along the sinusoids which reacted simultaneously to CD68, Gal-3, MHC class II or CD204. Although double immunofluorescence for CD163/Iba-1 was not carried out, because of difficulty in combination of different antibodies, $Iba\text{-}1^+$ cells were also seen along the sinusoids. These findings indicated that Kupffer cells can partly express such antigens as CD68, Gal-3, Iba-1, MHC class II and CD204 in normal rat livers (Golbar et al., 2012), because their numbers were usually smaller in contrast to the $CD163^+$ cell number. Interestingly, in addition to the absence of $Gal\text{-}3^+$ and $CD204^+$ cells in the GS area, the kinetic of cells reacting to CD68, Iba-1, Gal-3, MHC class II and CD204 was different from that of $CD163^+$ cells after CLD injection, particularly in that $CD163^+$ cells were almost completely depleted during the observation period; on the contrary, cells reacting to CD68, Iba-1 and Gal-3 were quickly reduced on PI day 1 and then gradually repopulated until PI day 12; the reduced number of cells reacting to MHC class II and CD204 were almost consistent on PI days 1-12, with approximately half to control levels. In double immunofluorescence analysis, additionally, all (100%) of $CD68^+$ or $CD204^+$ cells examined on PI days 1 and 12 reacted also to CD163, whereas, on PI days 1 and 12, respectively, $Gal\text{-}3^+$ cells expressing simultaneously CD163 were 9% and 57%, and MHC class II^+ cells expressing simultaneously CD163 were 24% and 44%. These findings indicated that the susceptibility of hepatic macrophages to CLD treatment in rats varied depending on immunophenotypes; $CD163^+$ Kupffer cells located along the sinusoids were the most susceptible to CLD treatment, whereas $CD204^+$ and MHC class II^+ cells (in particular, in the GS area) were less sensitive.

Influence of hepatic macrophage depletion after CLD injection on hepatic homeostasis

Kupffer cells may have a role in the clearance of serum enzymes by their unidentified surface receptors (Smit et al., 1987). Under the reduction of Kupffer cells in

rats by CLD, hepatic enzymes such as AST and ALT were significantly increased within 48 h after the treatment (Radi et al., 2011). In addition to AST and ALT, the present study showed that levels of ALP, γ-GTP and T. Bil mainly on PI days 1-5 were also increased after CLD injection, corresponding to PI days of depleting Kupffer cells. In HE-stained sections, there were no marked histopathological changes in CLD-treated rats (Radi et al., 2011). CLD is not considered hepatotoxicant (Cullen et al., 2013). These findings indicated that Kupffer cells are responsible for clearance of serum enzymes which are being produced under physiological condition.

Interestingly, however, BrdU immunohistochemistry showed that the number of positive hepatocytes was transiently increased on PI day 1. The comprehensive gene profile analysis also confirmed the increase in gene profiles relating to “cell cycle” which showed up- or down-regulation; among gene profiles analyzed, the “cell cycle-associated genes” was the greatest in the number. The proliferating activity of hepatocytes might be due to transient imbalance between hepatocytes and Kupffer cells immediately after CLD injection (Xu et al., 2012). However, the detail reason should be investigated in future study.

Additionally, the author analyzed expressions of cytokines, because hepatic macrophages are a major source of inflammatory mediators. MCP-1, a member of the chemokine family, acts as a highly potent chemotactic factor for blood-monocytes and resident macrophages (Zamara et al., 2007; Sakai et al., 2006). CSF-1 is a macrophage growth factor which regulates the proliferation, differentiation, and maturation of Kupffer cells (Dai et al., 2002; Cecchini et al., 1994). MCP-1 and CSF-1 mRNAs were increased transiently on PI day 1. Furthermore, IL-6 and IL-4 mRNAs were also increased exclusively on PI day 1. IL-6 is a possible factor for induction and activation of M1 macrophages (Martinez, 2011; Pello et al., 2011), whereas M2 macrophages can be induced by IL-4 (Martinez, 2011; Martinez, 2008; Meghari et al., 2007). The temporary increase in MCP-1, CSF-1, IL-6 and IL-4 on PI day 1 might be related to reactive phenomenon to hepatic macrophage depletion to re-constitute liver structure by inducing blood-derived monocytes or from local precursors (Ju et al., 2002; Meijer et al., 2000).

These factors might be produced from hepatocytes and sinusoidal cells (Fainboim et al., 2007; Ishihara and Hirano, 2002).

On the contrary, MCP-1 mRNA was significantly decreased in the hepatic macrophage repopulating stage on PI days 5-12. Furthermore, mRNAs of IL-1β, IL-10 and TGF-β1 were decreased on PI day 1 and subsequent repopulating days until PI day 12. IL-1β is known as a pro-inflammatory factor, and IL-10 and TGF-β1 act as anti-inflammatory factors; these factors may be produced by M2 macrophages in inflammation (Wijesundera et al., 2014b; Sica et al., 2013; Njoku et al., 2009). The decreased expressions of these factors during the observation period imply that repopulating macrophages are not inflammatory cells, but re-constituting cells necessary for liver homeostasis.

In conclusion, the present study showed that immunophenotypical characterization of depleting and repopulating hepatic macrophages after CLD injection by using different antibodies specific for rat macrophages; $CD163^+$ Kupffer cells were the most susceptible, whereas $CD204^+$ and MHC class II^+ cells were less susceptible. CLD may be very useful to know the conditions of depleted hepatic macrophages in normal and pathological lesions (Bautista et al., 2013; Cullen et al., 2013; Sturm et al., 2005). Under depletion of hepatic macrophages, in addition to increased number of proliferating hepatocytes, cytokines for macrophage induction and activation were increased and inflammation-related factors were decreased; these alterations might be related to re-constitute to keep liver homeostasis. Furthermore, under hepatic macrophage depletion, it was found that hepatic enzymes such as AST and ALT were significantly increased. Some chemicals may have potential activity to reduce macrophage functions without being accompanied by histopathological changes. It may be important for toxicologic pathologists to take hepatic macrophage conditions into consideration when such chemicals are evaluated in hepatotoxicity.

Summary

Hepatic macrophages (including Kupffer cells) play a crucial role in homeostasis and act as mediators of inflammatory response in liver. Hepatic macrophages were depleted in male F344 rats by a single intravenous injection of liposomal clodronate (CLD; 50 mg/kg body weight). Immunophenotypical characteristics of depleting and repopulating macrophages were analyzed by different antibodies specific for macrophages. $CD163^+$ Kupffer cells were almost completely depleted on post-injection (PI) days 1-12. Macrophages reacting to CD68, Iba-1 and Gal-3 were drastically reduced in number on PI day 1 and then recovered gradually until PI day 12. MHC class II^+ and $CD204^+$ macrophages were moderately decreased during the observation period. Although hepatic macrophages detectable by different antibodies were reduced in varying degrees, Kupffer cells were the most susceptible to CLD. Liver situation influenced by depleted hepatic macrophages was also investigated. No marked histological changes were seen in the liver, but the proliferating activity of hepatocytes was significantly increased, supported by changes of gene profiles relating to cell proliferation on microarray analysis on PI day 1; the values of AST and ALT were significantly elevated; macrophage induction/activation factors (such as MCP-1, CSF-1, IL-6 and IL-4) were increased exclusively on PI day 1, whereas anti-inflammatory factors such as IL-10 and TGF-β1 remained significantly decreased after macrophage depletion. The present study confirmed importance of hepatic macrophages in liver homeostasis. The condition of hepatic macrophages should be taken into consideration when chemicals capable of inhibiting macrophage functions are evaluated.

Table 1. Details of antibodies used for immunohistochemistry.

Antibody	Type	Fixative	Dilution	Pretreatment	Source
CD68 (ED1)	Mouse monoclonal	PLP	1/500	MW in citrate buffer, 20 min	AbD Serotec, Oxford, UK
CD163 (ED2)	Mouse monoclonal	PLP	1/300	100µg/ml Proteinase K, 10 min	AbD Serotec, Oxford, UK
CD204 (SRA-E5)	Mouse monoclonal	Zamboni's solution	1/1000	MW in citrate buffer, 20 min	Transgenic Inc., Kumamoto, Japan
MHC class II (OX6)	Mouse monoclonal	PLP	1/1000	MW in citrate buffer, 20 min	AbD Serotec, Oxford, UK
Iba-1	Rabbit polyclonal	Zamboni's solution	1/1000	MW in citrate buffer, 20 min	Wako Pnure Chemical Industries, Osaka, Japan
Galectin-3 (Gal-3)	Rabbit polyclonal	Zamboni's solution	1/500	MW in citrate buffer, 20 min	Santa Cruz Biotechnology, Santa Cruz, CA, USA
BrdU	Mouse monoclonal	NBF	1/500	4N HCl, 30 min and 100µg/ml Proteinase K, 10 min	Dako Corp, Glostrup, Denmark

PLP: periodate-lysine-paraformaldehyde; MW: microwave; BrdU: bromo-2-deoxyuridine; NBF: neutral buffered formalin.

Table 2. Up-regulated (more than 2-fold) genes in the liver of clodronate (CLD)-treated versus control rats.

Functional category	Gene symbol	Gene description	Fold change
Cell proliferation	Lcn2	Rattus norvegicus lipocalin 2 (Lcn2), mRNA [NM_130741]	16.56
	Map3k5	Rattus norvegicus mitogen-activated protein kinase kinase kinase 5 (Map3k5), mRNA [NM_001277694]	7.58
	Rab27b	Rattus norvegicus RAB27B, member RAS oncogene family (Rab27b), mRNA [NM_053459]	5.57
	Tgfb2	Rattus norvegicus transforming growth factor, beta 2, mRNA (cDNA clone IMAGE:7938703), complete cds. [BC100663]	5.02
	Sphk1	Rattus norvegicus sphingosine kinase 1 (Sphk1), transcript variant 6, mRNA [NM_133386]	4.66
	Pdgfd	Rattus norvegicus platelet derived growth factor D (Pdgfd), mRNA [NM_023962]	3.98
	Dbp	Rattus norvegicus D site of albumin promoter (albumin D-box) binding protein (Dbp), mRNA [NM_012543]	3.91
	Map4k3	Rattus norvegicus mitogen-activated protein kinase kinase kinase kinase 3 (Map4k3), mRNA [NM_133407]	2.92
	Wnt5b	Rattus norvegicus wingless-type MMTV integration site family, member 5B (Wnt5b), mRNA [NM_001100489]	2.41
	Wsb1	Rattus norvegicus WD repeat and SOCS box-containing 1 (Wsb1), transcript variant 1, mRNA [NM_001042561]	2.20
	Cdca7	Rattus norvegicus cell division cycle associated 7 (Cdca7), mRNA [NM_001025693]	2.09
Hepatic secretory proteins	mt1a	Rattus norvegicus metallothionein 1a (Mt1a), mRNA [NM_138826]	2.04
Cell surface and structural protein	Krt1	Rattus norvegicus keratin 1 (Krt1), mRNA [NM_001008802]	12.43
	Krt1	Rattus norvegicus keratin 12 (Krt12), mRNA [NM_001008761]	4.52
	Orm1	Rattus norvegicus orosomucoid 1 (Orm1), mRNA [NM_053288]	3.13
	H19	Rattus norvegicus H19, imprinted maternally expressed transcript (non-protein coding) (H19), long non-coding RNA [NR_027324]	2.72
Signal transduction and transcription factors	Hnf4g	Rattus norvegicus hepatocyte nuclear factor 4, gamma (Hnf4g), mRNA [NM_001108939]	5.18
	Onecut1	Rattus norvegicus one cut homeobox 1 (Onecut1), mRNA [NM_022671]	2.12
Apoptosis	Bik	Rattus norvegicus BCL2-interacting killer (apoptosis-inducing) (Bik), mRNA [NM_053704]	2.08

Table 3. Down-regulated (less than 0.5-fold) genes in the liver of clodronate (CLD)-treated versus control rats.

Functional category	Gene symbol	Gene description	Fold change
Cell proliferation	Cdca7l	Rattus norvegicus cell division cycle associated 7 like (Cdca7l), mRNA [NM_001034953]	0.49
	P2ry13	Rattus norvegicus purinergic receptor P2Y, G-protein coupled, 13 (P2ry13), mRNA [NM_001002853]	0.47
	Fgfr2	Rattus norvegicus fibroblast growth factor receptor 2 (Fgfr2), transcript variant a, mRNA [NM_012712]	0.46
	Socs3	Rattus norvegicus suppressor of cytokine signaling 3 (Socs3), mRNA [NM_053565]	0.39
	Rassf4	Rattus norvegicus Ras association (RalGDS/AF-6) domain family member 4 (Rassf4), mRNA [NM_001024275]	0.34
	Rab32	Rattus norvegicus RAB32, member RAS oncogene family (Rab32), mRNA [NM_001108902]	0.27
	P2ry12	Rattus norvegicus purinergic receptor P2Y, G-protein coupled, 12 (P2ry12), mRNA [NM_022800]	0.22
	Tlr2	Rattus norvegicus toll-like receptor 2 (Tlr2), mRNA [NM_198769]	0.13
	Fgfr1	Rattus norvegicus Fibroblast growth factor receptor 1 (Fgfr1), mRNA [NM_024146]	0.11
Growth factors and their receptors	thrsp	Rattus norvegicus thyroid hormone responsive (Thrsp), mRNA [NM_012703]	0.34
Signal transduction and transcription factors	Nr0b2	Rattus norvegicus nuclear receptor subfamily 0, group B, member 2 (Nr0b2), mRNA [NM_057133]	0.44
Apoptosis	Stk17b	Rattus norvegicus serine/threonine kinase 17b (Stk17b), mRNA [NM_133392]	0.41
	Vopp1	Rattus norvegicus vesicular, overexpressed in cancer, prosurvival protein 1 (Vopp1), mRNA [NM_001108630]	0.31

Figure legends

Fig. 1. A-E: Blood biochemical analyses in control and clodronate (CLD)-injected rats on post-injection (PI) days 1-12. Aspartate transaminase (AST) (A), alanine transaminase (ALT) (B), alkaline phosphatase (ALP) (C), γ-glutamyl transferase (γ-GTP) (D) and total bilirubin (T. Bil) (E). Dunnett's test. *, $P<0.05$, significantly different from control rats. d: day.

Fig. 2. A-B: Histopathology of livers of control and CLD-injected rats. The control rats shows normal hepatic architecture (A). Hepatic architecture is normal in CLD-injected rats on PI day 1 (B). C-D: BrdU-positive hepatocytes are seen in livers of control (C) and CLD-injected rats on PI day 1 (D). E. The kinetic of BrdU-positive hepatocytes in the liver of control and CLD-injected rats on PI days 1-12; the number of positive hepatocytes is significantly increased on PI day 1. Dunnett's test. *, $P<0.05$, significantly different from control rats. d: day, CV: central vein, BrdU: bromo-2-deoxyuridine. Bar = 50 μm.

Fig. 3. The kinetics of macrophages reacting to CD163 (A), CD68 (B), Iba-1 (C), Gal-3 (D), MHC class II (E) and CD204 (F) in the perivenular (PV) (■), periportal (PP) (▨) and Glisson's sheath (GS) (□) areas in livers of control and CLD-injected rats on PI days 1-12. Dunnett's test. *, $P<0.05$, significantly different from control rats. d: day.

Fig. 4. Immunohistochemistry in control and CLD-injected rats on PI day 1 or 12 in the perivenular area of livers. Many macrophages reacting to CD163 (A), CD68 (D), Iba-1 (G), Gal-3 (J), MHC class II (M) and CD204 (P) are seen (arrowheads) in control rats. Almost complete depletion of macrophages are seen (arrowheads) on PI day 1 in CLD-injected rats: CD163 (B), CD68 (E), Iba-1 (H), Gal-3 (K), MHC class II (N) and CD204 (Q). Repopulating macrophages (arrowheads) reacting to CD163 (C), CD68 (F), Iba-1 (I), Gal-3 (L), MHC class II (O) and CD204 (R) are seen on PI day 12 in CLD-injected rats. d: day, CV: central vein. Bar = 100 μm.

Fig. 5. Immunohistochemistry in control and CLD-injected rats on PI day 1 or 12 in the periportal area including the GS of livers. Many macrophages (arrowheads) reacting to CD163 (A), CD68 (D), Iba-1 (G), Gal-3 (J), MHC class II (M) and CD204 (P) are seen in control rats. A few macrophages (arrowheads) are seen on PI day 1 in CLD-injected rats: CD163 (B), CD68 (E), Iba-1 (H); Gal-3 (K), MHC class II (N) and CD204 (Q). Macrophages (arrowheads) reacting to CD163 (C), CD68 (F), Iba-1 (I), Gal-3 (L), MHC class II (O) and CD204 (R) are seen on PI day 12 in CLD-injected rats. d: day, GS: Glisson's sheath. Bar = 100 μm.

Fig. 6. Double immunofluorescence for CD68/CD163 (A-C), CD204/CD163 (D-F), Gal-3/CD163 (G-I) and MHC class II/CD163 (J-L) in the livers of control and CLD-injected rats on PI day 1 or 12. Yellow color indicates double positive reaction (arrows). Blue is nuclei stained with 4′, 6-diamidino-2-phenylindole (DAPI). d: day. Bar = 40 μm.

Fig. 7. The percentage (%) of double immunopositive macrophages for CD68/CD163 (A), CD204/CD163 (B), Gal-3/CD163 (C) and MHC class II/CD163 (D) in control and CLD-injected rats on PI day 1 or 12. d: day.

Fig. 8. mRNA expressions for cytokines such as MCP-1 (A), CSF-1 (B), IL-6 (C), IL-4 (D), IL-1β (E), IL-10 (F) and TGF-β1 (G) in control and CLD-treated rats on days 1-12. Expression levels are normalized to β-actin mRNA level. Dunnett's test. *, $P<0.05$, significantly different from control rats. d: day.

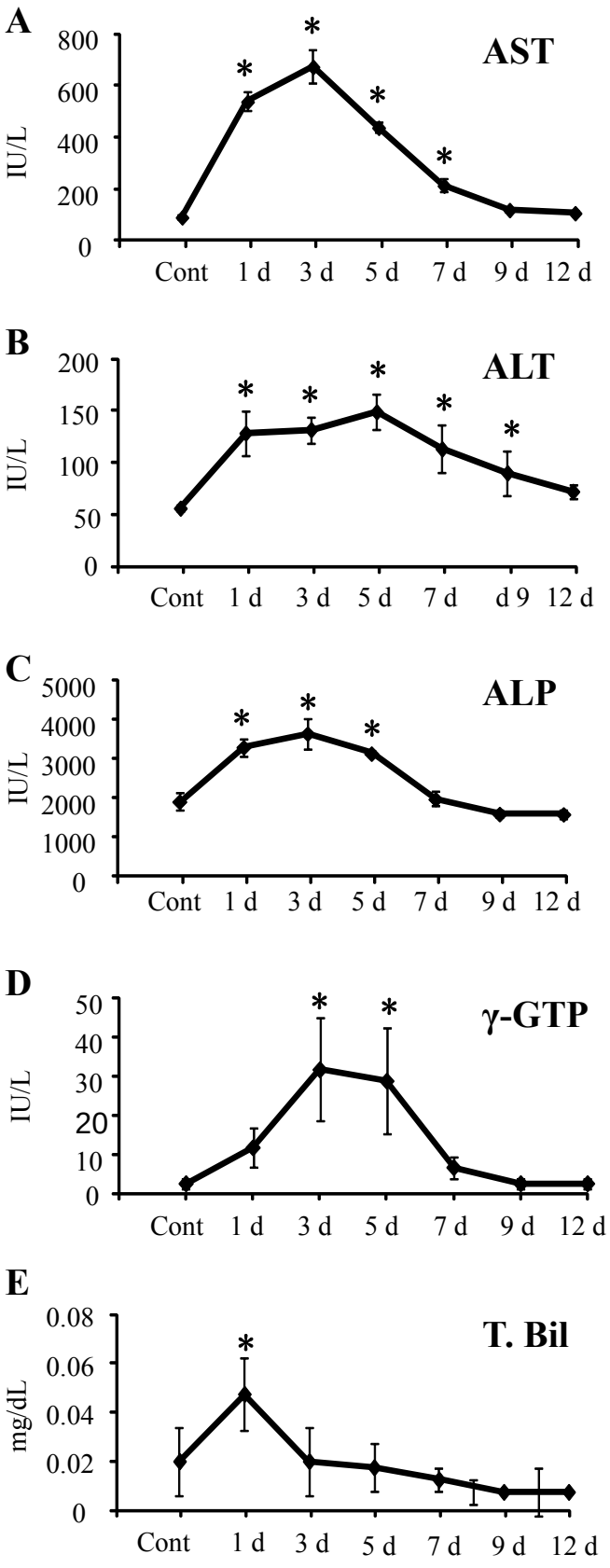
A
AST
IU/L
800
600
400
200
0
Cont 1 d 3 d 5 d 7 d 9 d 12 d
B
ALT
IU/L
200
150
100
50
0
Cont 1 d 3 d 5 d 7 d d 9 12 d
C
ALP
IU/L
5000
4000
3000
2000
1000
0
Cont 1 d 3 d 5 d 7 d 9 d 12 d
D
γ-GTP
IU/L
50
40
30
20
10
0
Cont 1 d 3 d 5 d 7 d 9 d 12 d
E
T. Bil
mg/dL
0.08
0.06
0.04
0.02
0
Cont 1 d 3 d 5 d 7 d 9 d 12 d

Fig. 1

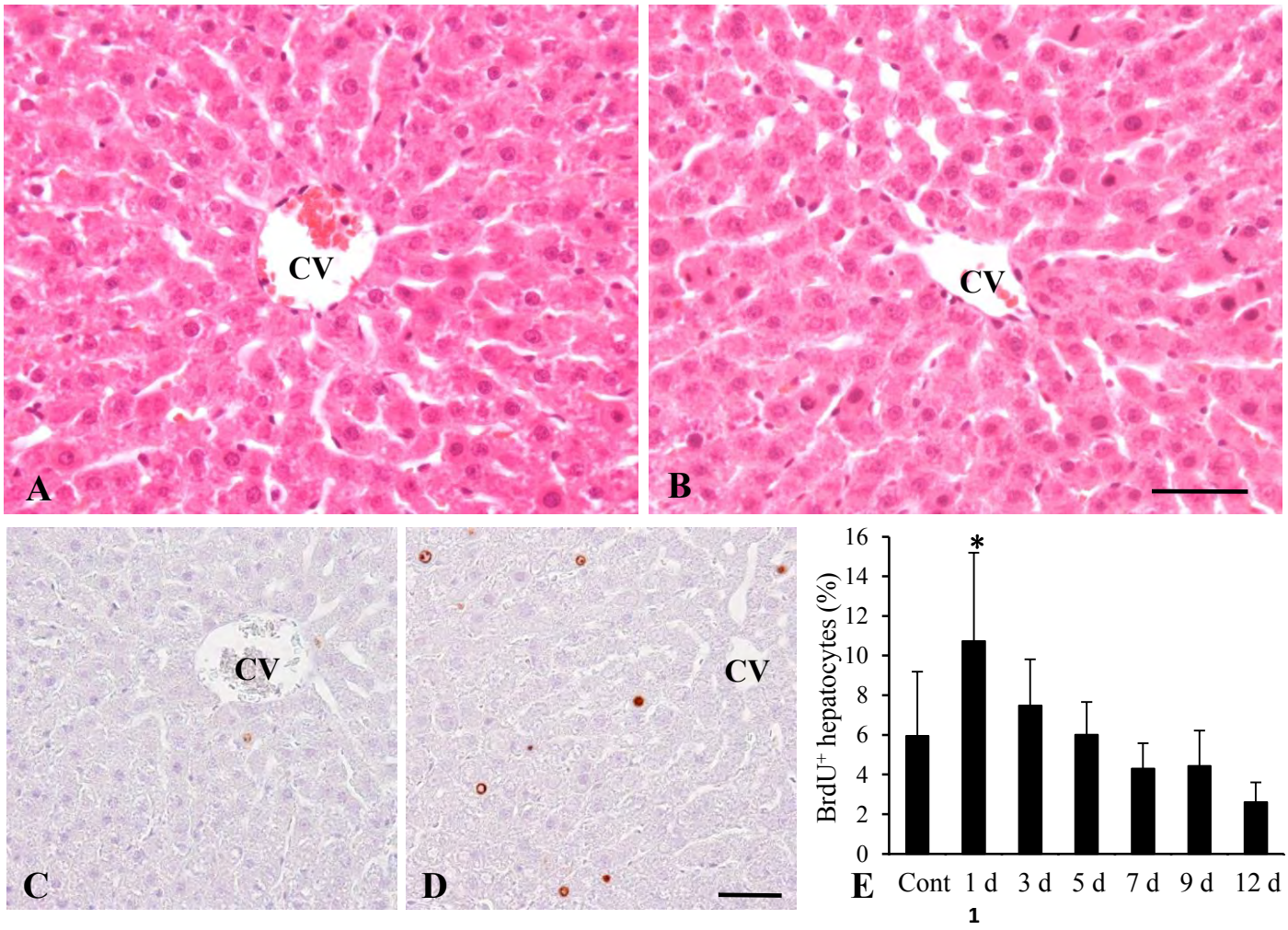
A
CV
B
CV
C
CV
D
CV
E
BrdU+ hepatocytes (%)
16
14
12
10
8
6
4
2
0
*
Cont
1 d
3 d
5 d
7 d
9 d
12 d

Fig. 2

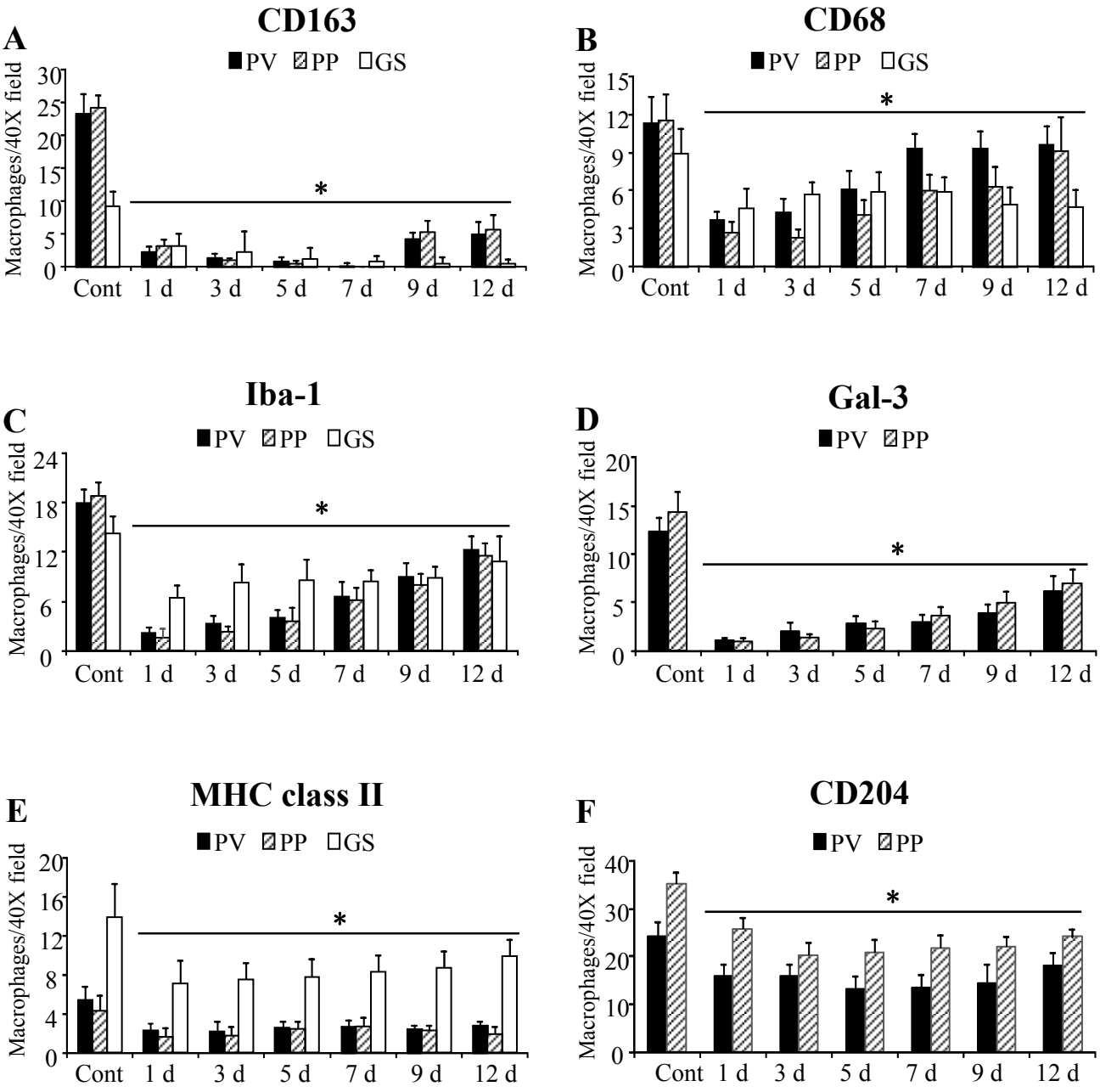
A
CD163
PV PP GS
Macrophages/40X field
30
25
20
15
10
5
0
*
Cont 1 d 3 d 5 d 7 d 9 d 12 d
B
CD68
PV PP GS
Macrophages/40X field
15
12
9
6
3
0
*
Cont 1 d 3 d 5 d 7 d 9 d 12 d
C
Iba-1
PV PP GS
Macrophages/40X field
24
18
12
6
0
*
Cont 1 d 3 d 5 d 7 d 9 d 12 d
D
Gal-3
PV PP
Macrophages/40X field
20
15
10
5
0
*
Cont 1 d 3 d 5 d 7 d 9 d 12 d
E
MHC class II
PV PP GS
Macrophages/40X field
20
16
12
8
4
0
*
Cont 1 d 3 d 5 d 7 d 9 d 12 d
F
CD204
PV PP
Macrophages/40X field
40
30
20
10
0
*
Cont 1 d 3 d 5 d 7 d 9 d 12 d

Fig. 3

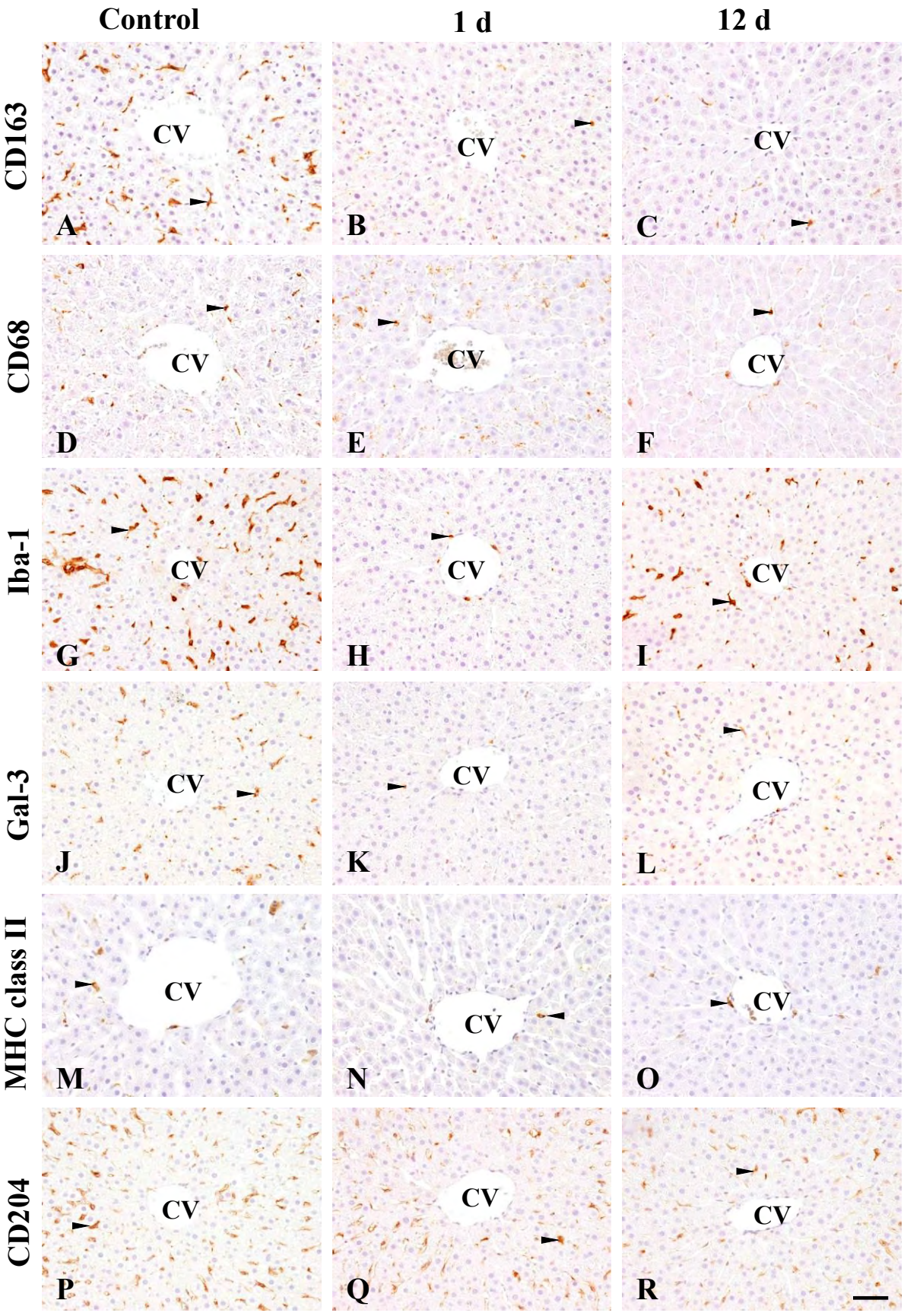
Control
1 d
12 d
CD163
CD68
Iba-1
Gal-3
MHC class II
CD204
CV
A
B
C
D
E
F
G
H
I
J
K
L
M
N
O
P
Q
R

Fig. 4

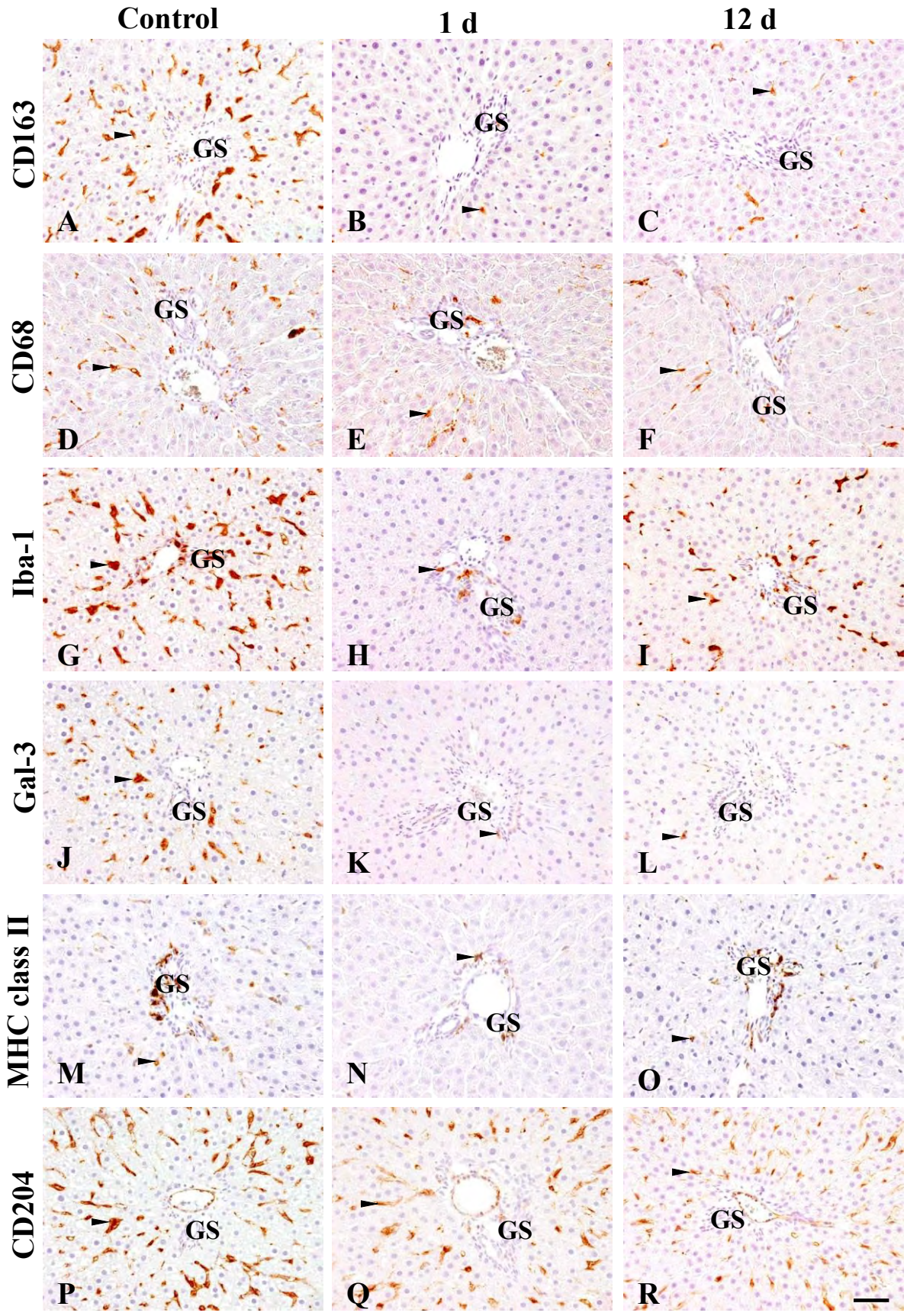
Control
1 d
12 d
CD163
CD68
Iba-1
Gal-3
MHC class II
CD204
GS
A
B
C
D
E
F
G
H
I
J
K
L
M
N
O
P
Q
R

Fig. 5

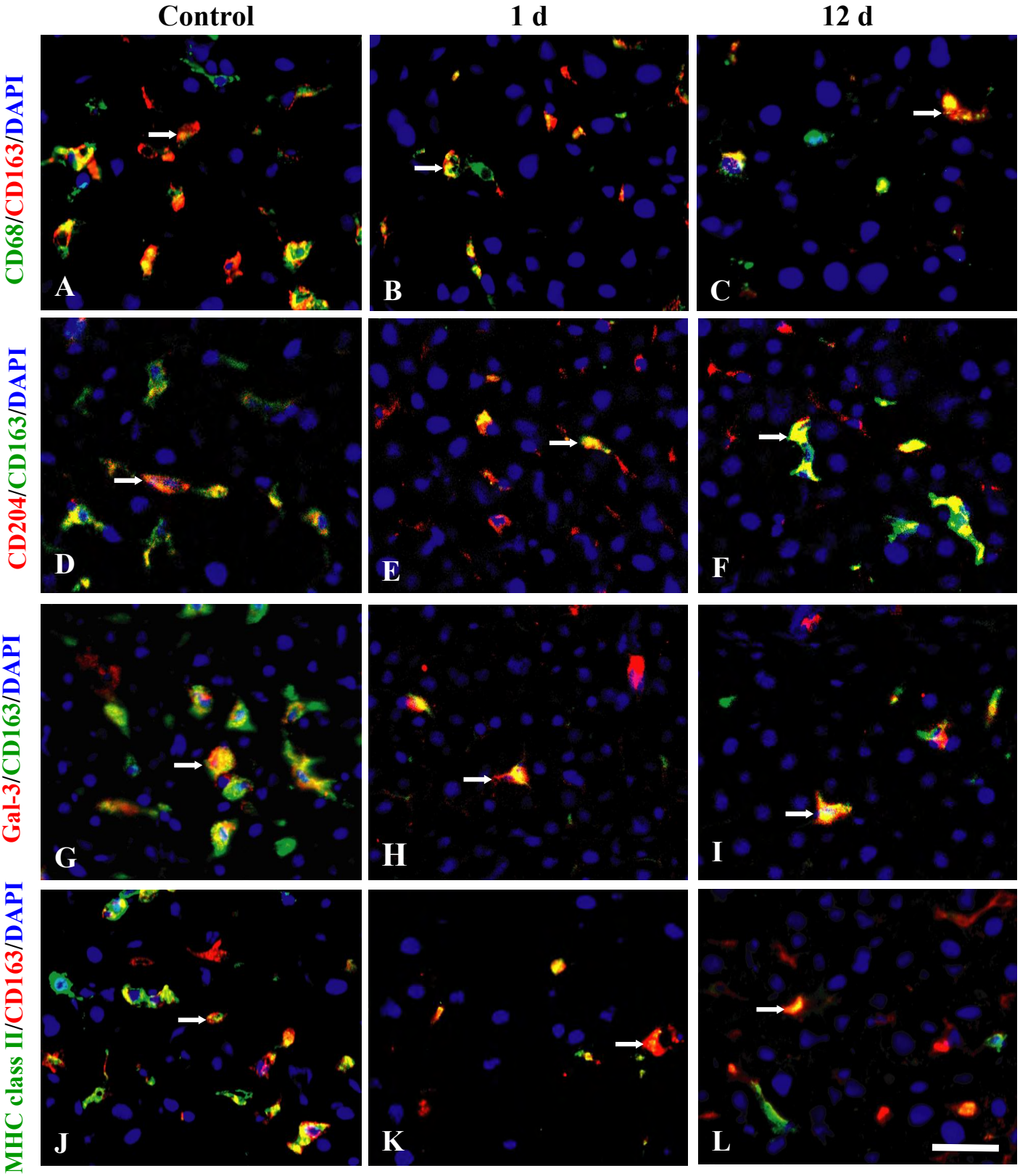
Control
1 d
12 d
CD68/CD163/DAPI
CD204/CD163/DAPI
Gal-3/CD163/DAPI
MHC class II/CD163/DAPI
A
B
C
D
E
F
G
H
I
J
K
L

Fig. 6

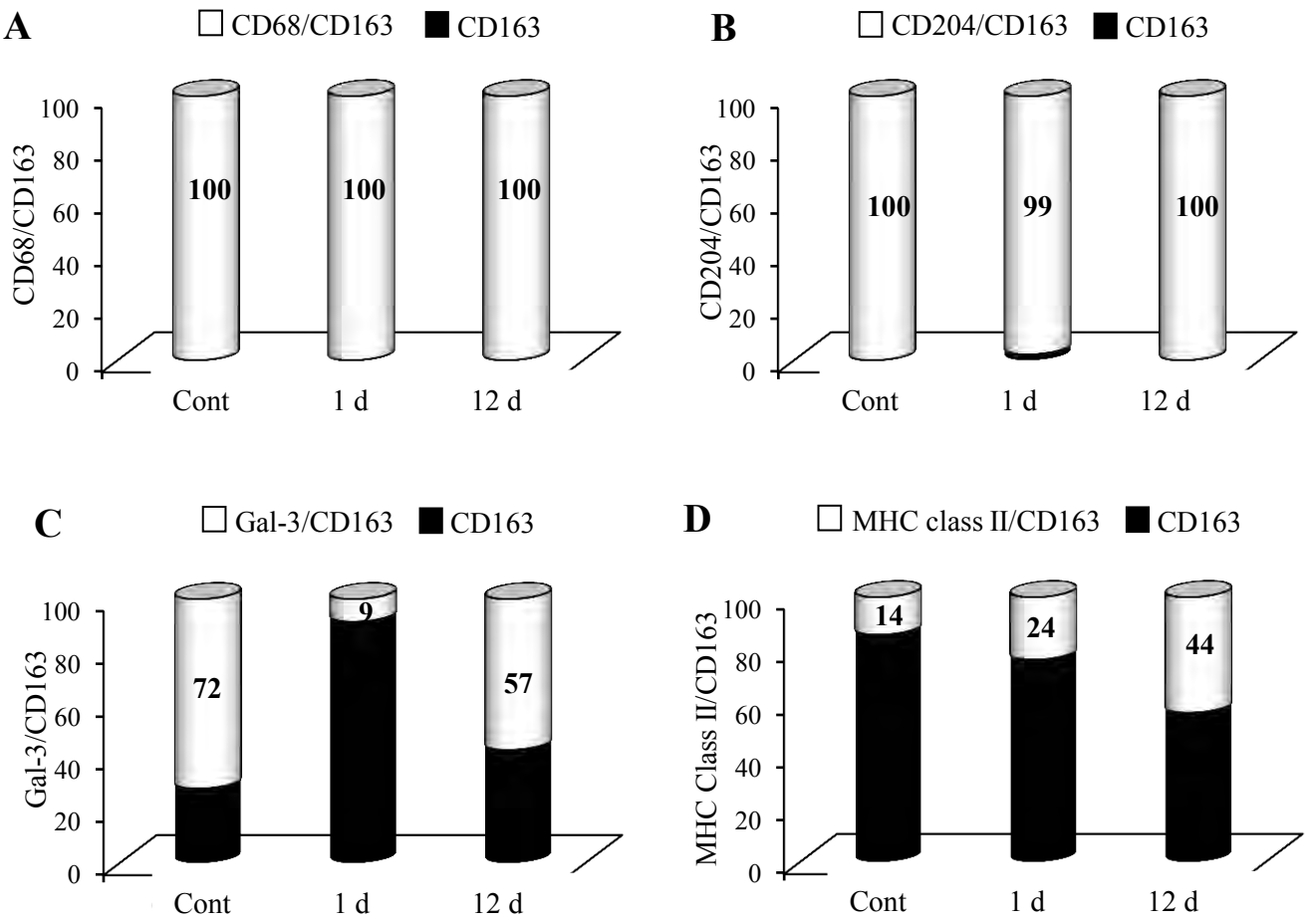
A
CD68/CD163
CD163
CD68/CD163
100
80
60
40
20
0
100
100
100
Cont
1 d
12 d
B
CD204/CD163
CD163
CD204/CD163
100
80
60
40
20
0
100
99
100
Cont
1 d
12 d
C
Gal-3/CD163
CD163
Gal-3/CD163
100
80
60
40
20
0
72
9
57
Cont
1 d
12 d
D
MHC class II/CD163
CD163
MHC Class II/CD163
100
80
60
40
20
0
14
24
44
Cont
1 d
12 d

Fig. 7

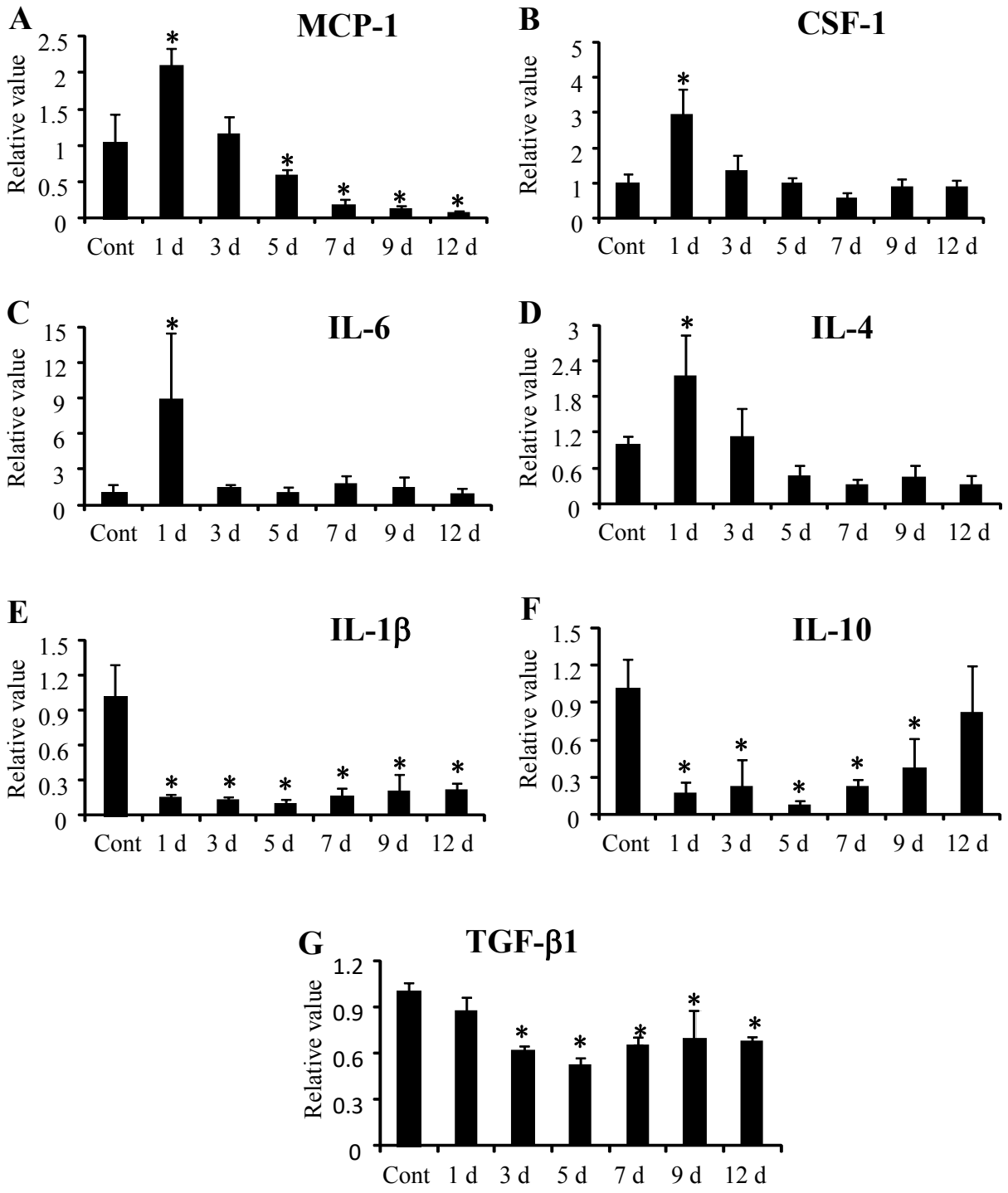
A
MCP-1
Relative value
2.5
2
1.5
1
0.5
0
Cont 1 d 3 d 5 d 7 d 9 d 12 d
B
CSF-1
Relative value
5
4
3
2
1
0
Cont 1 d 3 d 5 d 7 d 9 d 12 d
C
IL-6
Relative value
15
12
9
6
3
0
Cont 1 d 3 d 5 d 7 d 9 d 12 d
D
IL-4
Relative value
3
2.4
1.8
1.2
0.6
0
Cont 1 d 3 d 5 d 7 d 9 d 12 d
E
IL-1β
Relative value
1.5
1.2
0.9
0.6
0.3
0
Cont 1 d 3 d 5 d 7 d 9 d 12 d
F
IL-10
Relative value
1.5
1.2
0.9
0.6
0.3
0
Cont 1 d 3 d 5 d 7 d 9 d 12 d
G
TGF-β1
Relative value
1.2
0.9
0.6
0.3
0
Cont 1 d 3 d 5 d 7 d 9 d 12 d

Fig. 8

Chapter 2

Characterization of hepatic macrophages and autophagy under lipopolysaccharide (LPS) treatment in rats

Section I

Effects of low dose of LPS on hepatic macrophages and regulatory inflammatory factors in clodronate-treated rats

Introduction

Hepatic macrophages play a vital role in inflammation and immune responses in the liver. Although Kupffer cells, which express CD163 of hemoglobin-haptoglobin complex receptors (Polfliet et al., 2006), are the majority of liver macrophages, liver harbours different populations of hepatic macrophages. They can be identified by their immunophenotypic characteristics using specific antibodies (Golbar et al., 2012). For example, CD68 is a glycoprotein on lysosomal membranes, particularly on the phagosomes of macrophages and thus, the expression level implies enhanced phagocytosis (Zhu et al., 2012; Damoiseaux et al., 1994). MHC class II is expressed on mature dendritic cells and activated macrophages (Ide et al., 2005; Yamashiro et al., 1994), being related to the activation of T cells and subsequent induction of other macrophages (Perrigoue et al., 2009). Galectin-3 (Gal-3) is a member of the galectin family of mammalian proteins and expressed on the surface of activated macrophages, which may be related to fibrogenesis (Dong and Hughes, 1997; Barondes et al., 1994). Iba-1 has actin-cross linking activity and may act in membrane ruffling and phagocytosis of activated macrophages (Sasaki et al., 2001; Ohsawa et al., 2000). CD204 expression is related to lipid metabolism in macrophages via scavenger receptors (Greaves et al., 1998). Therefore, hepatic macrophages may show heterogeneous functions depending on microenvironments. They actively participate not only in maintaining the liver homeostasis but also in the development of hepatic lesions.

Hepatic macrophages respond to a variety of classical biological factors including bacterial toxins. Lipopolysaccharide (LPS), a potent inducer of inflammation, is the major

structural component of gram-negative bacterial cell wall. LPS elicits a wide variety of pathophysiological effects in liver. Large doses of LPS administration produce liver injury characterized by sinusoidal neutrophilia and midzonal hepatocellular necrosis (Yee et al., 2000). However, LPS itself is not hepatotoxic at low concentrations; rather, its ability to stimulate an inflammatory response may account for pathogenicity in liver (Ganey and Roth, 2001). In mammalian body, generally, a large number of gram-negative bacteria colonize in the intestine, and thus, the liver is continuously exposed to some amounts of LPS via the translocation from the intestinal lumen into portal venous blood (Ganey and Roth, 2001). Due to the location of Kupffer cells in liver sinusoids, they are the initial macrophages, which are exposed to gastrointestinal-derived bacteria and bacterial products including LPS. Kupffer cells phagocytize LPS from the circulation and remove most of the LPS (Martinez and Gordon, 2014). LPS-stimulated Kupffer cells via Toll-like-receptors (TLRs) lead to the production of inflammatory mediators (Vodovotoz et al., 2001; Means et al., 2000). This activated state of macrophages acts as a cofactor in the pathogenesis of liver injury. Therefore, the precise roles of hepatic macrophages in liver homeostasis and pathological lesions should be investigated in detailed.

To better understand the definite roles of divergent macrophage populations in liver, selective depletion of macrophages by using a single intravenous injection of liposome-encapsulated dichloromethylene diphosphonate clodronate (CLD), a bisphosphaonate molecule, is used in studies on hepatopathology. CLD causes selective killing of macrophages by intracellular release of the calcium-binding drug from the liposomes upon phagocytosis (Bakker et al., 1998; Van Rooijen et al., 1996). The present study was undertaken to clarify the pathophysiological effect of low dose of LPS on hepatic macrophage populations and liver specific regulatory inflammatory factors in normal and hepatic macrophage-depleted rat livers by CLD.

Materials and methods

Animals and experimental procedures

Forty eight 5-week-old male F344 rats purchased from Charles River Japan (Hino, Shiga, Japan) were used in this experiment. Rats were maintained in a room at 21±3°C with a 12 h light-dark cycle, and fed a standard diet for rats (DC-8, CLEA Japan, Tokyo, Japan) and supplied with tap water *ad libitum*. After one-week acclimatization, the rats were randomly divided into two groups: CLD-treated macrophage-depleted group (CLD + LPS; 24 rats) and vehicle liposome (Lipo)-treated control group (Lipo + LPS; 24 rats). A liposome-encapsulated CLD (5 mg/ml suspension; Foundation Clodronate Liposomes, Amsterdam, the Netherlands) at the dose of 50 mg/kg body weight (Pervin et al., 2016) or Lipo was injected intravenously once via tail vein in CLD + LPS and Lipo + LPS rats, respectively. After 24 h of CLD or Lipo administration, LPS was injected intraperitoneally at the dose of 0.1 mg/kg body weight (*Escherechia coli* 055:B5, Sigma-Aldrich, St Louis, MO, USA) in 20 rats of each group. Four rats in each group were euthanized by exsanguination under deep isoflurane anesthesia on LPS post-injection (PI) at 6, 12, 24, 48 and 72 h. The remaining four rats from each group were injected with sterile 0.9% NaCl (CLD + saline or Lipo + saline) instead of LPS and sacrificed immediately after injection (0 h). At necropsy, blood samples were collected from abdominal aorta and separated sera were subjected to biochemical assay for aspartate transaminase (AST), alanine transaminase (ALT), alkaline phosphatase (ALP) and γ-glutamyl transferase (γ-GTP) by SRL Inc. (Tokyo, Japan). The animal experiments were conducted under the institutional guidelines approved by the ethical committee of Osaka Prefecture University for the Care and Use of Experimental Animals.

Histopathology and immunohistochemistry

Liver tissues from the left lateral lobe were collected and immediately fixed in 10% neutral buffered formalin (NBF) and periodate-lysine-paraformaldehyde (PLP) solution processed by PLP-AMeX (acetone, methyl benzoate and xylene) method (Pervin et al., 2016). NBF-fixed tissues were dehydrated and embedded in paraffin and sectioned at 3-4 μm in thickness. The deparaffinized sections were stained with hematoxylin and eosin (HE) for histopathological examination.

Tissue sections fixed in PLP were deparaffinized and used in immunohistochemistry for CD163, CD68, Gal-3, Iba-1, CD204 and MHC class II staining. After pretreatment, tissue sections were stained by the Histostainer (Histofine, Nichirei Bioscience Inc., Tokyo, Japan). Briefly, sections were incubated with 5% skimmed milk for 10 min, followed by 1 h incubation with primary antibodies. Details of antibodies are listed in Table 1. After treatment with 3% H_2O_2 for 15 min, horseradish peroxidase-conjugated secondary antibody (Histofine simple stain MAX PO®; Nichirei Inc., Tokyo, Japan) was applied for 30 min. Then, they were incubated with 3, 3'-diaminobenzidine (DAB) (Nichirei Inc., Tokyo, Japan) for 5 min. Sections were counterstained with hematoxylin for 1 min. For negative controls, tissue sections were treated with mouse or rabbit non-immunized serum instead of the primary antibody. Cells expressing CD163, CD68, MHC class II, Iba-1, Gal-3 and CD204 were counted per 40X field in randomly selected five areas in the perivenular (PV) and periportal (PP) areas including the Glisson's sheath (GS) of the liver.

Double immunofluorescence staining

Fresh frozen liver sections from Lipo + LPS and CLD + LPS rats on PI 0 h, 6 h, 24 h and 48 h were used in double immunofluorescence using CD163 in combination with CD68, Gal-3, MHC class II and CD204. Briefly, after fixation in cold acetone: methanol (1:1) for 10 min at 4°C, the sections were incubated with 10% normal goat serum for 30 min at room temperature followed by reaction with the primary antibody overnight at 4°C. For CD163/Gal-3 combination, both primary antibodies were used together for overnight at 4°C. After rinsing with phosphate buffered saline (PBS), the sections were incubated for 45 min at room temperature with the secondary antibody goat anti-mouse IgG-conjugated with Alexa 568 (Invitrogen, Carlsbad, CA, USA) for CD163 and CD204; and goat anti-rabbit IgG-conjugated with Alexa 488 (Invitrogen, Carlsbad, CA, USA) for Gal-3. Then, the sections were incubated with the second primary antibody labeled with fluorescent dye-conjugated secondary antibody: Alexa 488-labeled CD163 (AbD Serotec, Oxford, UK) for CD163/CD204; Alexa 488-labeled MHC class II (AbD Serotec,Oxford, UK) for CD163/MHC class II; Alexa 488-labeled CD68 (AbD Serotec, Oxford, UK) for

CD68/CD163. The sections were visualized with Vectashield™ mounting medium containing 4', 6-diamidino-2-phenylindole (DAPI) (Vector Laboratories Inc., Burlingame, CA, USA) for nuclear staining, and analyzed by a virtual slide scanner (VS-120, Olympus, Tokyo, Japan).

Real time reverse transcriptase-polymerase chain reaction (RT-PCR)

Liver samples from the left median lobe were immediately immersed in RNAlater® (Qiagen GmbH, Hilden, Germany) overnight at 4°C and stored at −80°C until use. Total RNA was extracted from liver tissues by using an SV total RNA isolation system (Promega, Madison, WI, USA) according to the manufacturer's instructions. Two and half μg of total extracted RNA was reverse-transcribed with Superscript VILO reverse transcriptase (Life Technologies, CA, USA). Real time PCR was performed using TaqMan gene expression assays (Life Technologies, Carlsbad, CA, USA) in a PikoReal Real-Time 96 PCR System (Thermo Scientific, CA, Massachusetts, USA). The TaqMan probes specific for the cytokines used were as follows (Assay IDs): monocyte chemoattractant protein-1 (MCP-1), Rn00580555_m1; interleukin-1β (IL-1β), Rn00580432_m1; colony stimulating factor-1 (for macrophages) (CSF-1), Rn00696122_m1; interferon-γ (IFN-γ), Rn00594078_m1; tumor necrosis factor-α (TNF-α), Rn01525859_g1; transforming growth factor-β1 (TGF-β1), Rn00572010_m1; interleukin-4 (IL-4), Rn01456866_m1; interleukin-6 (IL-6), Rn01410330_m1; interleukin-10 (IL-10), Rn00563409_m1; toll like receptor-2 (TLR-2); Rn02133647_s1; toll like receptor-4 (TLR-4), Rn00569848_m1 and β-actin, Rn00667869_m1. The mRNA expression was normalized against the expression of β-actin mRNA as the internal control. The data were analyzed using the comparative C_t method ($^{\Delta\Delta}C_t$ method).

Statistical evaluation

Data obtained were expressed as mean ± standard deviation (SD). Statistical analysis was performed using Tukey-Kramer test. Significance was considered at $P < 0.05$.

Results

Histopathology of liver and serum biochemistry

There was no detectable gross lesion in livers of Lipo + LPS and CLD + LPS rats. In HE-stained sections, normal histoarchitectures of livers were seen without any hepatic injury in both groups (Fig. 1A-F); histological evaluation revealed no hepatic injury even after LPS exposure at the dose used in this study. Administration of low dose of LPS did not change serum hepatic enzymes such as AST, ALP and γ-GTP in Lipo + LPS rats (Fig. 2A, C, D); however, the ALT value was initially increased on PI 6 h after LPS injection in this group with a statistical significance (Fig. 2B). On the other hand, in CLD + LPS rats, administration of low dose of LPS did not change AST and ALT levels in comparison with 0 h controls (Fig. 2A, B); the values of ALP and γ-GTP were significantly increased on 72 h or 24 h to 72 h, respectively (Fig. 2C, D). In addition, the values of AST, ALT, ALP and γ-GTP were significantly increased in all observation points including 0 h in CLD + LPS rats as compared with those in Lipo + LPS rats (Fig. 2A-D), which might be due to the depletion of hepatic macrophages as reported previously (Pervin et al., 2016).

Kinetics of hepatic macrophages in rat livers

The kinetics of hepatic macrophages reacting to CD163, CD68, Gal-3, Iba-1, CD204 and MHC class II in the PV and PP areas is shown in Figs. 3A-F and 4A-F, respectively and representative findings are presented in Fig. 5A-H for the PV areas and Figs. 5I-P and 6A-X for the PP including the GS areas.

$CD163^+$ cells

CD163 antigen is mainly expressed on the cell surface of resident macrophages (Kupffer cells), located mainly along sinusoids in the PV and PP areas (Pervin et al., 2016). In Lipo + LPS rats, $CD163^+$ Kupffer cells were significantly increased at PI 6 h to 72 h as compared with those of 0 h controls (Figs. 3A and 4A) both in PV and PP areas (Fig. 5A-D, I-L). On the contrary, LPS injection did not show any effect on $CD163^+$ cells in

macrophage-depleted CLD + LPS rats (Figs. 3A, 4A and 5E-H, M-P). In addition, $CD163^+$ Kupffer cells were significantly decreased in CLD + LPS rats at all examination points as compared with those of Lipo + LPS rats (Figs. 3A and 4A). In short, these findings indicated that LPS is a potential Kupffer cell activator in normal condition.

$CD68^+$, $Iba\text{-}1^+$, $Gal\text{-}3^+$ and $CD204^+$ cells

Exposure of LPS resulted in a significant increase of $CD68^+$, $Gal\text{-}3^+$, $Iba\text{-}1^+$ and $CD204^+$ hepatic macrophages both in PV and PP areas of Lipo + LPS rats (Figs. 3B-E and 4B-E). Particularly, the numbers of $CD68^+$ macrophages were markedly increased at PI 6 h and 12 h in PV areas, whereas the numbers remained increased up to 24 h in PP areas and then, returned to normal level as seen in 0 h controls (Figs. 3B, 4B and 6A-D). $Gal\text{-}3^+$ macrophages were significantly increased immediately within 6 h to 12 h after LPS exposure in PV areas and at 6 h in PP areas (Figs. 3C and 4C). The macrophages reacting to Iba-1 showed significant increase at 6 h, 12 h and 72 h after LPS administration in PV areas, which remained increased in all observation points in PP areas (Figs. 3D, 4D and 6I-L). The number of $CD204^+$ macrophages showed kinetics similar to that of $CD163^+$ macrophages. $CD204^+$ macrophages were significantly increased throughout the observation periods as compared with those of 0 h controls both in PV and PP areas (Figs. 3E and 4E).

On the other hand, these hepatic macrophages were not changed in CLD + LPS rats after LPS treatment in contrast to those of 0 h controls (Figs. 3B-E, 4B-E and 6E-H, M-P). In addition, $CD68^+$, $Gal\text{-}3^+$, $Iba\text{-}1^+$ and $CD204^+$ hepatic macrophages were significantly lower in CLD + LPS rats at all examination points as compared with those of Lipo + LPS rats (Figs. 3B-E and 4B-E), indicating that LPS is a potent macrophage activator in normal rat livers rather than macrophage-depleted livers, as seen in $CD163^+$ cells mentioned above.

MHC class II^+ cells

In the parenchyma of liver, the numbers of MHC class II^+ cells were lower in comparison with other hepatic macrophages reacting to CD163, CD68, Iba-1, Gal-3 and

CD204. MHC class II^+ cells were mainly located in the GS (Fig. 6Q-X), indicative of the antigen presenting dendritic cells (Pervin et al., 2016; Golbar et al., 2012). In Lipo + LPS rats, LPS treatment significantly increased MHC class II^+ macrophages initially at 6 h in PV area and at 6 h to 12 h in PP area as compared with those of 0 h controls (Figs. 3F, 4F and 6Q-T). Interestingly, thereafter, the number of MHC class II^+ macrophages was significantly decreased at 24 h to 72 h as compared with that of 0 h controls both in PV and PP areas (Figs. 3F and 4F). In agreement with other hepatic macrophages, no significant changes were seen in CLD + LPS rats (Figs. 3F, 4F and 6U-X). In addition, between these groups, MHC class II^+ cells were significantly decreased in CLD + LPS rats at PI 6 h as compared with those of Lipo + LPS rats. Furthermore, unlike other macrophage markers, a significant increase in MHC class II^+ cells was observed in PV areas of CLD + LPS rats at PI 24 h as compared with those of Lipo + LPS rats (Figs. 3F and 4F).

Immunophenotypes of $CD163^+$ Kupffer cells

To find out the functional properties of Kupffer cells, double immunofluorescence for $CD163^+$ cells with antibodies against CD68, MHC class II, Gal-3, or CD204 were done in the liver of Lipo + LPS and CLD + LPS rats at PI 0 h, 6 h, 24 h and 48 h.

Almost all $CD68^+$ cells reacted simultaneously to CD163 in Lipo + LPS rats at all examination points, whereas 70% of $CD68^+$ cells reacted simultaneously to CD163 in CLD + LPS rats (Fig. 7A, C, E). In Lipo + LPS rats, 80-90% of MHC class II^+ cells showed a positive reaction to CD163; in CLD + LPS rats, the percentage of MHC class II^+CD163^+ cells were decreased (40-60%) at different examination points (Fig.7B, D, F). Eighty-two % to 87% Gal-3^+ cells showed a positive reaction to CD163 in Lipo + LPS rats; the $CD163^+$Gal-3^+cell number was decreased (2-12%) in CLD + LPS rats at different examination points (Fig. 7G). Almost all $CD204^+$ cells coexpressed CD163 in livers of both groups (Fig. 7H). The number of macrophages reacting to CD68, Gal-3, MHC class II and CD204 was smaller than that of $CD163^+$ cells, indicating that $CD163^+$ cells do not always express antigens of CD68, Gal-3, MHC class II or CD204. However, the coexpression ratios of $CD163^+$ Kupffer cells with other macrophage markers were lower in

CLD + LPS rats in comparison with those in Lipo + LPS rats, indicating that LPS treatment may increase Kupffer cell activity in normal rat livers.

Expressions of M1/M2 macrophage-related factors

At mRNA level, expressions of M1 macrophage-related factors such as MCP-1, IL-1β, IL-6, TNF-α and TLR-2 were abruptly increased as early as PI 6 h in Lipo + LPS rats as compared with those of 0 h controls, with a statistical significance (Fig. 8A-E). On the other hand, these factors were not changed in CLD + LPS rats (Fig. 8A-E). Additionally, in comparison between these groups, the mRNAs of IL-1β, IL-6, TNF-α and TLR-2 were significantly decreased at PI 6 h in CLD + LPS rats as compared with those of Lipo + LPS rats (Fig. 8A-E). Unlike other M1 macrophage-related factors, IFN-γ expression was significantly increased in CLD +LPS rats on PI 6 h, but no change was seen in Lipo + LPS rats. Between these groups, a significant higher expression in IFN-γ was seen in CLD + LPS rats at PI 6 h as compared with that of Lipo + LPS rats (Fig. 8F). In addition, TLR-4 mRNA was not changed in Lipo + LPS or CLD + LPS rats; however, the expression was significantly decreased in all observation points including 0 h in CLD + LPS rats as compared with those in Lipo + LPS rats (Fig. 8G).

Expression of M2 macrophage-related factors such as IL-4 (Fig. 9A) and CSF-1 (Fig. 9B) did not show any significant change in Lipo + LPS rats after LPS treatment. Interestingly, in CLD + LPS rats, IL-4 mRNA was significantly elevated at PI 6 h (Fig. 9A); CSF-1 mRNA was also increased initially at 6 h, but significantly decreased later at PI 24 h to 72 h (Fig. 9B). In comparison between these groups, IL-4 and CSF-1 mRNAs were significantly increased in CLD + LPS rats in contrast to those in Lipo + LPS rats at 6 h (Fig. 9A, B). IL-10 is a potent M2 macrophage-related factor, and showed mRNA expressions similar to M1 macrophage-related factors; IL-10 mRNA was significantly increased at PI 6 h in Lipo + LPS rats, which was reduced under macrophage depletion condition in CLD + LPS rats (Fig. 9C). There was no significant change in TGF-β1 mRNA expression after LPS treatment in Lipo + LPS or CLD + LPS rats; however, on 12 h, a significant difference was seen between these groups (Fig. 9D).

Discussion

Effects of LPS on liver histopathology and serum biochemistry

Hepatic macrophages play important roles in liver homeostasis as well as liver pathology through phagocytosis, cytokine/growth factor production, and antigen presentation (Ju and Tacke, 2016; Schumann et al., 2000). Systemic administration of LPS at high dose leads to liver injury in rats. Hepatic macrophages, especially Kupffer cells, rapidly act to remove LPS from circulation. However, in patients with liver failure, Kupffer cells could not properly clear gut-derived LPS, resulting in severe endotoxemia. This endogenous endotoxemia may contribute to the pathogenesis of concomitant exposure of hepatotoxicants in the liver. In the present study, low dose of LPS (0.1 mg/kg body weight) did not produce any histopathological alterations in the liver either in liposome-treated control rats (Lipo + LPS rats) or CLD-treated hepatic macrophage-depleted rats (CLD + LPS rats). Consistently, no change in serum hepatic enzymes was seen after exposure of low dose of LPS in Lipo + LPS rats, excluding ALT value which showed an increased level at early PI 6 h; the ALT finding might be related to the effects of LPS; however, the other hepatic enzymes remained unchanged throughout the observation periods. These findings indicated that the administration of present LPS dose (0.1 mg/kg body weight) is non-injurious to liver. On the contrary, the increased value of ALP at PI 72 h and γ-GTP at 24 h to 72 h in CLD + LPS rats indicated that CLD pretreatment might be induced more susceptible condition to rat livers as well as biliary injury, because of hepatic macrophage depletion. In addition, hepatic enzymes such as AST, ALT, ALP and γ-GTP were significantly increased in CLD-treated macrophage-depleted (CLD + LPS) rats including 0 h before LPS injection; these increased values of hepatic enzymes might be also related to depletion of Kupffer cells, because Kupffer cells have roles in liver homeostasis via clearance of such enzymes (Pervin et al., 2016; Radi et al., 2011).

Effects of LPS on different immunophenotypes of hepatic macrophages

Macrophages are heterogenous cell populations, belonging to the mononuclear phagocyte system. Hepatic macrophages display different immunophenotypes and may exert distinct functions in hepatotoxicity (Yamate et al., 2000; Takahashi et al., 1996). Based on the type 1 or type 2 helper T-cell polarization concept, macrophages appearing in pathological settings are recently grouped as classically activated macrophages (M1) and alternatively activated macrophages (M2) (Yamate et al., 2016; Martinez and Gordon 2014; Sica and Mantovani, 2012). CD68, Iba-1 and MHC class II-expressing macrophages are considered as M1 macrophages, whereas M2 macrophages work through CD163, Gal-3 and CD204 expressions (Yamate et al., 2016; Wijesundera et al., 2014b; Mantovani et al., 2002). The appearance of different hepatic macrophages in hepatic lesions may reflect their important roles in hepatotoxicity (Ju and Tacke, 2016; Yamate et al., 2000). In this study, CLD pretreatment significantly reduced the macrophage numbers detectable by various markers (CD163, CD68, Gal-3, Iba-1, CD204 and MHC class II) throughout the observation periods in CLD + LPS rats as compared with those in Lipo + LPS rats, indicating that CLD effectively depleted both M1 and M2 macrophages (Golbar et al., 2016; Pervin et al., 2016).

The LPS administration at low dose of 0.1 mg/kg body weight resulted in significant increase both in M1 macrophages (expressing CD68, Iba-1 and MHC class II) and M2 macrophages (expressing CD163, Gal-3 and CD204) in Lipo + LPS rats. However, LPS-mediated activation to hepatic macrophages varied with their immunophenotypical characteristics. M2 macrophages express CD163, of which antigen expression is regarded as Kupffer cells, and also co-express high levels of scavenger receptor molecule type A (CD204) (Gordon, 2003). In this study, the number of $CD163^+$ and $CD204^+$ macrophages was significantly increased at PI 6 h to 72 h both in PV and PP areas following LPS injection in Lipo + LPS rats, which might be related to the production of proinflammatory factors and phagocytosis (Polfliet et al., 2006; Fabreik et al., 2005). On the other hand, M1 macrophages expressing CD68, MHC class II and Iba-1 were activated immediately after LPS injection in Lipo + LPS rats. It is well known that M1 macrophages function mainly

in early inflammatory reactions with tissue destruction (Martinez et al., 2008). There was no difference in the increase of hepatic macrophages between the PV and PP areas following low dose of LPS injection in Lipo + LPS rats; however, the macrophages in PP area remained increased during observation period in contrast to those in PV area. Because macrophages present in PP areas are closer to intralobular blood vessels in the Glisson's sheath, they may be quickly activated in response to LPS. On the other hand, the hepatic macrophage populations were not changed in CLD-treated macrophage-depleted (CLD + LPS) rats after LPS treatment, indicating that LPS act as a potent macrophage activator in the presence of hepatic macrophages in rat livers, possibly via TLR-dependent activation pathway (Seki et al., 2007; Schwabe et al., 2006); this is supported by mRNA expressions of TLR-2, which was clearly increased in Lipo + LPS rats, but did not change in CLD + LPS rats. These findings suggest that TLRs work as a receptor for LPS and that Kupffer cells are the most sensitive to LPS via TLRs (Seki et al., 2007).

Phenotypic properties of $CD163^+$ Kupffer cells

Additionally, the author analyzed phenotypic properties of Kupffer cells, because macrophage polarizations are the major determinant of macrophage functions (Patel et al., 2012). In the present study, $CD163^+$ Kupffer cells located along the sinusoids reacted simultaneously to CD68, Gal-3, MHC class II or CD204 in livers of all rats; however, the expression levels of such antigens (CD68, Gal-3, Iba-1, MHC class II or CD204) in Kupffer cells was much lower in CLD + LPS rats in comparison with those in Lipo + LPS rats after LPS treatment. Therefore, LPS enhanced Kupffer cell immunoexpression in normal rat liver in Lipo + LPS rats; however, LPS did not effect repopulating Kupffer cells in livers of CLD + LPS rats. These findings may indicate that repopulating hepatic macrophages after CLD treatment are functionally less active.

Effects of LPS on regulatory inflammatory factors

Kupffer cells are important initiator of inflammatory responses to liver injury by producing M1 macrophage-related proinflammatory factors (Ju and Tacke, 2016; Laskin et al., 2011; Soehnlein and Lindbom, 2010). In the present study, after LPS injection at low

dose, proinflammatory M1 macrophage-related factors (IL-1β, IL-6, TNF-α, MCP1) were abruptly increased in Lipo + LPS rats at early stage, indicating the pivotal role of Kupffer cells in the production of proinflammatory cytokines (Zizzo et al., 2012; Soehnlein and Lindbom, 2010; Mori et al., 2009). Increased level of TLR-2 may promote proinflammatory signaling pathway (Schwabe et al., 2006). In addition, after LPS injection at low dose, M1 macrophage-related factors were decreased in CLD + LPS rats in comparison with those in Lipo + LPS rats, indicating that these proinflammatory factors are major source of hepatic macrophages. Therefore, macrophage-depleted liver condition in CLD + LPS rats may be more sensitive to development of hepatic lesions in the concomitant exposure of hepatotoxin. Recently, it is reported that hepatic macrophage depletion enhanced the thioacetamide-induced liver injury in rats with the prolonged hepatocyte coagulation necrosis (Golbar et al., 2016). The action of M1 macrophages is regulated by M2 macrophages, which are primarily involved in down-regulation of inflammation to recover the hepatic lesions (Laskin et al., 2011; Martinez et al., 2008). M2 macrophages, which can release anti-inflammatory cytokines (IL-4 and IL-10), contribute to the resolution of inflammation by phagocytizing cell debris and producing growth factors (TGF-β1) important in tissue remodeling (Novak and Koh, 2013; La Flamme et al., 2012; Martinez, 2011). In this study, M2 macrophage-related factors (IL-4 and CSF-1) were significantly increased in CLD + LPS rats and did not show significant changes in Lipo + LPS rats after LPS treatment. These findings indicate that liver cells other than Kupffer cells also play an important role in providing anti-inflammatory milieu during liver homeostasis.

In conclusion, the present study showed that LPS can activate hepatic macrophages with different immunophenotypes in rat liver without showing liver lesions, and did not effect on repopulating hepatic macrophages. LPS at low dose also effected potentially liver microenvironments by the production of inflammatory mediators, which may enhance or suppress the liver injury. Therefore, the present findings would provide the baseline information for evaluating liver injury, particularly in hepatic macrophage-based hepatotoxicity.

Summary

Hepatic macrophages play a central role in maintaining liver homeostasis and pathogenesis of liver injury. Here, the author investigated the pathophysiological significance in appearance of hepatic macrophages and expression of regulatory inflammatory factors in normal and hepatic macrophage-depleted rat livers using low dose of lipopolysaccharide (LPS). Male F344 rats were pretreated with clodronate (CLD; 50 mg/kg body weight, intravenously) (CLD + LPS rats) or vehicle liposome (Lipo) (Lipo + LPS rats) 24 h before LPS injection (0.1 mg/kg body weight, intraperitoneally) or saline. Low dose of LPS did not alter histoarchitectures of the liver, and changes on serum hepatic enzymes (AST, ALP, ALT and γ-GTP) were not seen. The kinetics of M1 macrophages (expressing CD68, Iba-1, MHC class II) and M2 macrophages (expressing CD163, Gal-3 and CD204) showed stimulatory effects to LPS in Lipo + LPS rats with increased numbers, and effects on repopulating Kupffer cells were not seen in CLD + LPS rats. M1 macrophage-related factors (IL-1β, IL-6, TNF-α and MCP-1) were dramatically increased at 6 h after LPS exposure in Lipo + LPS rats, which was attenuated by macrophage depletion in CLD + LPS rats. On the contrary, significant elevation of M2 macrophage-related factors (IL-4 and CSF-1) were seen in CLD + LPS rats, but no change was seen in Lipo + LPS rats. These results indicate that low dose of LPS used herein can activate the hepatic macrophages in rat liver without hepatic lesion and did not effect repopulating hepatic macrophages; furthermore, the LPS administration can effect potentially liver microenvironments by the production of inflammatory mediators. Therefore, the present findings would provide a significant insight into the development of macrophage-based hepatopathology.

Table 1. Details of antibodies used for the immunohistochemistry and immunofluorescence.

Antibody	Clone	Type	Dilution	Pretreatment	Source
CD163	ED2	Mouse monoclonal	1/300	100µg/ml Proteinase K, 10 min	AbD Serotec, Oxford, UK
CD68	ED1	Mouse monoclonal	1/500	Microwaving in citrate buffer, 20 min	AbD Serotec, Oxford, UK
Iba-1	-	Rabbit polyclonal	1/1000	Microwaving in citrate buffer, 20 min	Wako Pure Chemical Industries, Osaka, Japan
MHC class II	OX6	Mouse monoclonal	1/1000	Microwaving in citrate buffer, 20 min	AbD Serotec, Oxford, UK
Galectin-3 (Gal-3)	-	Rabbit polyclonal	1/500	Microwaving in citrate buffer, 20 min	Santa Cruz Biotechnology, Santa Cruz, CA, USA
CD204	SRA-E5	Mouse monoclonal	1/1000	Microwaving in citrate buffer, 20 min	Transgenic Inc., Kumamoto, Japan

Figure legends

Fig. 1. A-F: Histopathology of liver in liposome-treated control (Lipo + LPS) and hepatic macrophage-depleted (CLD + LPS) rats. No histopathological change of hepatic architecture is seen in both groups. h: hour, CV: central vein. Bar = 100 μm.

Fig. 2. A-D: Blood biochemical analyses in Lipo + LPS and CLD + LPS rats. Aspartate transaminase (AST) (A), alanine transaminase (ALT) (B), alkaline phosphatase (ALP) (C) and γ-glutamyl transferase (γ-GTP) (D). Tukey's test; *, $P<0.05$, significantly different from 0 h in Lipo + LPS and CLD + LPS rats; †, $P<0.05$, significantly different between Lipo + LPS and CLD + LPS rats at respective examination points. h: hour.

Fig. 3. The kinetics of macrophages reacting to CD163 (A), CD68 (B), Gal-3 (C), Iba-1 (D), CD204 (E) and MHC class II (F) in the perivenular area of the liver in Lipo + LPS (□) and CLD + LPS (■) rats. Tukey's test; *, $P<0.05$, significantly different from 0 h in Lipo + LPS and CLD + LPS rats; †, $P<0.05$, significantly different between Lipo + LPS and CLD + LPS rats at respective examination points. h: hour.

Fig. 4. The kinetics of macrophages reacting to CD163 (A), CD68 (B), Gal-3 (C), Iba-1 (D), CD204 (E) and MHC class II (F) in the periportal area of the liver in Lipo + LPS (□) and CLD + LPS (■) rats. Tukey's test; *, $P<0.05$, significantly different from 0 h in Lipo + LPS and CLD + LPS rats; †, $P<0.05$, significantly different between Lipo + LPS and CLD + LPS rats at respective examination points. h: hour.

Fig. 5. $CD163^+$ Kuppfer cells (arrows) seen along the sinusoid in the perivenular (A-H) and periportal (I-P) areas of liver parenchyma in Lipo + LPS and CLD + LPS rats. Kupffer cells are rarely seen in the perivenular and periportal areas of CLD + LPS rats. h: hour, CV: central vein, GS: Glisson's sheath. Bar = 100 μm.

Fig. 6. Distribution of macrophages (arrows) in the periportal area of liver in Lipo + LPS and CLD + LPS rats, showing immunophenotypes for CD68 (A-H), Iba-1 (I-P),

and MHC class II (Q-X). CD68, Iba-1 and MHC class II expressing macrophage numbers are decreased in the periportal area of CLD + LPS rats in comparison with those of Lipo + LPS rats. h: hour, GS: Glisson's sheath. Bar = 100 μm.

Fig. 7. Double immunofluorescence for CD68/CD163 and MHC class II/CD163 in the livers of Lipo + LPS (A, B) and CLD + LPS (C, D) rats. Yellow color indicates double positive reaction (arrows). Blue is nuclei stained with 4′, 6-diamidino-2-phenylindole (DAPI). E-H: Graph represents the percentage (%) of double positive macrophages for CD68/CD163 (E), MHC class II/CD163 (F), Gal-3/CD163 (G), CD204/CD163 (H). h: hour, LL: Lipo + LPS rats, CL: CLD + LPS rats. Bar = 50 μm.

Fig. 8. A-G: mRNA expressions for M1 macrophage-related factors in Lipo + LPS (□) and CLD + LPS (■) rats. M1 macrophage-related factors such as MCP-1 (A), IL-1β (B), IL-6 (C), TNF-α (D), TLR-2 (E), IFN-γ (F) and TLR-4 (G) are significantly increased in Lipo + LPS rats at post-injection (PI) 6 h, showing significant difference from CLD + LPS rats. Expression levels are normalized to β-actin mRNA level. Tukey's test; *, $P<0.05$, significantly different from 0 h in Lipo + LPS and CLD + LPS rats; †, $P<0.05$, significantly different between Lipo + LPS and CLD + LPS rats at respective examination points. h: hour.

Fig. 9. mRNA expressions for M2 macrophage-related factors such as IL-4 (A), CSF-1 (B), IL-10 (C) and TGF-β1 (D) in Lipo + LPS (□) and CLD + LPS (■) rats. The expression of mRNA for IL-4 and CSF-1 are significantly increased in CLD + LPS rats at PI 6 h, showing significant difference from Lipo + LPS rats. Expression levels are normalized to β-actin mRNA level. Tukey's test; *, $P<0.05$, significantly different from 0 h in Lipo + LPS and CLD + LPS rats; †, $P<0.05$, significantly different between Lipo + LPS and CLD + LPS rats at respective examination points. h: hour.

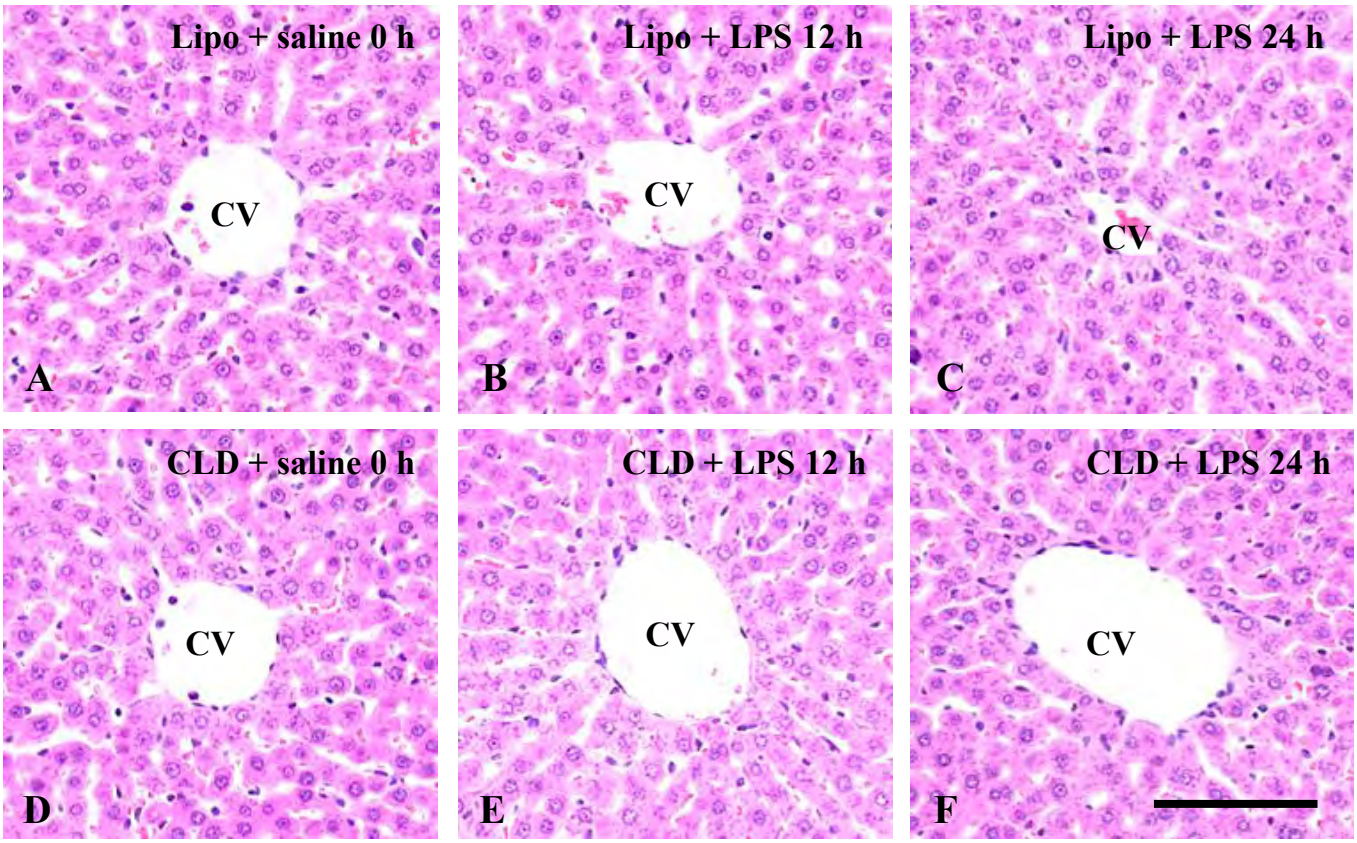
Lipo + saline 0 h
CV
A
Lipo + LPS 12 h
CV
B
Lipo + LPS 24 h
CV
C
CLD + saline 0 h
CV
D
CLD + LPS 12 h
CV
E
CLD + LPS 24 h
CV
F

Fig. 1

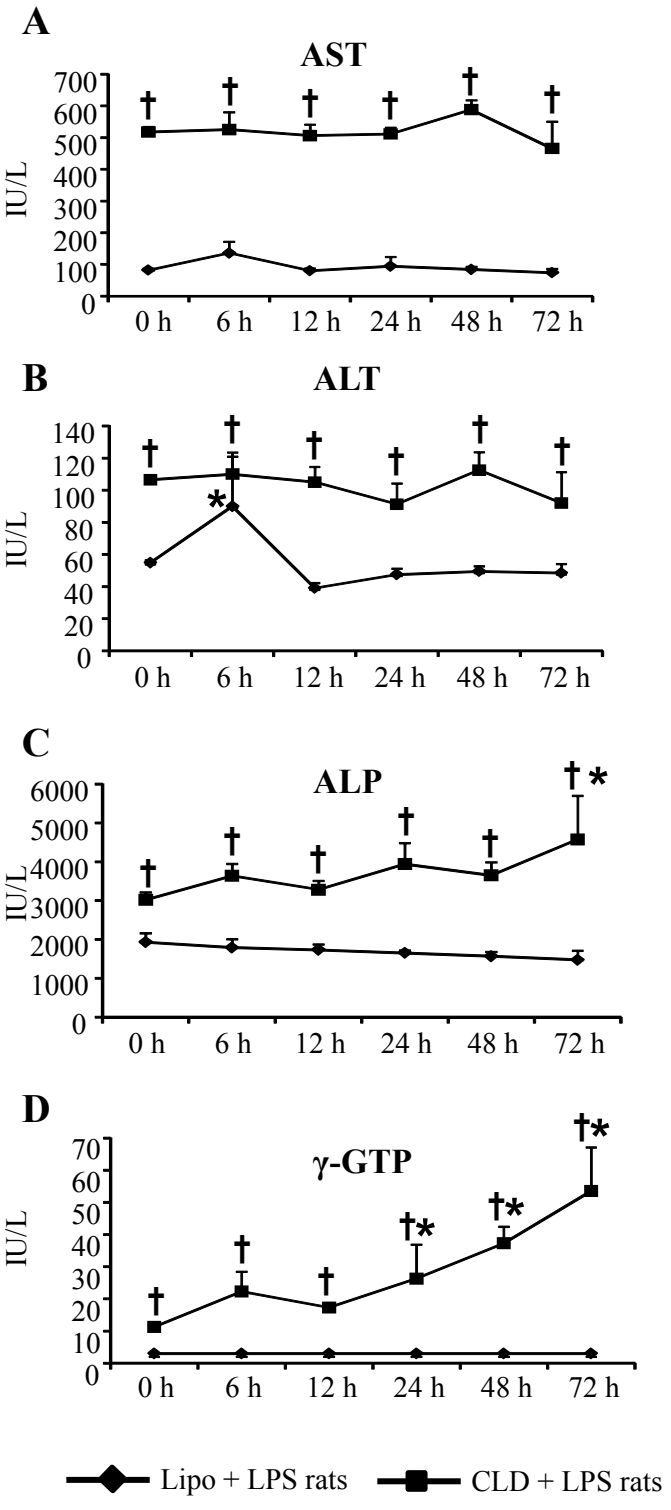
A
AST
IU/L
700
600
500
400
300
200
100
0
0 h
6 h
12 h
24 h
48 h
72 h
B
ALT
IU/L
140
120
100
80
60
40
20
0
C
ALP
IU/L
6000
5000
4000
3000
2000
1000
0
D
γ-GTP
IU/L
70
60
50
40
30
20
10
0
Lipo + LPS rats
CLD + LPS rats

Fig. 2

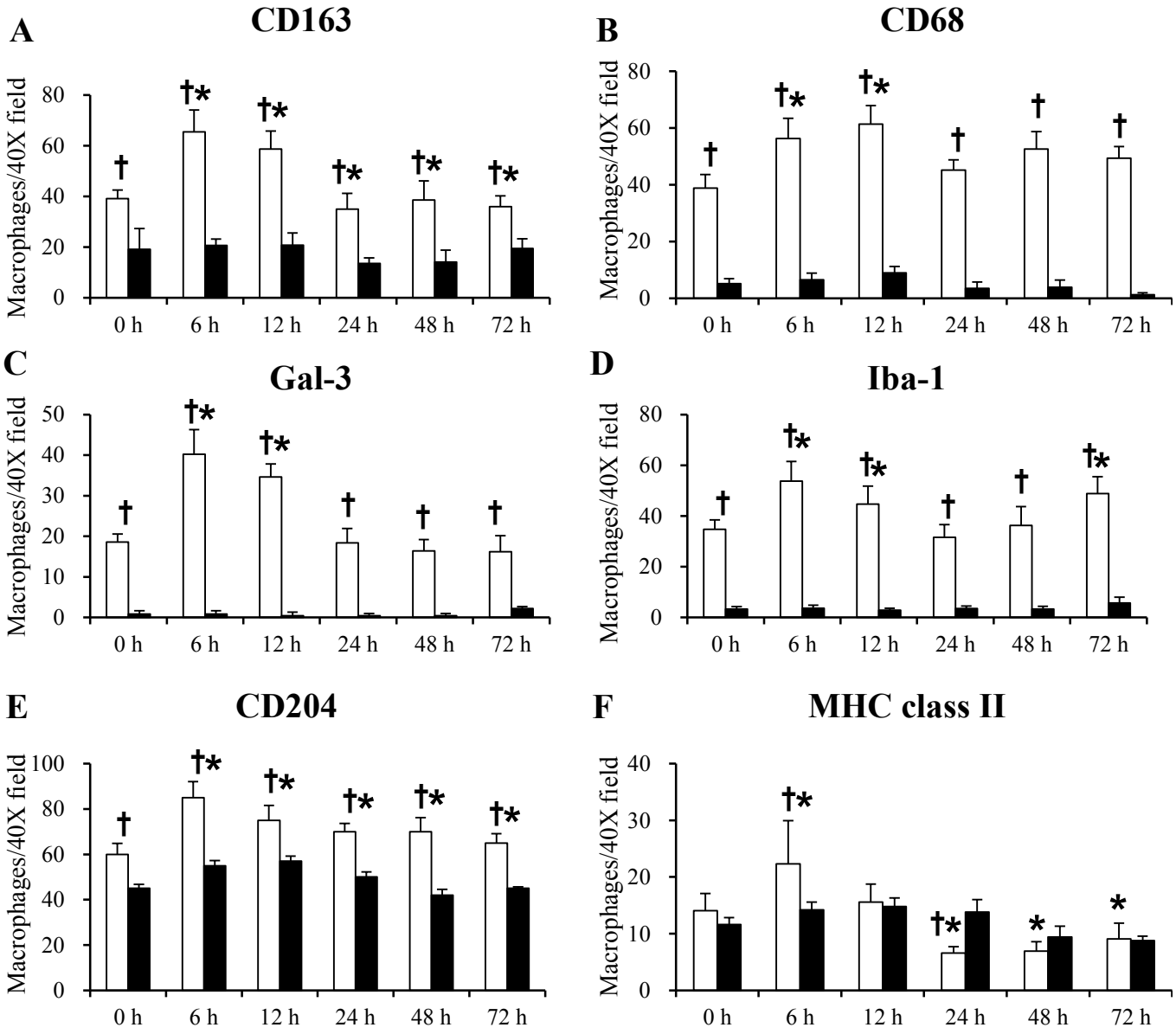
A
CD163
Macrophages/40X field
0 h
6 h
12 h
24 h
48 h
72 h
B
CD68
C
Gal-3
D
Iba-1
E
CD204
F
MHC class II
†
†*
*

Fig. 3

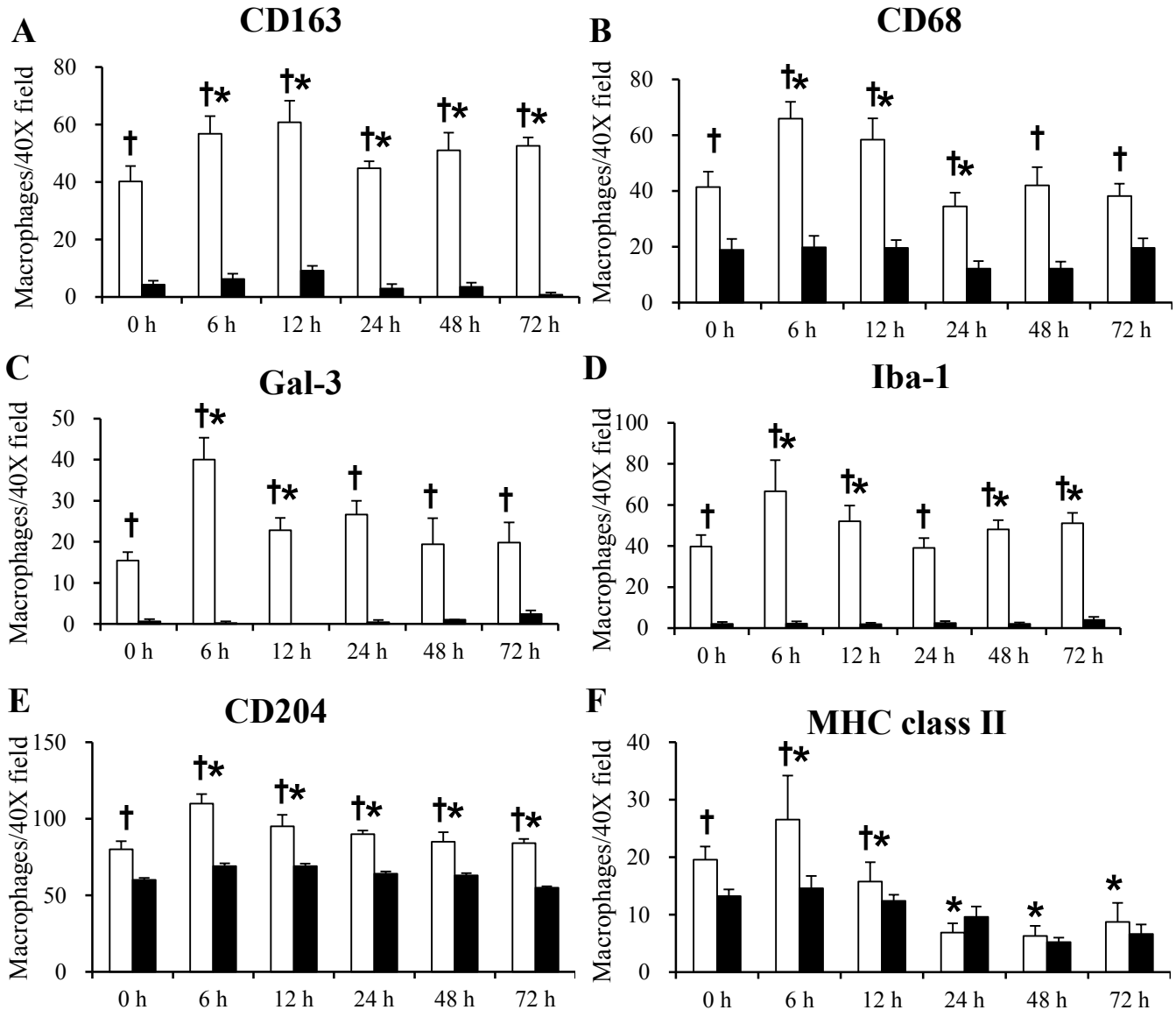
A
CD163
Macrophages/40X field
0 h
6 h
12 h
24 h
48 h
72 h
B
CD68
C
Gal-3
D
Iba-1
E
CD204
F
MHC class II

Fig. 4

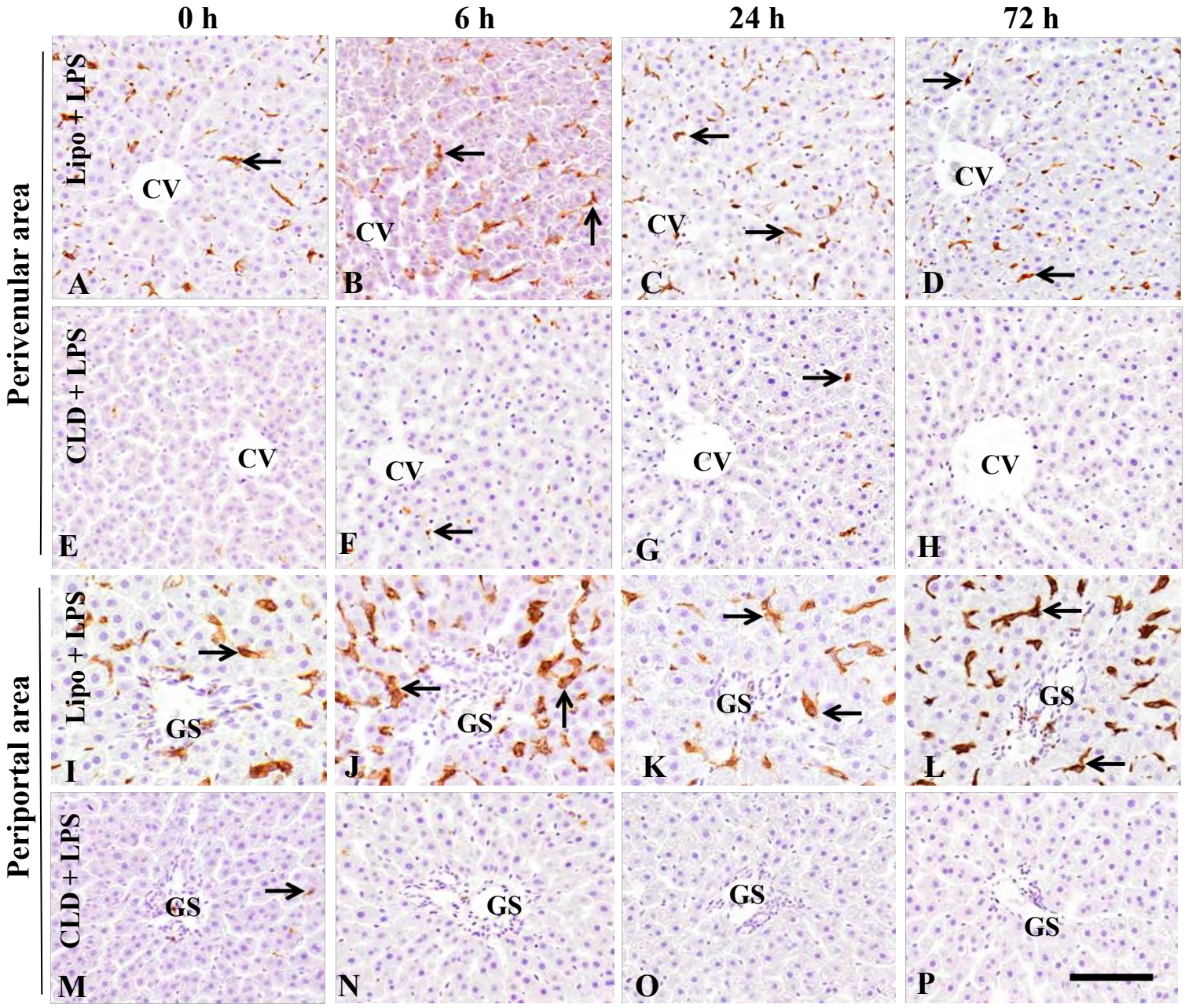
0 h
6 h
24 h
72 h
Perivenular area
Periportal area
Lipo + LPS
CLD + LPS
Lipo + LPS
CLD + LPS
CV
GS
A
B
C
D
E
F
G
H
I
J
K
L
M
N
O
P

Fig. 5

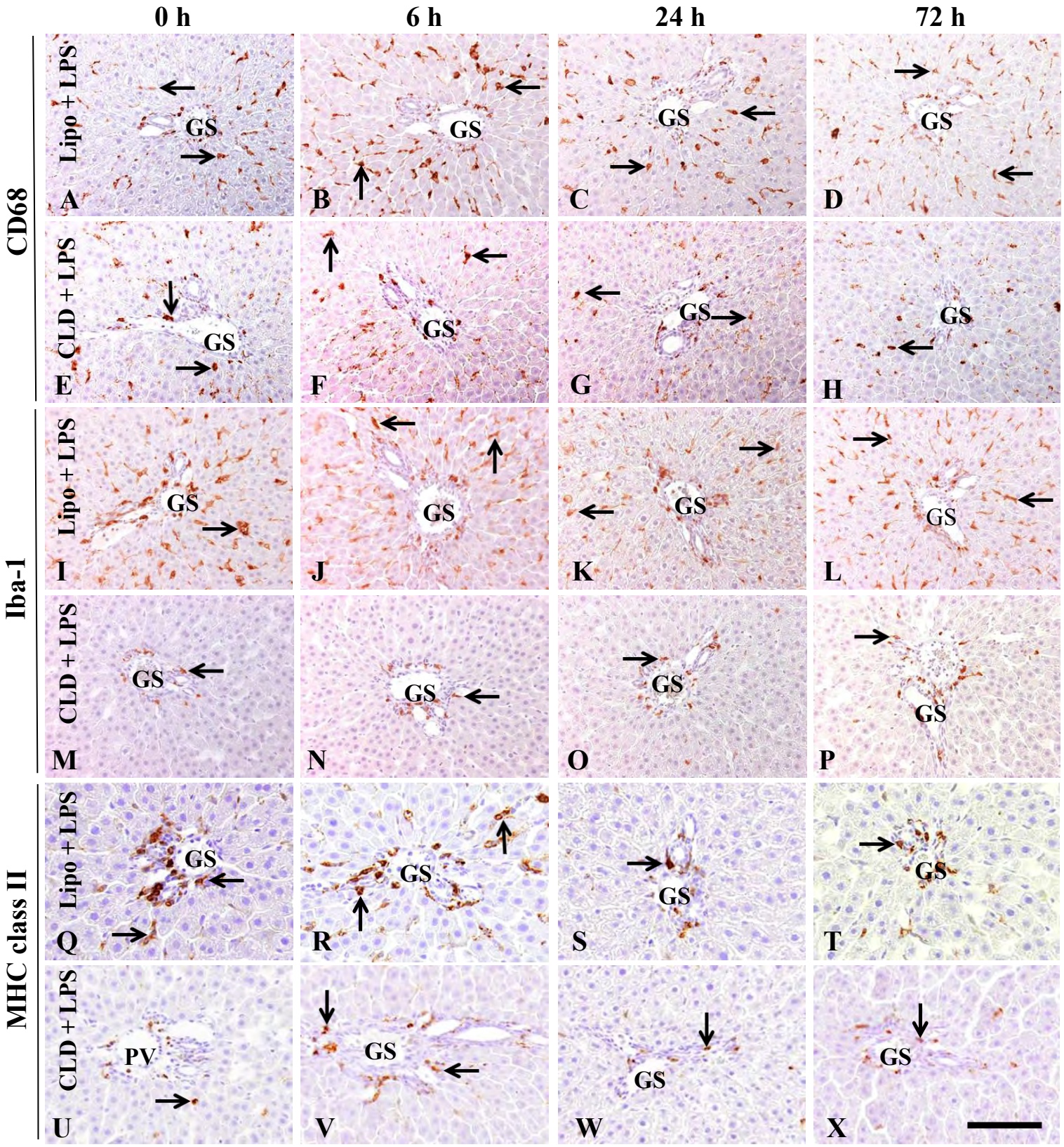
0 h
6 h
24 h
72 h
CD68
Iba-1
MHC class II
Lipo + LPS
CLD + LPS
GS
PV
A
B
C
D
E
F
G
H
I
J
K
L
M
N
O
P
Q
R
S
T
U
V
W
X

Fig. 6

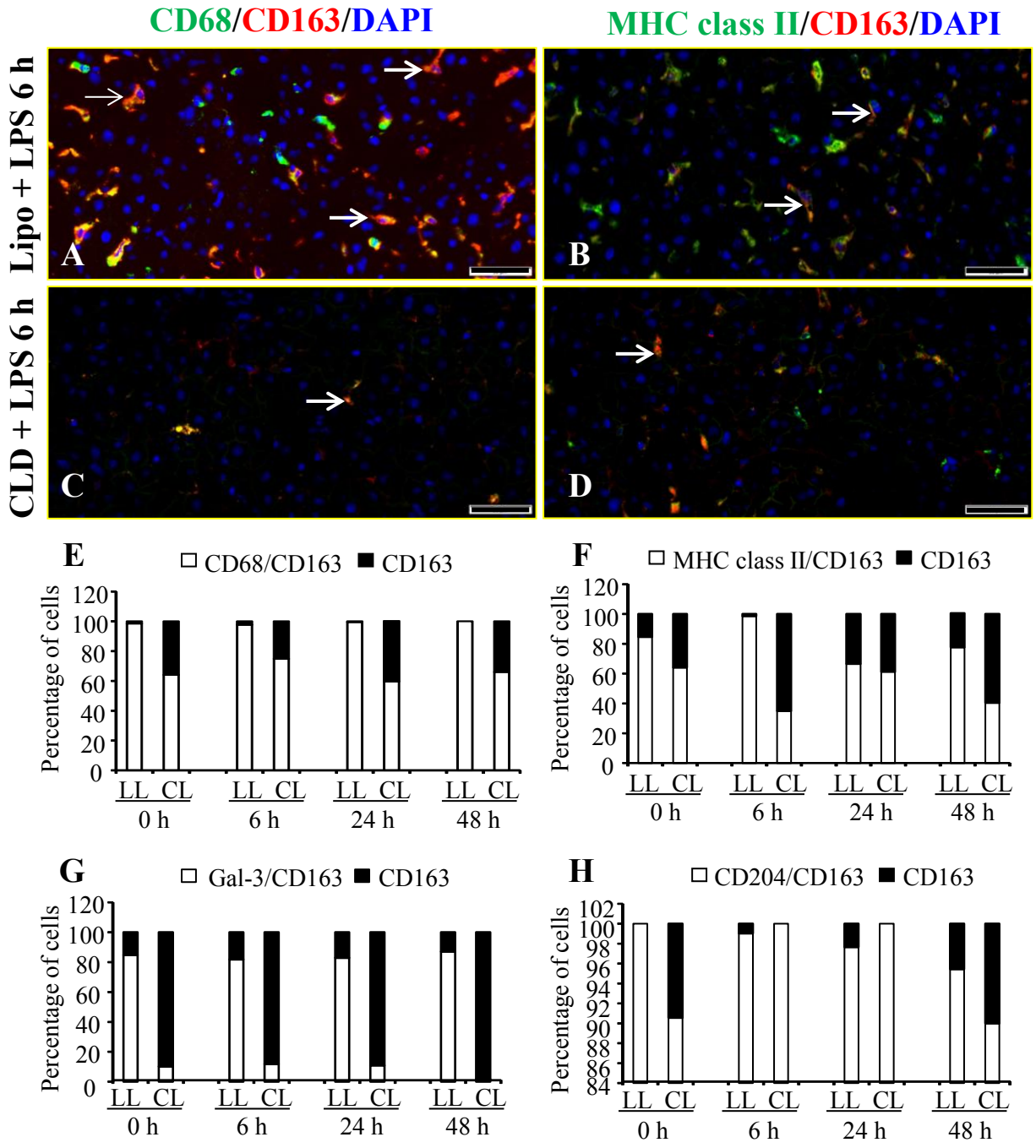
CD68/CD163/DAPI
MHC class II/CD163/DAPI
Lipo + LPS 6 h
CLD + LPS 6 h
A
B
C
D
E
CD68/CD163
CD163
Percentage of cells
LL CL
0 h
6 h
24 h
48 h
F
MHC class II/CD163
CD163
G
Gal-3/CD163
CD163
H
CD204/CD163
CD163

Fig. 7

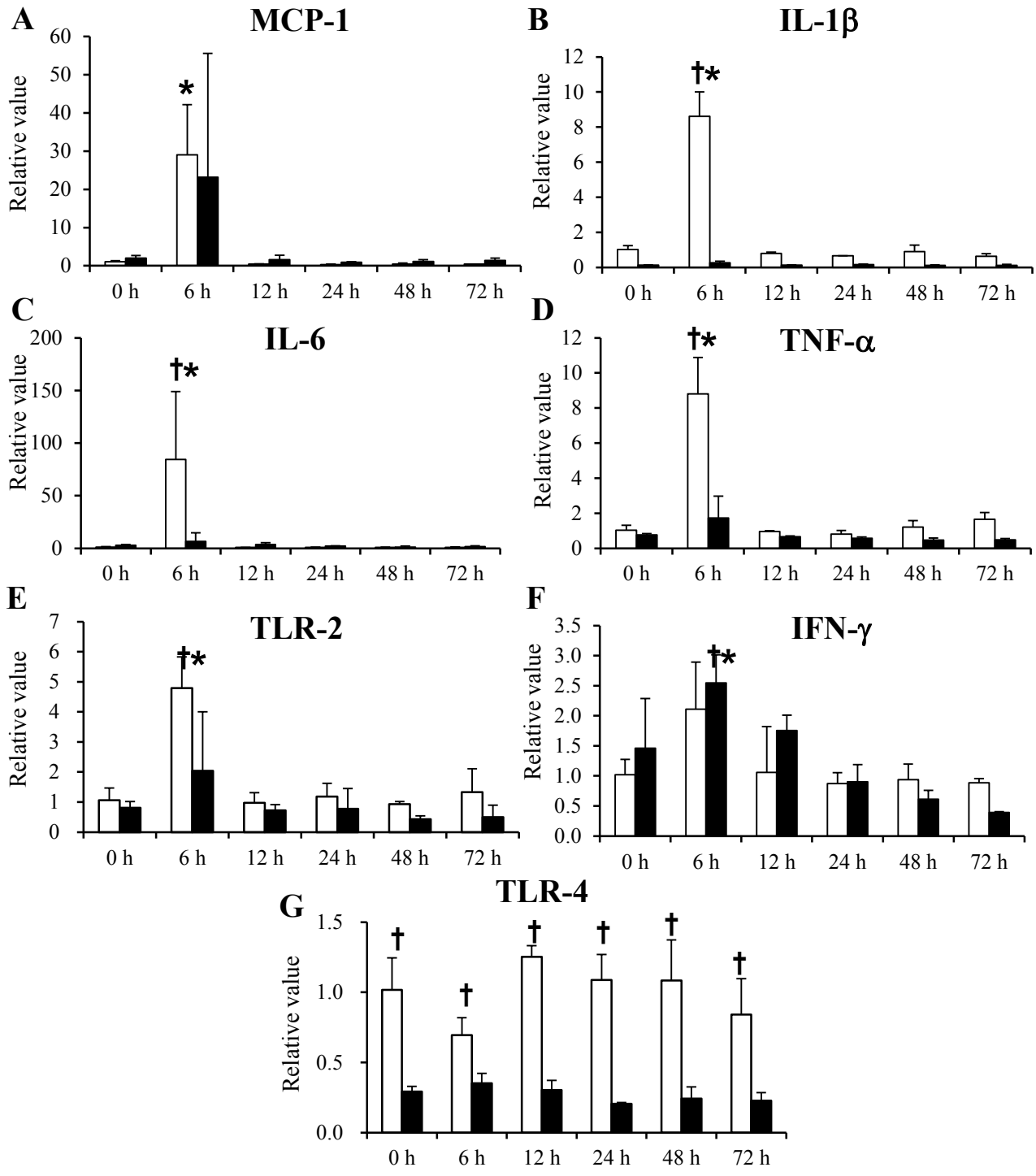
A
MCP-1
Relative value
60
50
40
30
20
10
0
*
0 h
6 h
12 h
24 h
48 h
72 h
B
IL-1β
Relative value
12
10
8
6
4
2
0
†*
C
IL-6
Relative value
200
150
100
50
0
†*
D
TNF-α
Relative value
12
10
8
6
4
2
0
†*
E
TLR-2
Relative value
7
6
5
4
3
2
1
0
†*
F
IFN-γ
Relative value
3.5
3.0
2.5
2.0
1.5
1.0
0.5
0.0
†*
G
TLR-4
Relative value
1.5
1.0
0.5
0.0
†

Fig. 8

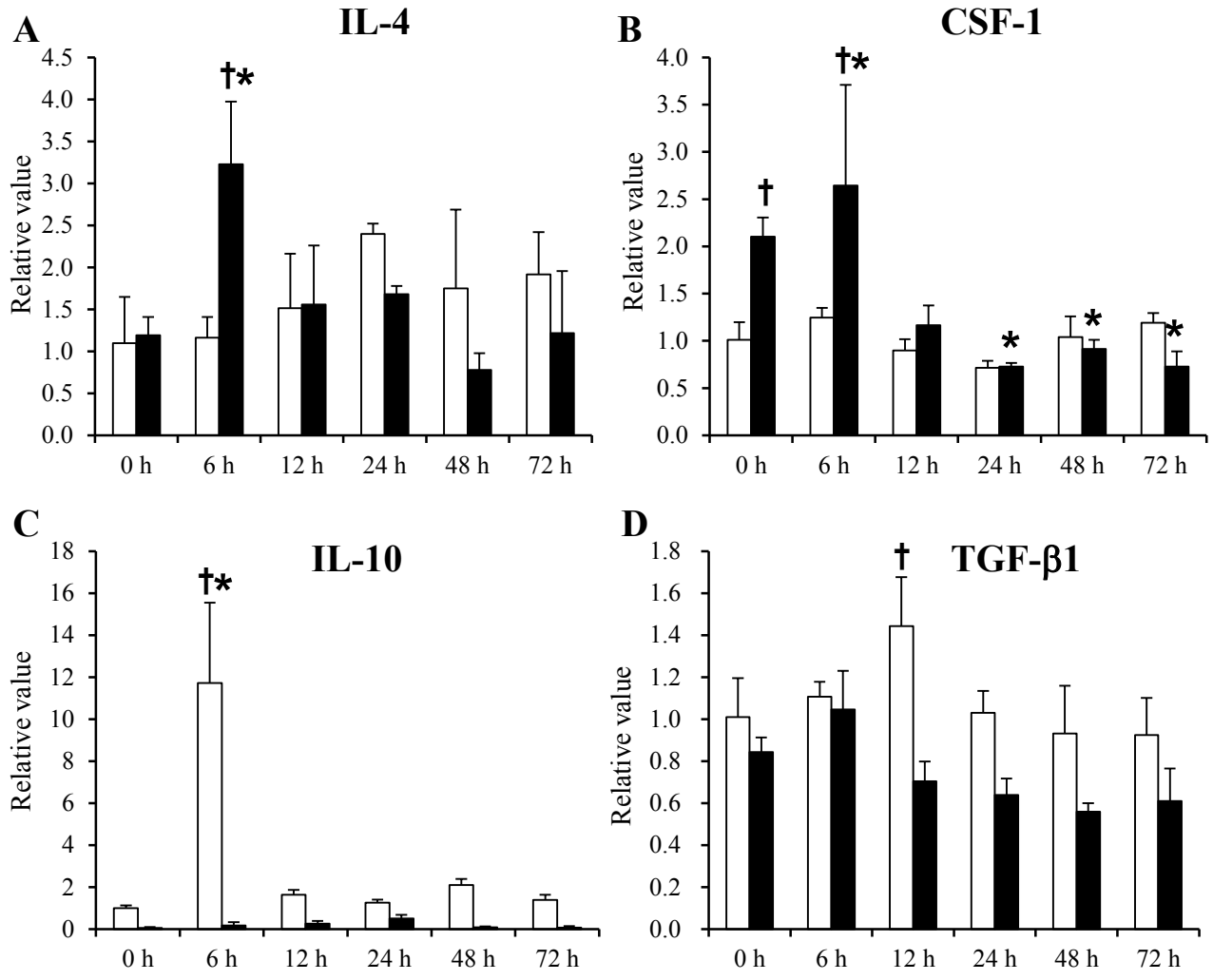
A
IL-4
Relative value
4.5
4.0
3.5
3.0
2.5
2.0
1.5
1.0
0.5
0.0
†*
0 h
6 h
12 h
24 h
48 h
72 h
B
CSF-1
Relative value
4.0
3.5
3.0
2.5
2.0
1.5
1.0
0.5
0.0
†*
†
*
*
*
0 h
6 h
12 h
24 h
48 h
72 h
C
IL-10
Relative value
18
16
14
12
10
8
6
4
2
0
†*
0 h
6 h
12 h
24 h
48 h
72 h
D
TGF-β1
Relative value
1.8
1.6
1.4
1.2
1.0
0.8
0.6
0.4
0.2
0.0
†
0 h
6 h
12 h
24 h
48 h
72 h

Fig. 9

Section II

Characterization of cell specific autophagy in liver and hepatic macrophages under treatment with low dose of LPS in clodronate-treated rats

Introduction

Autophagy (Greek for ‘‘self eating”) is an evolutionarily conserved and strictly regulated lysosomal pathway for intracellular degradation. The autophagy was first discovered by Christian de Duve in 1963 in liver. Autophagy plays an important role in defending the cell not only from physiologically damaged organelles, misfolded proteins or energy balance (Ishida and Nagata, 2009; Komatsu et al., 2005) but also from invading pathogens (Nakagawa et al., 2004). The process of autophagy begins with the formation of a double-membrane autophagosome, which fuses with a lysosome to form an autolysosome, where the cellular contents are sequestered and degraded by lysosomal enzymes. Microtubule-associated protein 1 light chain 3 beta (LC3B) is an essential component of autophagosomes, which exists in two molecular forms. LC3-I (18 kDa) is cytosolic and the other component, LC3-II (16 kDa), is tightly membrane-bound to the autophagosome (Mizushima et al., 2010). LC3B consisting of LC3-I and LC3-II is a classic marker used for autophagy study.

Autophagy is an important regulator of liver homeostasis under physiological conditions. However, the autophagy is also activated by a variety of liver diseases (including viral hepatitis, hepatocellular carcinoma and drug toxicity) as well as pharmacological or physiological stress stimuli (Ueno and Komatsu, 2017; King et al., 2011). Inappropriate stimulation of autophagy promotes autophagic cell death (Debnath et al., 2005), whereas appropriate induction of autophagy plays a cytoprotective role in liver

injuries (Chen et al., 2014; Amir et al., 2013; Ni et al., 2012). Increasing evidences indicate that autophagy is likely to contribute to the pathogenesis of hepatotoxicity (Ueno and Komatsu, 2017).

Lipopolysaccharide (LPS) is a well-known, as a gram-negative bacteria-derived cell membrane component that induces a wide variety of pathophysiological effects in humans and animals. LPS has been reported to stimulate autophagy in hepatocytes (Unuma et al., 2013), which may provide cytoprotective effects during liver injuries (Amir et al., 2013; Ni et al., 2012; Ding et al., 2010), in addition to contribution to liver homeostasis (Ueno and Komatsu, 2017).

In this study, low dose of LPS was used to determine the pathophysiological significance of autophagic responses in liver parenchymal cells (hepatocytes) and non-parenchymal cells (hepatic macrophages, hepatic stellate cells (HSCs) and cholangiocytes), and to demonstrate the role of hepatic macrophages in relation to liver autophagy.

Materials and methods

Animals and experimental procedures

Thirty six 5-week-old male F344 rats purchased from Charles River Japan (Hino, Shiga, Japan) were used. Rats were maintained at 21 ± 3°C with a 12 h light-dark cycle, and fed a standard diet for rats (DC-8, CLEA Japan, Tokyo, Japan) and supplied with tap water *ad libitum*. After one-week acclimatization, four rats (untreated normal controls) were euthanized under deep isoflurane anesthesia and liver sample were collected to evaluate the basal level of autophagy in the liver tissue. The remaining 32 rats were randomly divided into two groups: clodronate (CLD)-treated macrophage-depleted group (CLD + LPS; 16 rats) and vehicle liposome (Lipo)-treated control group (Lipo + LPS; 16 rats). A liposome-encapsulated CLD (5 mg/ml; Foundation Clodronate Liposomes, Amsterdam, the Netherlands) was injected intravenously once via tail vein in CLD + LPS group at a dose of 50 mg/kg body weight (Pervin et al., 2016); one day after CLD injection, 12 rats were injected intraperitoneally once with LPS (*Escherechia coli* 055:B5; Sigma-

Aldrich, St Louis, MO, USA) at low dose of 0.1 mg/kg body weight; four rats were euthanized under deep isoflurane anesthesia LPS-post injection (PI) at 6 h, 12 h and 24 h. The remaining four rats received sterile 0.9% NaCl instead of LPS and were sacrificed immediately after injection at PI 0 h; (CLD + saline). Rats in Lipo + LPS group received empty Lipo (10 ml/kg body weight, intravenously), followed by injection of LPS or saline intraperitoneally, and liver samples were collected similarly. The animal experiments were conducted under the institutional guidelines approved by the ethical committee of Osaka Prefecture University for the Care and Use of Experimental Animals.

Immunohistochemistry

Liver tissues from the left lateral lobe were collected and immediately fixed in periodate-lysine-paraformaldehyde (PLP) solution processed by PLP-AMeX (acetone, methyl benzoate and xylene) method (Pervin et al., 2016). Tissue sections were deparaffinized and used in immunohistochemistry for LC3B. After pretreatment in citrate buffer (pH 6.0) by microwaving for 20 min, tissue sections were stained by the Histostainer (Histofine, Nichirei Bioscience Inc., Tokyo, Japan). Briefly, sections were incubated with 5% skimmed milk for 10 min, followed by 1 h incubation with primary rabbit polyclonal anti-LC3B antibody. Antibody details are listed in Table 1. After treatment with 3% H_2O_2 for 15 min, horseradish peroxidase-conjugated secondary antibody (Histofine simple stain MAX PO®; Nichirei Inc., Tokyo, Japan) was applied for 30 min. Slides were then incubated with 3, 3'-diaminobenzidine (DAB) (Nichirei Inc., Tokyo, Japan) for 5 min. Sections were counterstained with hematoxylin for 1 min. For negative controls, tissue sections were treated with rabbit non-immunized serum instead of the primary antibody. Cytoplasmic LC3B-positive granules within hepatocytes were counted in at least 100 hepatocytes in randomly selected five different perivenular or periportal areas of the liver.

Immunofluorescence staining

Fresh frozen liver sections (10 µm in thickness) from vehicle control (Lipo + LPS) and macrophage-depleted (CLD + LPS) rats at PI 0 h, 6 h, 12 h and 24 h were used. Single

immunofluorescence was performed using LC3B antibody, to confirm the expression pattern of LC3B protein.

Double immunofluorescence was carried out using LC3B antibody in combination with lysosomal marker (lysosome-associated membrane protein 1 (Lamp 1)), macrophage markers (CD163, CD68, MHC class II), HSC marker (glial fibrillary acidic protein (GFAP) and cholangiocyte marker (CK19). Briefly, after fixation in cold acetone : methanol (1:1) for 10 min at 4°C, the sections were incubated with 10% normal goat serum for 30 min. The sections were reacted with the primary antibody overnight at 4°C. After rinsing with phosphate buffered saline (PBS), the sections were incubated for 45 min with the secondary anti-rabbit IgG-conjugated with Alexa 488 and anti-mouse IgG-conjugated with Alexa 568 (Invitrogen, Carlsbad, CA, USA). The sections were visualized with Vectashield^{TM} mounting medium containing 4′, 6-diamidino-2-phenylindole (DAPI) (Vector Labora-tories Inc., Burlingame, CA, USA) for nuclear staining, and analyzed by a virtual slide scanner (VS-120, Olympus, Tokyo, Japan).

Western blot analysis

Frozen liver tissues were homogenized, and the total protein extracts were prepared as previously described (Izawa et al., 2015). Frozen liver tissues (about 25 mg) were lysed in RIPA assay buffer (20 mM Tris-HCl pH 7.5, 150 mM NaCl, 1 mM EDTA, 1 mM ethylene glycol tetraacetic acid, 1% NP-40, 0.1% deoxycholate, 0.1% SDS, 1 mM NaF, 100 mM Na3VO4, 1 mM phenylmethylsulfonyl fluoride, and protease I cocktail; Nakarai Tesque, Kyoto, Japan) for 30 min on ice. Supernatants were collected after centrifugation at 12,000 rpm at 4^{o}C for 10 min. The protein concentration was determined by an absorption spectrometer using protein assay (Bio-Rad Laboratories, CA). The supernatants were incubated at 95^{o}C for 5 min with SDS sample buffer (Cosmo Bio, Tokyo, Japan) containing 10% beta-mercaptoethanol. The samples were run on 10% polyacrylamide gel and transferred to polyvinylidene difluoride membrane (Bio-Rad Laboratories). The membranes were reacted with rabbit polyclonal anti-LC3B, anti-MyD88, anti-TRAM1 antibodies overnight at 4°C. Details of antibodies are listed in Table 1. The membranes

were reacted with peroxidase-conjugated secondary antibody (Histofine simple stain MAX PO®; Nichirei Inc., Tokyo, Japan) and were incubated with ECL Prime Western Blotting Detection Reagent (GE Healthcare, NJ). Signals were detected by using LAS-3000 imaging system (GE Healthcare). Band intensity was analyzed by Multi Gauge software, Version 1.0, Fujifilm (Fujiflim, Tokyo, Japan).

Real time reverse transcriptase-polymerase chain reaction (RT-PCR)

Liver samples from left median lobe were collected and immediately immersed in RNAlater® (Qiagen GmbH, Hilden, Germany) overnight at 4°C and stored at −80°C until use. Total RNA was extracted from liver tissues by using an SV total RNA isolation system (Promega, Madison, WI, USA) according to the manufacturer's instructions. Two and half μg of total extracted RNA was reverse-transcribed with Superscript VILO reverse transcriptase (Life Technologies, CA, USA). Real time PCR was performed using TaqMan gene expression assays (Life Technologies, Carlsbad, CA, USA) in a PikoReal Real-Time 96 PCR System (Thermo Scientific, CA, Massachusetts, USA). The TaqMan probes specific for the cytokines used were as follows (Assay IDs): microtubule associated protein 1 light chain 3 beta (LC3B), Rn02132764_s1; beclin 1, Rn00586976_n1; sequestosome 1 (Sqstm1/p62), Rn00709977_m1; lysosomal associated membrane protein 2 (Lamp 2), Rn00567053_m1; autophagy related gene 5 (Atg 5), Rn01767063_m1; autophagy related gene 7 (Atg 7), Rn01492725_m1; toll like receptor-2 (TLR-2); Rn02133647_s1; toll like receptor-4 (TLR-4), Rn00569848_m1 and β-actin, Rn00667869_m1. The mRNA expression was normalized against the expression of β-actin mRNA as the internal control. The data were analyzed using the comparative C_t method ($^{\Delta\Delta}C_t$ method).

Statistical evaluation

Obtained data were presented as mean ± standard deviation (SD). Statistical analysis was performed using Tukey-Kramer's test. $P < 0.05$ was considered significant.

Results

Cell specific autophagy in rat livers

Autophagy in hepatocytes

To evaluate the autophagy activity in hepatocytes of macrophage-depleted rats, immunohistochemistry or immunofluorescence was performed for LC3B in the liver of untreated normal, Lipo + LPS and CLD + LPS rats. In control (Lipo + saline or CLD + saline at PI 0 h) rats, LC3B-positive cytoplasmic granules/dots in hepatocytes were detected at basal level, showing similar reaction in each group rats (Fig. 1A, E). Compared to expression in control rats at PI 0 h, LC3B-positve hepatocyte numbers with intra-cytoplasmic LC3B-labeled dots were increased in Lipo + LPS and CLD + LPS rats at PI 6 h and 12 h (Fig. 1B, C, F, G). In addition, the LC3B-positive hepatocyte numbers were apparently lower in CLD + LPS rats compared with those of Lipo + LPS rats. At PI 24 h, LC3B reactivity was low in livers of both groups (Fig. 1D, H). In single immunofluorescence, a basal level of LC3B was also observed in liver of untreated control rats (Fig. 1I), but LPS injection resulted in a notable increase of LC3B reactivity in Lipo + LPS rats at PI 12 h (Fig. 1J). Semi-quantitative analysis showed that LC3B-labeled cytoplasmic dots per hepatocyte was markedly increased in Lipo + LPS and CLD + LPS rats at PI 6 h and 12 h (Fig. 1K). However, at PI 12 h, LC3B-positive cytoplasmic dots per hepatocyte was significantly decreased in CLD + LPS rats as compared with those of Lipo + LPS rats.

Lysosomal activity in hepatocyte was evaluated using double immunofluorescence with lysosomal marker Lamp 1 and autophagy marker LC3B (Fig. 2A-C). Expression of Lamp 1 was increased in livers of Lipo + LPS and CLD + LPS rats at PI 6h or 12h (Fig. 2B, C). Most of the Lamp 1-positive hepatocytes expressed LC3B in both groups (Fig. 2A-C), indicating formation of autolysosomes from lysosomes.

Consistent with immunohistochemistry, Western blot analysis confirmed the increased expression of LC3B (LC3-I or LC3-II) in liver of Lipo + LPS and CLD + LPS

rats at PI 6 h and 12 h (Fig. 3A). However, the band intensity was weaker in CLD + LPS rats. Statistically, LC3-II expression was significantly decreased in CLD + LPS rats at PI 12 h as compared with that of Lipo + LPS rats (Fig. 3B). Expressions of TLR adaptor proteins MyD88 and TRAM1 were not changed in CLD + LPS rats, whereas these factors were markedly increased in Lipo + LPS rats at PI 12 h (Fig. 3A).

Autophagy in non-parenchymal liver cells

Autophagy activity in non-parenchymal cells in liver was evaluated using double immunofluorescence with autophagy marker protein LC3B and non-parenchymal cell specific markers such as CD68, CD163 and MHC class II for hepatic macrophages, GFAP for HSCs and CK19 for cholangiocytes (Figs. 4-6). Double immunofluorescence for LC3B with macrophage markers revealed that hepatic macrophage autophagy was markedly increased in Lipo + LPS rats at PI 6 h and 12 h (Fig. 4A-F; inset); particularly, 17 to 26% of $CD68^+$, $CD163^+$ and MHC class II^+ macrophages co-expressed LC3B in 0 h control rats (Fig. 4G-I), indicating a basal level of autophagy in hepatic macrophages. After LPS treatment, 97 to 98% of the $CD68^+$ and $CD163^+$ hepatic macrophages co-expressed LC3B at PI 12 h (Fig. 4G, H) and approximately 56% of MHC class II^+ macrophages showed simultaneous LC3B reactivity at PI 12 h (Fig. 4I).

In double immunofluorescence, a small number of GFAP-expressing HSCs also expressed LC3B in untreated control rats at PI 0 h (Fig. 5A). Co-expression of GFAP-positive HSCs with LC3B was clearly increased in Lipo + LPS and CLD + LPS rats (Fig. 5B, C) at PI 6 h or 12 h without significant difference between these groups. Induction of autophagy in HSCs resulted from the effect of LPS, but there was no significant effect of CLD-induced hepatic macrophage depletion in CLD + LPS rats.

In cholangiocytes, low levels of LC3B expression were seen in untreated control rats at PI 0 h by immunohistochemistry (Fig. 6A). LC3B expression was not changed in cholangiocytes of Lipo + LPS and CLD + LPS rats after LPS injection (Fig. 6B, C). Similar results were obtained in double immunofluorescence for CK19 and LC3B (Fig.

6D-F), indicating that LPS injection or CLD-induced hepatic macrophage depletion did not affect cholangiocyte autophagy.

Expression of autophagy-related genes

LC3B mRNA expression was significantly increased in Lipo + LPS rats at PI 6 h or 12 h and in CLD + LPS rats at PI 6 h (Fig. 7A). However, at PI 12 h, LC3B mRNA expression was significantly decreased in CLD + LPS rats as compared with that of Lipo + LPS rats. Other autophagy-related genes, beclin 1, p62, Lamp 2, Atg 5 and Atg 7 did not show any significant change within Lipo + LPS or CLD + LPS rats (Fig. 7B-F). However, at PI 6 h, mRNAs of these factors were significantly increased in CLD + LPS rats compared with those of Lipo + LPS rats. TLR-2 mRNA expression was significantly increased in Lipo + LPS rats at PI 6 h (Fig. 7G) and between the groups, TLR-2 mRNA expression was significantly decreased in CLD + LPS rats. TLR-4 mRNA was decreased significantly at all examination points in CLD + LPS rats in contrast to that in Lipo + LPS rats, which might be related to Kupffer cell depletion due to CLD injection (Fig. 7H).

Discussion

Autophagy contributes to cell physiology and also acts as a protective cellular mechanism in response to various stimuli. In this study, a basal level of autophagy was seen in hepatocytes and non-parenchymal cells such as Kupffer cells, HSCs and cholangiocytes of normal rat livers, which may reflect the steady-state presence of autophagy. It is recognized that hepatocytes have a basal level of autophagy which can regulate cellular metabolism (Madrigal-Matute and Cuervo, 2016). The basal level autophagy has also been observed in HSCs and bile ductular cells in mouse and rat livers (Hung et al., 2015; Hernandez-Gea et al., 2012). Autophagy in hepatocytes and non-parenchymal liver cells is essential for their survival and physiological functions (Ueno and Komatsu, 2017; Zhang et al., 2012).

LPS induces autophagy in rat livers

The dose of LPS used in this study resulted in a marked increase of autophagy in hepatocytes, hepatic macrophages and HSCs in Lipo + LPS and CLD + LPS rats. LC3-II protein expression in mouse liver and isolated primary hepatocytes have been reported to be increased after LPS treatment (5 mg/kg body weight) *in vivo* and *in vitro*, respectively (Chen et al., 2014). In mouse heart, LPS (0.5 to 1.5 mg/kg body weight) also induced autophagy in cardiomyocytes (Yuan et al., 2009). Although autophagy in non-parenchymal liver cells was not studied, LPS (15 mg/kg body weight) also induced autophagy in hepatocytes of rat livers (Unuma et al., 2013). Taken together, these findings including data of the present study indicate that LPS is a potent autophagy inducer in rat livers.

Hepatic macrophage depletion reduces hepatocyte autophagy in rats via decreased TLR signaling

The decrease in hepatocyte autophagy in CLD + LPS rats is most likely due to decreased levels of TLR adapter proteins (MyD88 and TRAM1) and TLR mRNAs, indicating the impairment of TLR signaling in autophagy (Anand et al., 2011). These factors were significantly higher in Lipo + LPS rats, suggesting that TLR signaling pathways influence autophagy in hepatocytes as well as macrophages. The TLR signaling is essential for LPS-induced autophagy; in particular, TLR-2 is crucial to autophagy activation during pathogen-induced autophagy in mice (Anand et al., 2011; Xu et al., 2007). Hepatocytes express and activate TLR-2 or TLR-4 in response to LPS (Chen et al., 2014; Vodovotz et al., 2001). LPS interacts with different cells (hepatocytes and granulocytes) and then, these cells contribute to endotoxin tolerance in mice (Freudenberg and Galanos, 1988). Isolated primary Kupffer cells treated with LPS showed inflammatory mediator production (TNF-α) and phagocytic capacity (Hafenrichter et al., 1994). Thus, hepatic macrophages influence not only inflammatory mediator production and phagocytic capacity, but also autophagy activity in hepatocytes via TLRs signaling, suggesting that Kupffer cells may contribute to cytoprotective roles in liver injury through the activation of autophagy.

LPS-mediated cell specific autophagy contributes to the pathogenesis of liver lesions in rats

The uptake of LPS in the liver is well established. Various molecular mechanisms may be involved in LPS-induced hepatoprotection against pathogen infection, toxins and chemicals (Anand et al., 2011; Nakagawa et al., 2004; Liu et al., 2000). The mechanisms include stimulation of Kupffer cells and reactive macrophages (Hafenrichter et al., 1994; Freudenberg and Galanos, 1988), release of cytokines (Leon et al., 1992), activation of transcription factors such as nuclear factor kappa B (NF-κB) (Yoza et al., 1998), stimulation of tissue repair machinery (Calabrese and Mehendale, 1996) and suppression of cytochrome P450 (Liu et al., 2000). The present results indicated that activation of autophagy in hepatocytes, HSCs and hepatic macrophages during liver injuries might be responsible for the hepatotoxicity.

Cell-specific autophagy is important for progression of liver diseases. Hepatocyte autophagy may provide cytoprotection for liver injuries (Amir et al., 2013; Ni et al., 2012; Ding et al., 2010). In fact, hepatic macrophage autophagy reduces acute toxin-induced liver injury in mice (Ilyas et al., 2016). Autophagy-impaired macrophages induce proinflammatory macrophage (M1) polarization and decrease anti-inflammatory macrophage (M2) polarization, suggesting that autophagy may regulate inflammation for M1 type macrophages or tissue repair for M2 type macrophages (Liu et al., 2015). Increased autophagy in HSCs regulates intracellular retinols (Zhang et al., 2012). HSC autophagy induction has been shown in carbon tetrachloride- and thioacetamide-induced liver injuries in mice (Hung et al., 2015; Hernandez-Gea et al., 2012). The present study showed that low dose of LPS (0.1 mg/kg body weight) could stimulate autophagy in HSCs and Kupffer cells in rat livers without affecting cell morphology, indicating that cell-specific autophagy may participate in the modulation of liver lesions. However, it is notice that hepatic macrophage depletion (in CLD + LPS rats) decreased autophagy in hepatocytes, indicating importance of relation of hepatic macrophages with autophagy expression in hepatocytes.

In conclusion, LPS could induce autophagy in hepatocytes, hepatic macrophages and HSCs, and liver autophagy was influenced by hepatic macrophages in rats. Therefore, low dose of LPS should be considered as a potential autophagy inducer in rat livers, and cell specific autophagy may play important roles in the pathogenesis of liver diseases including hepatotoxicity.

Summary

Autophagy is important for liver homeostasis and in the pathogenesis of liver diseases. The author investigated autophagy in normal and hepatic macrophage-depleted rat livers after treatment with lipopolysaccharide (LPS). Hepatic macrophages were depleted with liposome-encapsulated clodronate (CLD; 50 mg/kg body weight, intravenously) followed by LPS injection (0.1 mg/kg body weight, intraperitoneally) (CLD + LPS rats). Rats received empty-liposome (Lipo) followed by LPS, which served as liposome controls (Lipo + LPS rats). Localization of LC3B (autophagy marker) was seen at basal level in hepatocytes, Kupffer cells, hepatic stellate cells (HSCs) and cholangiocytes in normal rat livers. LPS administration resulted in a markedly increased LC3B expression in hepatocytes of Lipo + LPS and CLD + LPS rats at LPS-post injection (PI) 6 h and 12 h. In comparisons between these groups, the number of LC3B-positive hepatocytes with cytoplasmic LC3B-labelling was lower in hepatic macrophage-depleted CLD + LPS rats. LC3B reactivity was increased in GFAP-expressing HSCs in both groups after LPS treatment. LPS also induced autophagy in $CD163^+$ Kupffer cells and $CD68^+$ macrophages of Lipo + LPS rats. At mRNA level, LC3B and TLR-2 were significantly increased at PI 6 h or 12 h in Lipo + LPS rats, while the levels of these factors was significantly lower in CLD + LPS rats. Collectively, low dose of LPS induced autophagy in hepatocytes and non-parenchymal liver cells, and depletion of hepatic macrophages reduced hepatocyte autophagy. The present results clearly demonstrate that LPS acts as a potent autophagy inducer in rat livers, and that hepatic macrophages may be important for liver autophagy functions.

Table 1. Details of antibodies for immunostaining and Western blotting.

Antibody	Clone	Type	Dilution	Source
LC3B	-	Rabbit polyclonal	1/2000	Sigma-Aldrich Co., MO, USA
CD163	ED1	Mouse monoclonal	1/300	AbD Serotec, Oxford, UK
CD68	ED2	Mouse monoclonal	1/500	AbD Serotec, Oxford, UK
MHC class II	OX-6	Mouse monoclonal	1/1000	AbD Serotec, Oxford, UK
MyD88	-	Rabbit polyclonal	1/500	Abcam plc., Cambridge, UK
TRAMP1	-	Rabbit polyclonal	1/1000	Abcam plc., Cambridge, UK
β-actin	-	Mouse monoclonal	1/10000	Sigma-Aldrich Co., MO, USA

Figure legends

Fig. 1. Lipopolysaccharide (LPS) induces autophagy in hepatocytes, and hepatic macrophage depletion reduces hepatocyte autophagy in rat livers. A-H: LC3B-labeled dots within hepatocytes show normal distribution (at basal level) in Lipo + LPS and CLD + LPS rats at post-injection (PI) 0 h (A, E) and are markedly increased at PI 6 h and 12 h in Lipo + LPS (B, C) and CLD + LPS (F, G) rats. Inset shows LC3B-labeled dots within hepatocyte of higher magnification. I-J: Immunofluorescence for LC3B in untreated control and Lipo + LPS rats at PI 12 h. Blue is nuclei stained with 4′, 6-diamidino-2-phenylindole (DAPI). K: The mean number of LC3B-labeled dots per hepatocyte is shown in graph. Tukey's test; *, $P<0.05$, significantly different from 0 h in Lipo + LPS (□) and CLD + LPS (■) rats; †, $P<0.05$, significantly different between Lipo + LPS and CLD + LPS rats at respective examination points. h: hour, CV: central vein. Bar = 100 μm.

Fig. 2. A: Western blot analysis for LC3B (LC3-I and LC3-II), MyD88 and TRAMP1 in Lipo + LPS and hepatic macrophage-depleted (CLD + LPS) rats. B: The intensity of LC3 II band was quantified using Multi Gauge software, Version 1.0, Fujifilm; β-actin is used as a loading control. Tukey's test; *, $P<0.05$, significantly different from 0 h Lipo + LPS (□) and CLD + LPS (■) rats; †, $P<0.05$, significantly different between Lipo + LPS and CLD + LPS rats at respective examination points. h: hour.

Fig. 3. LPS-induced autophagy in hepatic macrophages. A-F: Double immunofluorescence for CD68/LC3B (A, B), CD163/LC3B (C, D) and MHC class II/LC3B (E, F) in Lipo + LPS rats at PI 0 h and 12 h. Yellow signals indicate hepatic macrophage positive for LC3B (arrows, inset). DAPI for nuclear stain. G-I: Graph represents the percentage (%) of LC3B-positive macrophages after LPS treatment. h: hour, CV: central vein, GS: Glisson's sheath. Bar = 100 μm.

Fig. 4. LPS-induced autophagy in hepatic stellate cells (HSCs) and hepatic macrophage depletion do not affect autophagy in HSCs. Dual-immunofluorescence for glial fibrillary acidic protein (GFAP) for HSCs and LC3B in Lipo + LPS (A, B) and CLD + LPS (C) rats. Yellow color indicates double positive reaction (arrows, inset). DAPI for nuclear stain. h: hour, CV: central vein. Bar = 50 μm.

Fig. 5. A-F: Expression of LC3B in ductular lining cells (cholangiocytes) in Lipo + LPS and CLD+LPS rats. A-C: Immunohistochemistry for LC3B shows low levels of LC3B localization (arrow) in cholangiocytes. D-F: Dual-immunofluorescence for CK19 (cholangiocyte marker) and LC3B. Yellow color indicates double positive reaction (arrow). DAPI for nuclear stain. h: hour, Bd: bile duct, GS: Glisson's sheath. Bar = 50 μm.

Fig. 6. A-C: LPS-induced lysosomal activity in Lipo + LPS and CLD + LPS rats. Dual-immunofluorescence for Lamp 1 (lysosome marker) and LC3B. Yellow color indicates double positive reaction (arrows). DAPI for nuclear stain. h: hour, CV: central vein. Bar = 50 μm.

Fig. 7. mRNA expressions for autophagy-related genes such as LC3B (A), beclin 1 (B), p62 (C), Lamp 2 (D), Atg 5 (E), Atg 7 (F), TLR-2 (G) and TLR-4 (H) in Lipo + LPS (□) and CLD + LPS (■) rats. Expression levels are normalized to β-actin mRNA level. Tukey's test; *, $P<0.05$, significantly different from 0 h in Lipo + LPS and CLD + LPS rats; †, $P<0.05$, significantly different between Lipo + LPS and CLD + LPS rats at respective examination points. h: hour.

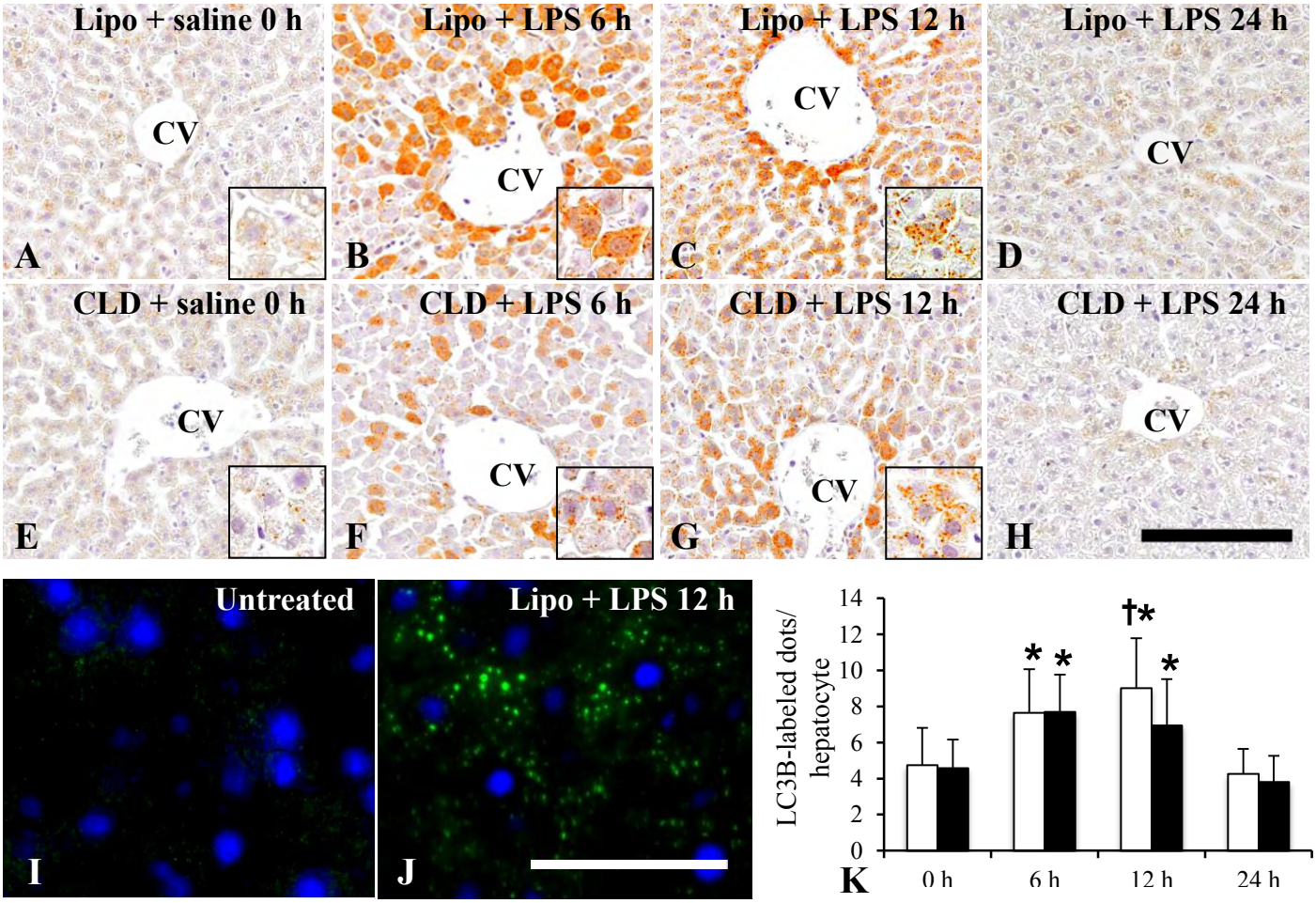
Lipo + saline 0 h
CV
A
Lipo + LPS 6 h
CV
B
Lipo + LPS 12 h
CV
C
Lipo + LPS 24 h
CV
D
CLD + saline 0 h
CV
E
CLD + LPS 6 h
CV
F
CLD + LPS 12 h
CV
G
CLD + LPS 24 h
CV
H
Untreated
I
Lipo + LPS 12 h
J
LC3B-labeled dots/ hepatocyte
14
12
10
8
6
4
2
0
*
*
†*
*
K
0 h
6 h
12 h
24 h

Fig. 1

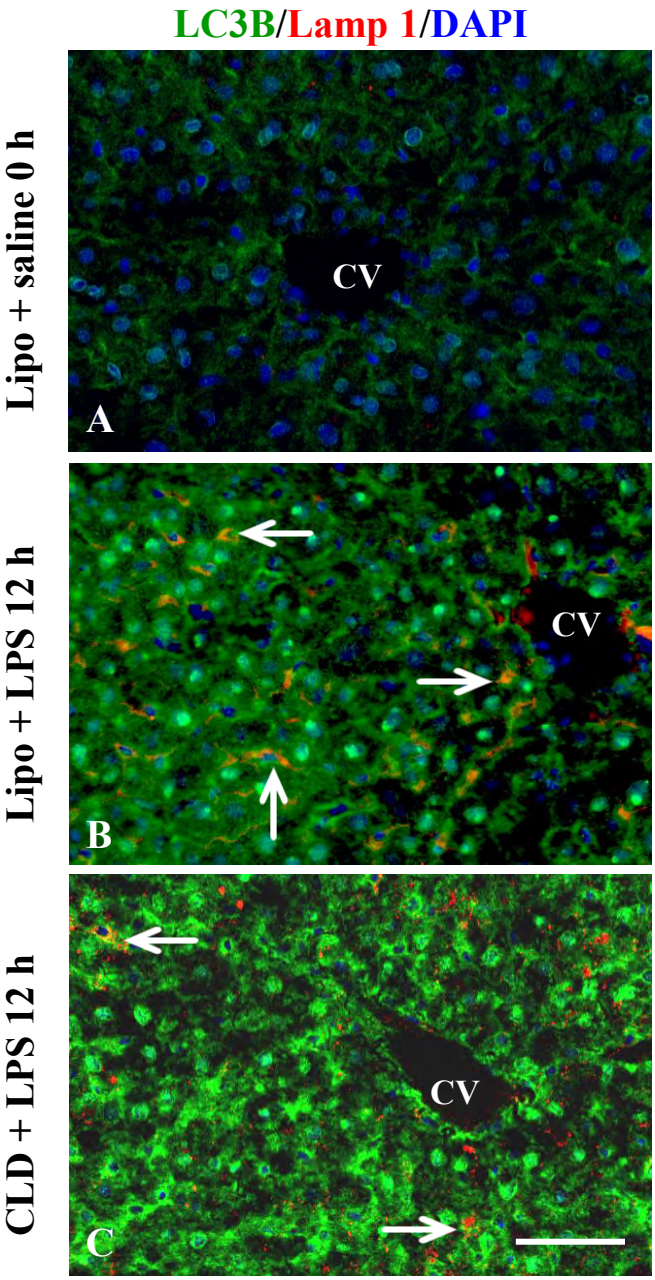
LC3B/Lamp 1/DAPI
Lipo + saline 0 h
CV
A
Lipo + LPS 12 h
CV
B
CLD + LPS 12 h
CV
C

Fig. 2

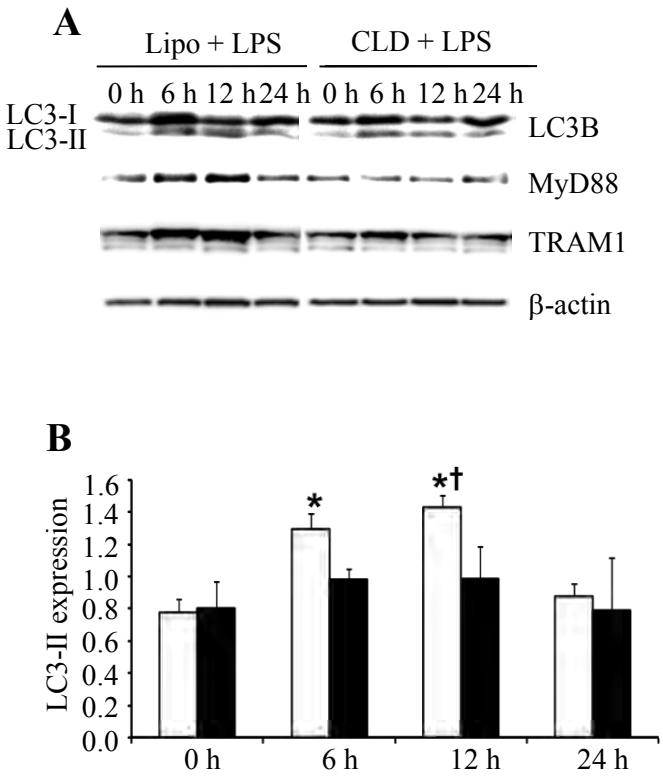
A
Lipo + LPS
CLD + LPS
0 h 6 h 12 h 24 h 0 h 6 h 12 h 24 h
LC3-I
LC3-II
LC3B
MyD88
TRAM1
β-actin
B
LC3-II expression
1.6
1.4
1.2
1.0
0.8
0.6
0.4
0.2
0.0
*
*†
0 h
6 h
12 h
24 h

Fig. 3

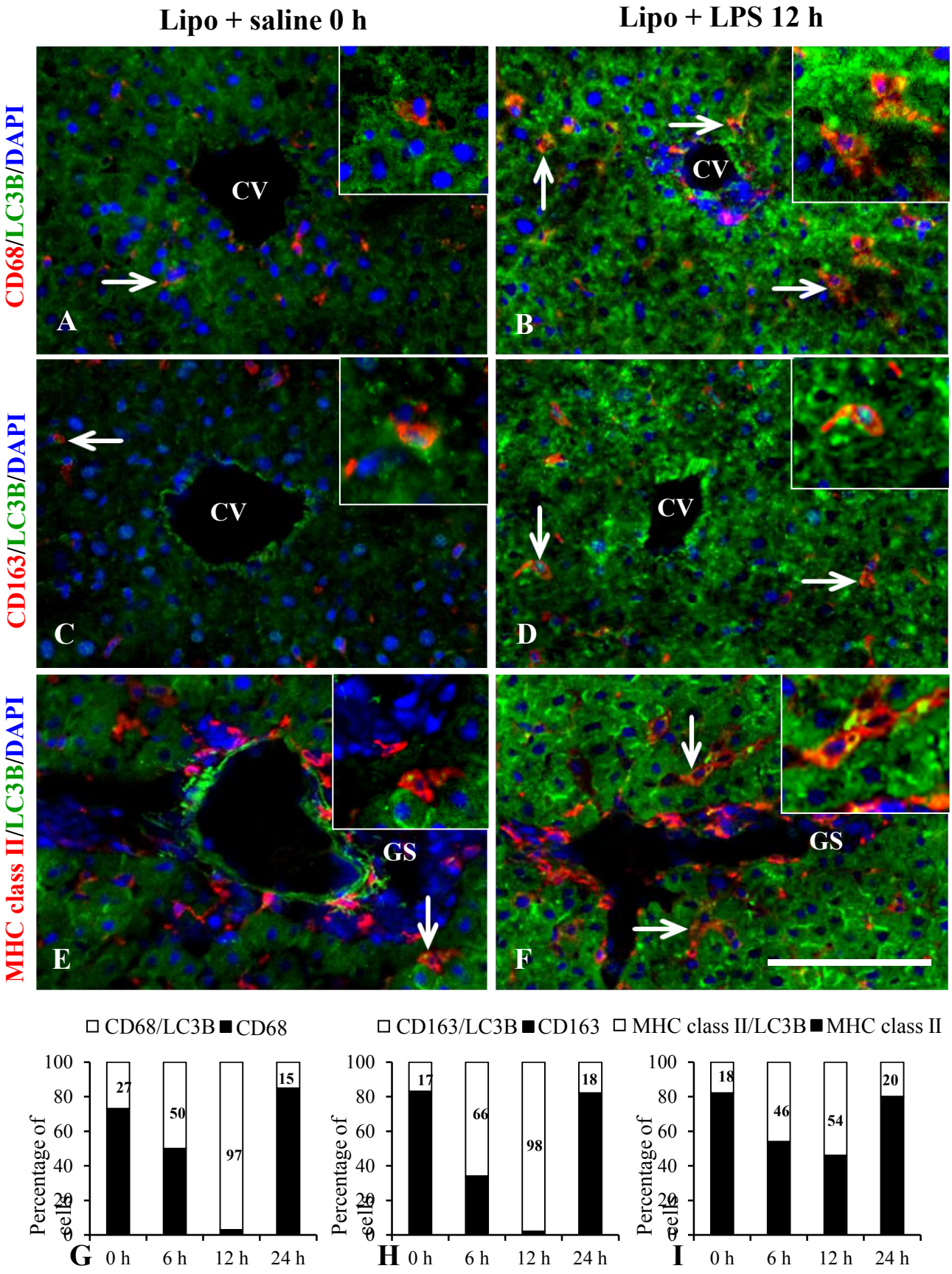
Lipo + saline 0 h
Lipo + LPS 12 h
CD68/LC3B/DAPI
CD163/LC3B/DAPI
MHC class II/LC3B/DAPI
CV
GS
A
B
C
D
E
F
CD68/LC3B
CD68
CD163/LC3B
CD163
MHC class II/LC3B
MHC class II
Percentage of cells
0 h
6 h
12 h
24 h
G
H
I
27
50
97
15
17
66
98
18
18
46
54
20

Fig. 4

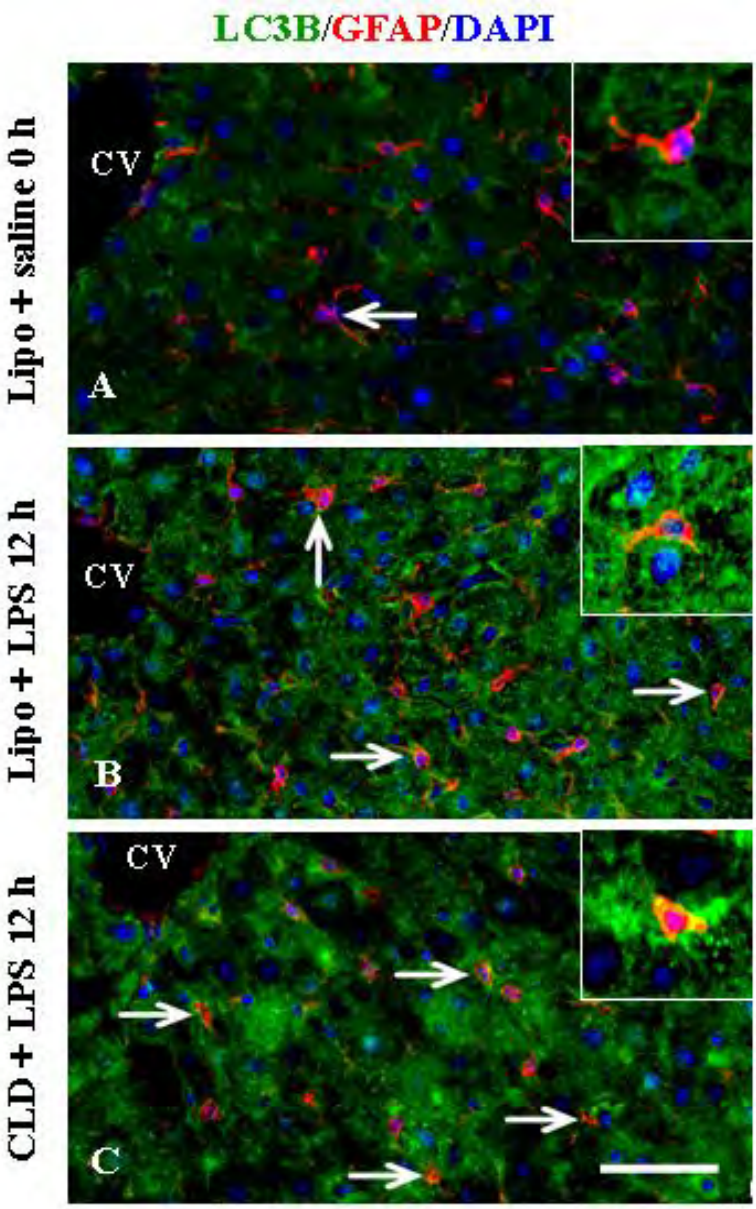
LC3B/GFAP/DAPI
Lipo + saline 0 h
CV
A
Lipo + LPS 12 h
CV
B
CLD + LPS 12 h
CV
C

Fig. 5

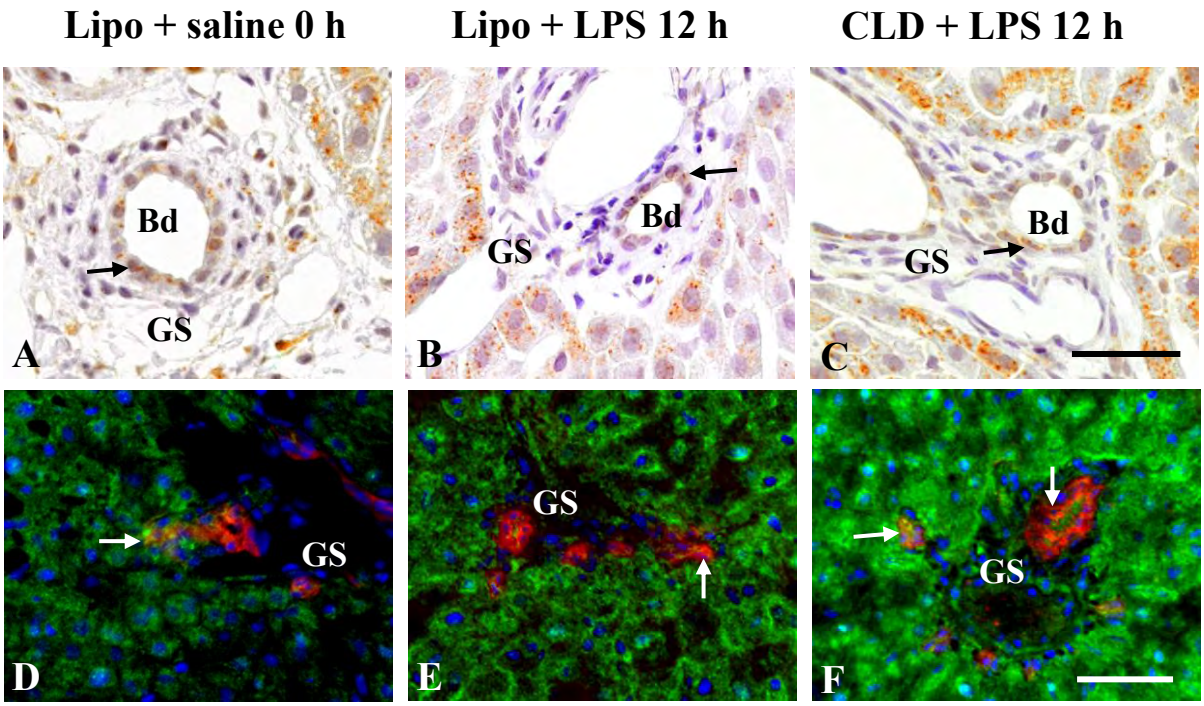
Lipo + saline 0 h
Lipo + LPS 12 h
CLD + LPS 12 h
Bd
GS
A
Bd
GS
B
Bd
GS
C
GS
D
GS
E
GS
F

Fig. 6

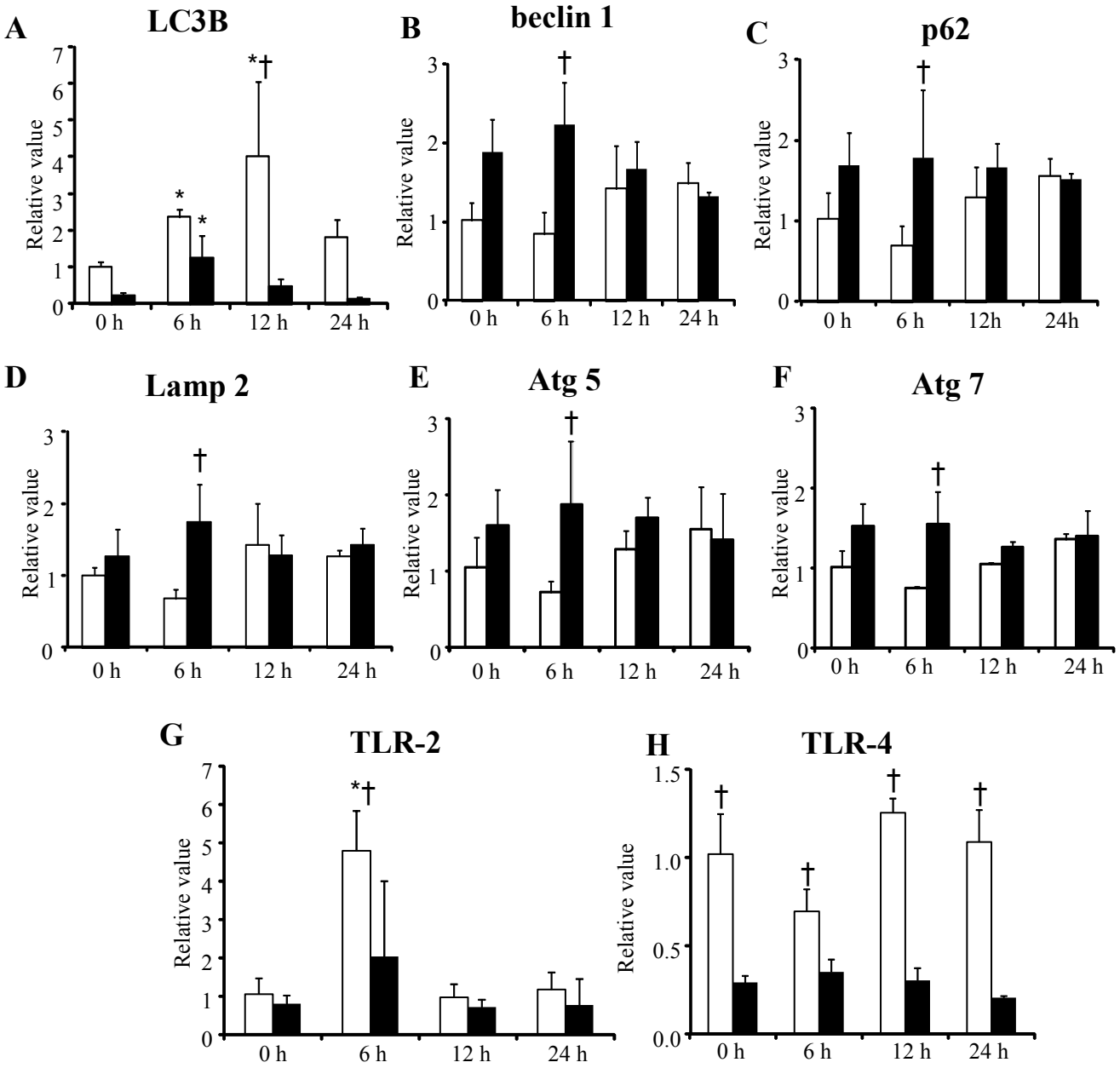
A
LC3B
Relative value
0 h
6 h
12 h
24 h
B
beclin 1
C
p62
12h
24h
D
Lamp 2
E
Atg 5
F
Atg 7
G
TLR-2
H
TLR-4

Fig. 7

Chapter 3

Roles of hepatic macrophages and autophagy in thioacetamide (TAA)-induced hepatotoxicity in lipopolysaccharide (LPS)-pretreated rats

Section I

Time dependent protection of LPS in TAA-induced acute liver injury in rats

Introduction

Liver is the main organ for detoxifying chemicals and drugs, because many chemicals and drugs are metabolized in the liver. Chemically-induced hepatotoxicity represents an important healthcare issue, which causes significant morbidity and mortality. Thus, chemically-induced hepatotoxicity is becoming a major concern in the drug development worldwide. To resolve this issue, various hepatotoxicants have been used for the studies of liver injury models. Thioacetamide (TAA) is one of the popular hepatotoxicant widely used to induce both acute and chronic liver injury (Yovchev et al., 2014). TAA-induced hepatotoxicity occurs through its S-oxide metabolite (TAA-S-dioxide), which interferes with the movement of RNA from the nucleus to the cytoplasm, resulting in structural and functional cellular deformation, including membrane injury (Yovchev et al., 2014; Chen, et al., 2005). The administration of TAA causes hepatocellular necrosis in centrilobular areas in rats (Ide et al., 2003).

Lipopolysaccharide (LPS) is a gram-negative bacterial endotoxin, which can modulate the liver injury in hepatotoxicity (Liu et al., 2000; Roth et al., 1997). Exposure of LPS increases the liver toxicity of some chemicals (galactosamine, ethanol, allyl alcohol and halothane) (Roth et al., 1997; Laskin, 1990); on the contrary, LPS can protect against the hepatotoxicity of some chemicals (acetaminophen and carbon tetrachloride) (Liu et al., 2000). It is well-known that liver is routinely exposed to small amounts of LPS, mainly from gut microbiota through the portal venous blood. Therefore, low dose of LPS might be an important determinant in the pathogenesis of hepatotoxicants. In Chapter 2, the author demonstrated that low dose of LPS (0.1 mg/kg body weight) can activate the hepatic

macrophages and also play a potential role for induction of autophagy in rat livers without altering the histological structures. Thus, the present study was undertaken to determine the roles of activated hepatic macrophages and autophagy in the presence of LPS by using TAA-induced acute liver injury in rats. The author focused on time-dependent effects of LPS before TAA injection

Materials and methods

Animals and experimental procedures

Twenty-four 5-week-old male F344 rats were obtained from Charles River Laboratories Japan (Hino, Shiga, Japan). Rats were maintained in a room under controlled environment at 21±3°C with a 12 h light-dark cycle, and fed a standard rodent chow (DC-8, CLEA Japan, Tokyo, Japan) and supplied with tap water *ad libitum*. After one-week acclimatization, a single intraperitoneal injection of LPS at the dose of 0.1 mg/kg body weight (*Escherechia coli* 055:B5, Sigma-Aldrich, St Louis, MO, USA) were given in 16 rats. Then, four rats at 2 h, 6 h, 12 h and 24 h after LPS injection were given an intraperitoneal injection of TAA dissolved in saline (100 mg/kg body weight; Wako Pure Chemicals, Osaka, Japan), which were expressed as LPS-pretreated TAA-injected rats at 2 h, 6 h, 12 h and 24 h, respectively. Four rats were injected only TAA and designated as alone TAA-injected control rats. The remaining four rats was administered an equal volume of saline and regarded as saline control rats. One day after injection of TAA or saline, all animals were euthanized under deep isoflurane anesthesia. At necropsy, liver tissues were fixed in 10% neutral buffered formalin (NBF) and periodate-lysine-paraformaldehyde (PLP) solution processed by PLP-AMeX (acetone, methyl benzoate and xylene) method (Pervin et al., 2016). A part of liver samples were also immersed in RNAlater^{TM} (Qiagen GmbH, D-40724 Hilden, Germany) and stored at −80^{o}C until mRNA extraction. Blood samples were collected from abdominal aorta at necropsy and separated sera were subjected to biochemical assay for aspartate transaminase (AST), alanine transaminase (ALT), alkaline phosphatase (ALP) and total bilirubin (T. Bil) by SRL Inc. (Tokyo, Japan). The animal experiments were conducted under the institutional guidelines

approved by the ethical committee of Osaka Prefecture University for the Care and Use of Experimental Animals.

Histopathology and immunohistochemistry

NBF-fixed tissues were dehydrated and embedded in paraffin and sectioned at 3-4 μm in thickness. The deparaffinized sections were stained with hematoxylin and eosin (HE) for histopathological examination.

PLP-fixed tissue sections were used in immunohistochemistry with mouse monoclonal antibodies specific for CD163 (clone ED2, 1:300, AbD Serotec, Oxford, UK), CD68 (clone ED1, 1:500, AbD Serotec, Oxford, UK), MHC class II (clone OX6, 1:1000, AbD Serotec, Oxford, UK) and rabbit polyclonal antibody specific for LC3B (1:2000, Sigma-Aldrich Co., MO, USA). After deparaffinization, sections to be labelled for CD68, MHC class II and LC3B were pretreated by microwaving for 20 min in citrate buffer (pH 6.0) and CD163 were pretreated by Proteinase K (100 μg/ml, Dako crop, Glosturb, Denmark) for 10 min at room temperature for antigen retrieval. Then, the tissue sections were stained by Histostainer (Histofine, Nichirei Bioscience Inc., Tokyo, Japan). Briefly, sections were incubated with 5% skimmed milk for 10 min, followed by 1 h incubation with the primary antibodies. After treatment with 3% H_2O_2 for 15 min, horseradish peroxidase-conjugated secondary antibody (Histofine simple stain MAX PO®; Nichirei Inc., Tokyo, Japan) was applied for 30 min. Then, they were incubated with 3, 3'-diaminobenzidine (DAB) (Nichirei Inc., Tokyo, Japan) for 5 min. Sections were counterstained with hematoxylin for 1 min. For negative controls, tissue sections were treated with mouse or rabbit non-immunized serum instead of the primary antibody. Cells expressing CD163, CD68 and MHC class II were counted per 40X field in randomly selected five areas in the perivenular areas of liver. Cytoplasmic LC3B-positive granules within hepatocytes were counted in at least 100 hepatocytes in randomly selected five different perivenular or periportal areas of liver.

Real time reverse transcriptase-polymerase chain reaction (RT-PCR)

Total RNA was extracted from the liver tissues using an SV total RNA isolation system (Promega, Madison, WI, USA) according to the manufacturer's instructions. Two and half μg of total extracted RNA was reverse-transcribed with Superscript VILO reverse transcriptase (Life Technologies, CA, USA). Real time PCR was performed using TaqMan gene expression assays (Life Technologies, Carlsbad, CA, USA) in a PikoReal Real-Time 96 PCR System (Thermo Scientific, CA, Massachusetts, USA). The TaqMan probes specific for the cytokines used were as follows (Assay IDs): monocyte chemoattractant protein-1 (MCP-1), Rn00580555_m1; interleukin-1β (IL-1β), Rn00580432_m1; interferon-γ (IFN-γ), Rn00594078_m1; tumor necrosis factor-α (TNF-α), Rn01525859_g1; transforming growth factor-β1 (TGF-β1), Rn00572010_m1; interleukin-4 (IL-4), Rn01456866_m1; interleukin-6 (IL-6), Rn01410330_m1; interleukin-10 (IL-10), Rn00563409_m1; microtubule associated protein 1 light chain 3 beta (LC3B), Rn02132764_s1; beclin 1, Rn00586976_n1; sequestosome 1 (Sqstm1/p62), Rn00709977_m1; lysosomal associated membrane protein 2 (Lamp 2), Rn00567053_m1; and eukaryotic 18S rRNA (18s rRNA), Hs99999901_s1. The mRNA expression was normalized against the expression of 18s rRNA mRNA as the internal control. The data were analyzed using the comparative C_t method ($^{\Delta\Delta}C_t$ method).

Statistical evaluation

Data obtained were expressed as mean ± standard deviation (SD). Statistical analysis was performed using Tukey-Kramer test. Significance was considered at $P < 0.05$.

Results

Histopathology of liver

In HE-stained sections, normal histology was seen in the liver of saline control rats (Fig. 1A). In alone TAA-injected rats, coagulation necrosis of hepatocytes was seen mainly around centrilobular vein (centrilobular area) of the hepatic lobules, accompanied by

infiltrates of mononuclear cells (Fig. 1B), which are similar to a previous report (Ide et al., 2003). LPS-pretreated TAA-injected rats at 2 h or 6 h showed the similar or slightly low hepatic lesions as compared with those of alone TAA-injected rats (Fig. 1C, D). Interestingly, the hepatic lesions were markedly decreased in LPS-pretreated TAA-injected rats at 12 h and 24 h (Fig. 1E, F).

Blood biochemistry

The values of AST, ALT and ALP were significantly increased in alone TAA-injected rats in comparison with saline control rats (Fig. 2A-C). LPS-pretreated TAA-injected rats at 2 h and 6 h also showed the significant elevation of serum hepatic enzymes in comparison with saline control rats (Fig. 2A-C). However, in LPS-pretreated TAA-injected rats at 12 h and 24 h, the values of AST and ALT did not change as compared with those in saline control rats (Fig. 2A, B). Together with ALP, the values were significantly decreased or tended to be decreased in LPS-pretreated TAA-injected rats at 12 h and 24 h as compared with those of alone TAA-injected rats (Fig. 2A-C). The value of T. Bil was not changed after TAA injection regardless of LPS pretreatment in comparison with saline control rats (Fig. 2D).

Hepatic macrophage populations in rat livers

The kinetics of hepatic macrophages reacting to CD163, CD68 and MHC class II is shown in Fig. 3A-C, respectively. The numbers of $CD163^+$, $CD68^+$ and MHC class II^+ macrophages in liver parenchyma were significantly increased following TAA injection, regardless of LPS pretreatment as compared with those of saline control rats (Fig. 3A-C). In addition, in comparison between alone TAA-injected and LPS-pretreated TAA-injected rats, Kupffer cells reacting to CD163 did not show any difference in their numbers (Fig. 3A). However, the $CD68^+$ exudative macrophages were significantly increased in LPS-pretreated TAA-injected rats at 12 h as compared with those in alone TAA-injected rats (Fig. 3B). By the contrary, the numbers of MHC class II^+ macrophages were significantly decreased in LPS-pretreated TAA-injected rats at 12 h than in alone TAA-injected rats (Fig. 3C).

Expression of mRNA of macrophage-related inflammatory factors

To evaluate the expressions of macrophage-related inflammatory factors, the author investigated the expression of regulatory cytokines and chemokines at mRNA level (Fig. 4A-H). The inflammatory-related factors such as MCP-1(Fig. 4A), IL-1β (Fig. 4B), IFN-γ (Fig. 4C) and IL-4 (Fig. 4G) mRNAs were significantly increased in alone TAA-injected rats as compared with those of saline control rats. In LPS-pretreated TAA-injected rats at 2 h, 12 h or 24 h, MCP-1 (Fig. 4A), IL-1β (Fig. 4B) and IL-4 (Fig. 4G) mRNAs were significantly increased as compared with those in saline control rats. Additionally, in comparison between the alone TAA-injected and LPS-pretreated TAA-injected rats, these factors were not changed statistically, except TNF-α in LPS-pretreated TAA-injected rats at 2 h (Fig. 4D).

Autophagy and autophagy-related factors

The immunohistochemistry with autophagy marker, LC3B, showed that LC3B-positive cytoplasmic granules/dots in hepatocytes were seen at basal level in saline control rats (Fig. 5A). Compared to the expression of saline control rats, LC3B-positive hepatocyte numbers as well as intra-cytoplasmic LC3B-labeled dots were increased in alone TAA-injected rats (Fig. 5B) and mainly localized around the necrotic areas. However, the LC3B expression was greatly increased in LPS-pretreated TAA-injected rats at 2 h to 24 h in comparison with saline control rats or alone TAA-injected rats (Fig. 5C-G).

At mRNA level, the autophagy-related genes such as LC3B, Lamp 2, beclin 1 and p62 did not show any significant difference in the alone TAA-injected or LPS-pretreated TAA-injected rats as compared with those of saline control rats (Fig. 6A-D). However, in LPS-pretreated TAA-injected rats at 2 h, the LC3B mRNA was significantly decreased than that in saline control rats (Fig. 6A).

Discussion

Alteration of TAA-induced hepatic lesions by LPS pretreatment

TAA is a thiono-sulphur containing compound that undergoes extensive metabolism by the mixed oxidase system functions in the liver (Fujisawa et al., 2011; Ramaiah et al., 2001). TAA-induced hepatic lesions are characteristically seen in the centrilobular areas of liver as hepatocyte necrosis/degeneration accompanied with inflammatory cells (Wijesundera et al., 2014b; Ide et al., 2003). Here, the author demonstrated that low dose of LPS pretreatment protected against TAA-induced acute liver injury depending on LPS injection time points before TAA treatment. LPS pretreatment at 2 h and 6 h before TAA injection did not clearly influence the TAA-induced hepatic lesions, which were also supported by liver enzymes; AST, ALT, ALP and T. Bil values showed no significant difference from the alone TAA-injected rats. Interestingly, on the contrary, LPS treatment before TAA injection at 12 h or 24 h showed a good protective phenomenon against TAA-induced hepatotoxicity; the hepatocyte necrosis was reduced markedly accompanied by decreased levels in AST, ALT and ALP in comparison with those of alone TAA-injected rats. These findings indicated that LPS pretreatment could protect the TAA-induced hepatotoxicity based on the time points before TAA injection, particularly with the greatest cytoprotection at 12 h and 24 h. It is reported that LPS pretreatment protected against acetaminophen- and carbon tetrachloride-induced liver injury (Ishikawa et al., 1990; Williams, 1988). On the contrary, simultaneous administration of LPS with some hepatotoxicants results in increased hepatotoxicity and lethality (Roth et al., 1997; Laskin, 1990).

The role of hepatic macrophages in the protection of TAA-induced hepatic lesions

Hepatic macrophages are important as non-parenchymal cells of liver comprising 10-20% of liver-constituting cells (Godoy et al., 2013). They are versatile in nature, playing crucial roles in regulation of inflammation and repair in various pathological conditions (Beljaars et al., 2014; Tacke and Zimmermann, 2014; Pellicoro et al., 2012). To identify the hepatic macrophages, the author used CD163, CD68 and MHC class II antibodies. In this study, the numbers of $CD163^{+}$, $CD68^{+}$ and MHC class II^{+} macrophages were significantly increased after TAA alone injection, indicating that macrophages with heterogeneous immunophenotypes participated in TAA-induced hepatic lesion

development. However, in LPS-pretreated TAA-injected rats, the number of Kupffer cells reacting to CD163 did not show any difference from alone TAA-injected rats, whereas the numbers of exudative macrophages expressing CD68 were significantly increased in LPS-pretreated TAA-injected rats at 12 h in comparison with those in alone TAA-injected rats; the increased number of $CD68^+$ exudative macrophages may imply the enhanced phagocytosis (Haralanova-Ileava et al., 2005; Damoiseaux et al., 1994). MHC class II^+ macrophages were significantly decreased in LPS-pretreated TAA-injected rats at 12 h. It is reported that MHC class II antigen is expressed in mature dendritic cells and activated macrophages as the antigen presenting cells (Ide et al., 2005; Yamashiro et al., 1994). The reduction of MHC class II-expressing macrophages in LPS-pretreated TAA-injected rats was unclear.

The protective effects of LPS pretreatment at 12 h and 24 h before TAA injection might be mediated by cytokines which are related to hepatic macrophage functions. In the present study, M1-related inflammatory factors such as MCP-1 and IL-1β were significantly increased in LPS-pretreated TAA-injected rats at 2 h, 12 h and 24 h. The hepatic macrophages are the main source for the production of these regulatory cytokines. LPS acts as a potent activator of hepatic macrophage populations, resulting in secretion of cytokines capable of modulating the inflammatory conditions. The relation of inflammatory factors with cytoprotection of LPS pretreatment in TAA hepatotoxicity was not clear.

The role of hepatocyte autophagy in the protection of TAA-induced hepatic lesions

Beside macrophages, autophagy may also contribute to liver physiology and pathology. Generally, autophagy is a highly dynamic and multistep process in eukaryotes involved degradation of cytoplasmic components by lysosomes. It is reported that the autophagy is involved in chemically-induced liver toxicity, although deep insights into the mechanisms remain unclear. In Section II of Chapter 2, the author also showed that low dose of LPS (0.1 mg/kg body weight) induced autophagy in hepatocytes as well as hepatic macrophages. In this study, TAA administration resulted in increased hepatocyte

autophagy, which is similar to findings in TAA-induced liver injury in mice (Hernandez-Gea et al., 2012). In addition, LPS treatment before TAA injection significantly increased the autophagy in hepatocytes in comparison with alone TAA-injected rats. Autophagy should serve as cellular protective mechanisms against acute liver injury by chemicals such as acetaminophen (Ni et al., 2012), ethanol (Wu et al., 2012; Ding et al., 2010) and efavirenez (Apostolova et al., 2011). Therefore, activated autophagy might be an important factor related to the decrease in TAA-induced hepatotoxicity, particularly at 12 h and 24 h.

In conclusion, the present study showed that LPS pretreatment protected against TAA-induced acute liver lesions depending on time points before TAA injection. Induced hepatic macrophages (particularly $CD68^+$ exudative macrophages) and activated autophagy might participate partly in the protective phenomenon. The present findings would provide a significant insight into the molecular mechanism of hepatotoxicity. However, detailed study is necessary for better understanding of the underlining molecular mechanisms.

Summary

Lipopolysaccharide (LPS), a bacterial endotoxin, can influence the pathogenesis of liver injury. Here, the author investigated the effects of low dose of LPS in TAA-induced hepatotoxicity as a protective mechanism. Male F344 rats were pretreated with LPS (0.1 mg/kg body weight, intraperitoneally) at 2 h, 6 h, 12 h and 24 h before TAA injection (100 mg/kg body weight, intraperitoneally). Histopathologically, TAA injection produced centrilobular necrosis in the liver. LPS-pretreated TAA-injected rats at 2 h and 6 h showed similar effect on the hepatic lesions to alone TAA-injected rats, but rats at 12 h and 24 h showed a marked reduction in the hepatic lesions as compared with those of alone TAA-injected rats. Consistently, AST, ALT and ALP values tended to be decreased in the LPS-pretreated rats at 12 h or 24 h. At each time point, LC3B-labeled cytoplasmic granules in hepatocytes were significantly increased in LPS-pretreated rats. Additionally, at each time point of LPS pretreatment, $CD163^+$, $CD68^+$ and MHC class II^+ macrophages were significantly increased after TAA injection; in particular, $CD68^+$ exudative macrophages were significant increased or tended to be increased in LPS-pretreated TAA-injected rats at 12 h or 24 h. Inflammatory-related factors such as MCP-1, IL-1β and IL-4 were significantly increased in LPS-pretreated rats. The present study demonstrated that LPS pretreatment protected against TAA-induced liver lesions depending on time points before TAA injection which might be related to the LPS-induced hepatic macrophages and LPS-activated hepatocyte autophagy. Therefore, the activation of hepatic macrophages and autophagy could constitute a therapeutic approach against hepatic complications induced by chemicals or drugs.

Figure legends

Fig. 1. A-F: Histopathology of livers in saline control, alone TAA-injected and LPS-pretreated TAA-injected rats on day 1 of TAA injection. The hepatic architecture is normal in saline control rats (A); centrilobular coagulation necrosis is seen in alone TAA-injected rats (B) and LPS-pretreated rats at 2 h (C) and 6 h (D). The lesions are markedly decreased in LPS-pretreated TAA-injected rats at 12 h (E) and 24 h (F). Dotted lines indicate the necrotic area. h: hour, CV: central vein. Bar = 200 μm.

Fig. 2. A-D: Blood biochemical analyses in saline control, alone TAA-injected and LPS-pretreated TAA-injected rats on day 1 of TAA injection. Aspartate transaminase (AST) (A), alanine transaminase (ALT) (B), alkaline phosphatase (ALP) (C) and total bilirubin (T. Bil) (D). Tukey's test; *, P <0.05, significantly different from saline control rats; †, P <0.05, significantly different from alone TAA-injected rats. h: hour.

Fig. 3. The kinetics of macrophages reacting to CD163 (A), CD68 (B) and MHC class II (C) in the liver of saline control, alone TAA-injected and LPS-pretreated TAA-injected rats on day 1 of TAA injection. Tukey's test; *, P <0.05, significantly different from saline control rats; †, P <0.05, significantly different from alone TAA-injected rats. h: hour.

Fig. 4. A-H: mRNA expressions for inflammatory-related factors in saline control, alone TAA-injected and LPS-pretreated TAA-injected rats on day 1 of TAA injection. Tukey's test; *, P <0.05, significantly different from saline control rats; †, P <0.05, significantly different from alone TAA-injected rats. h: hour.

Fig. 5. A-F: LC3B Immunohistochemistry of livers in saline control, alone TAA-injected and LPS-pretreated TAA-injected rats on day 1 of TAA injection. The LC3B-positive dots are present as basal level in saline control rats (A); the activated expression is seen in alone TAA-injected rats (B) and LPS-pretreated TAA-injected rats at 2 h (C), 6 h (D), 12 h (E) and 24 h (F). Inset shows LC3B-labeled dots

within hepatocyte of higher magnification. G. The mean number of LC3B-labeled cytoplasmic dots per hepatocyte is shown in graph. h: hour, CV: central vein. Bar = 100 μm.

Fig. 6. A-D: mRNA expressions for autophagy-related genes in saline control, alone TAA-injected and LPS-pretreated TAA-injected rats on day 1 of TAA injection. LC3B mRNAs (A) are significantly decreased in LPS-pretreated rats at 2 h, whereas Lamp 2 (B), beclin 1 (C) and p62 (D) mRNAs do not show any change. Tukey's test; *, $P < 0.05$, significantly different from saline control rats. h: hour.

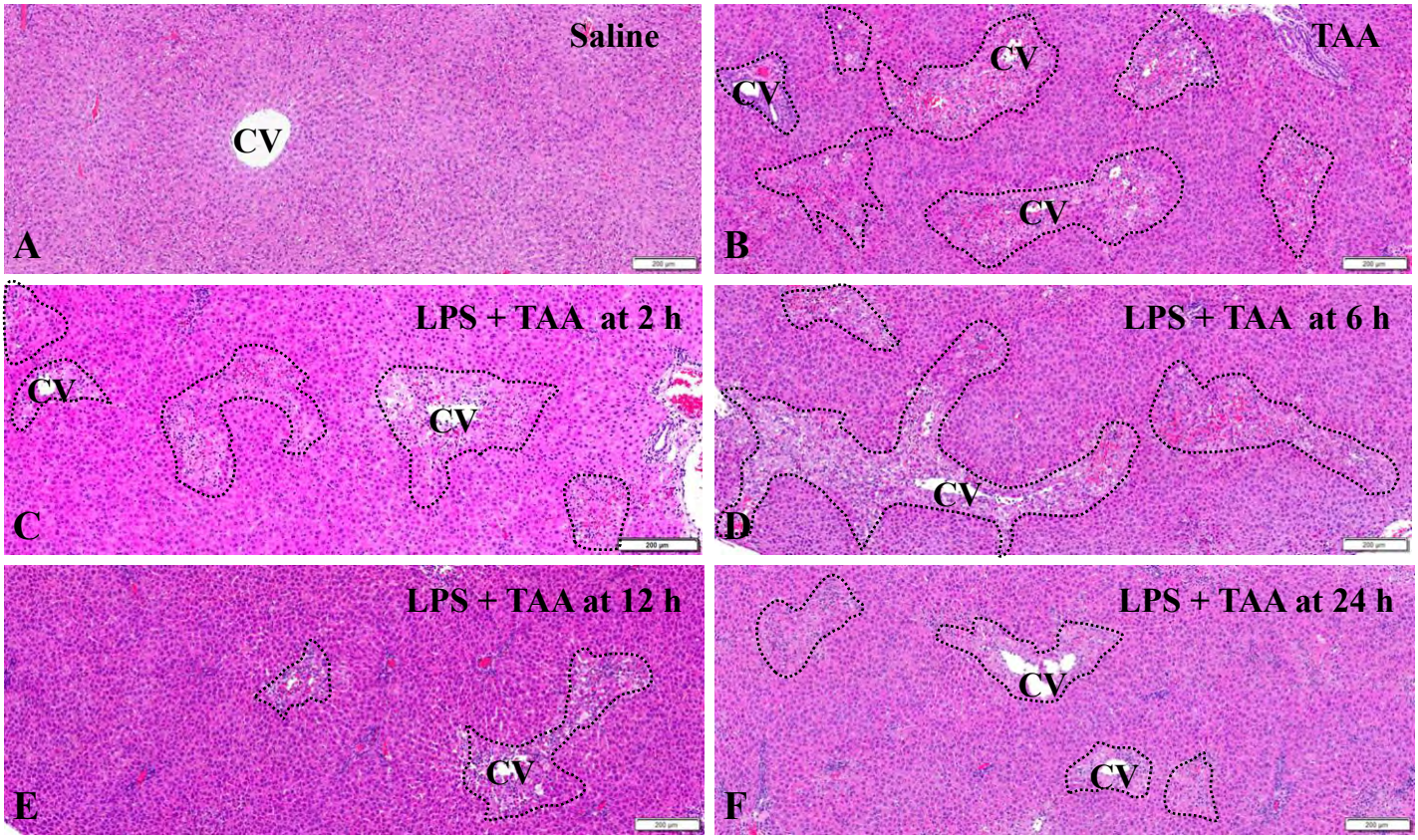
Saline
CV
A
TAA
CV
CV
CV
B
LPS + TAA at 2 h
CV
CV
C
LPS + TAA at 6 h
CV
D
LPS + TAA at 12 h
CV
E
LPS + TAA at 24 h
CV
CV
F

Fig. 1

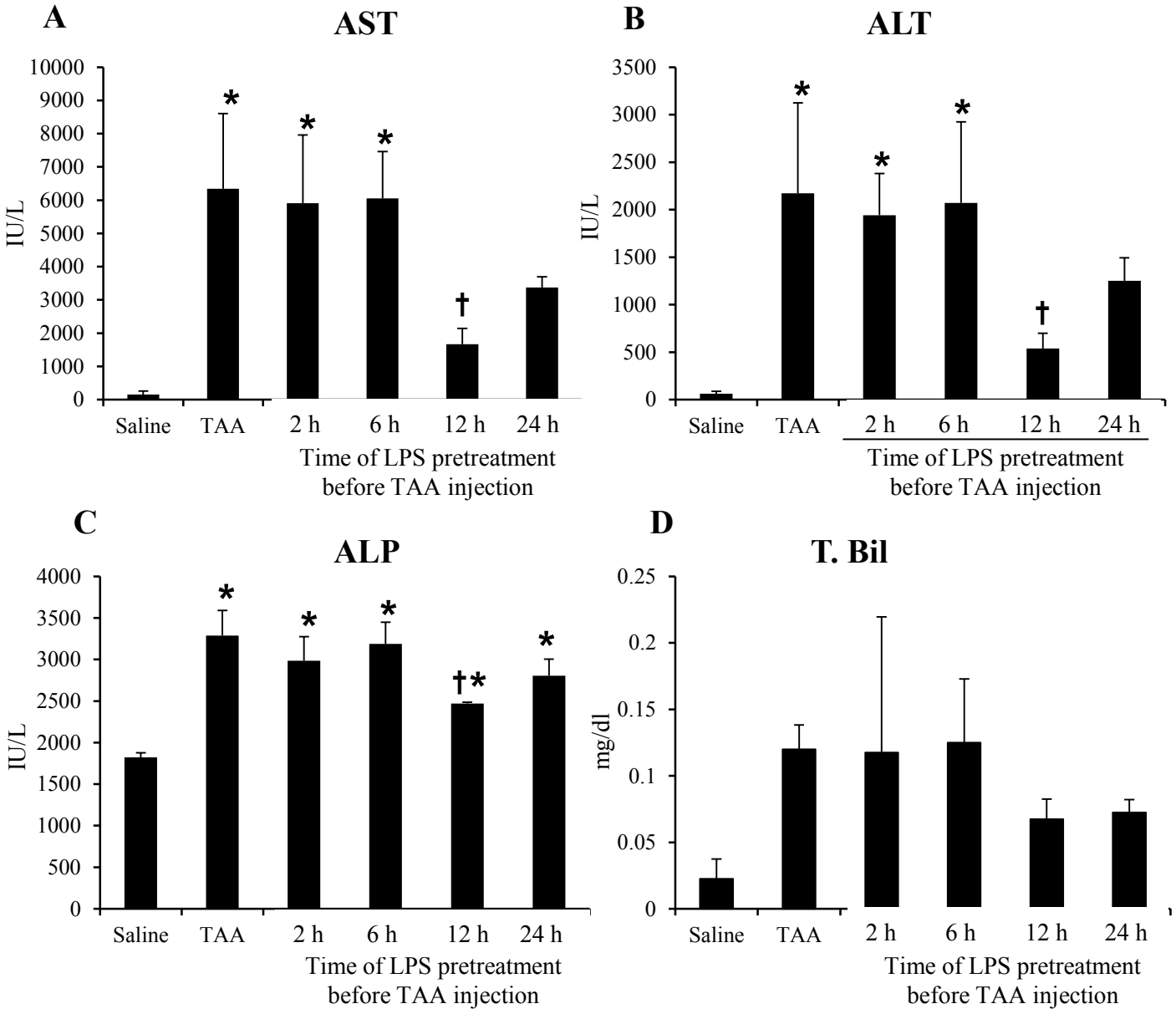
A
AST
IU/L
10000
9000
8000
7000
6000
5000
4000
3000
2000
1000
0
Saline
TAA
2 h
6 h
12 h
24 h
Time of LPS pretreatment
before TAA injection
B
ALT
IU/L
3500
3000
2500
2000
1500
1000
500
0
Saline
TAA
2 h
6 h
12 h
24 h
Time of LPS pretreatment
before TAA injection
C
ALP
IU/L
4000
3500
3000
2500
2000
1500
1000
500
0
Saline
TAA
2 h
6 h
12 h
24 h
Time of LPS pretreatment
before TAA injection
D
T. Bil
mg/dl
0.25
0.2
0.15
0.1
0.05
0
Saline
TAA
2 h
6 h
12 h
24 h
Time of LPS pretreatment
before TAA injection

Fig. 2

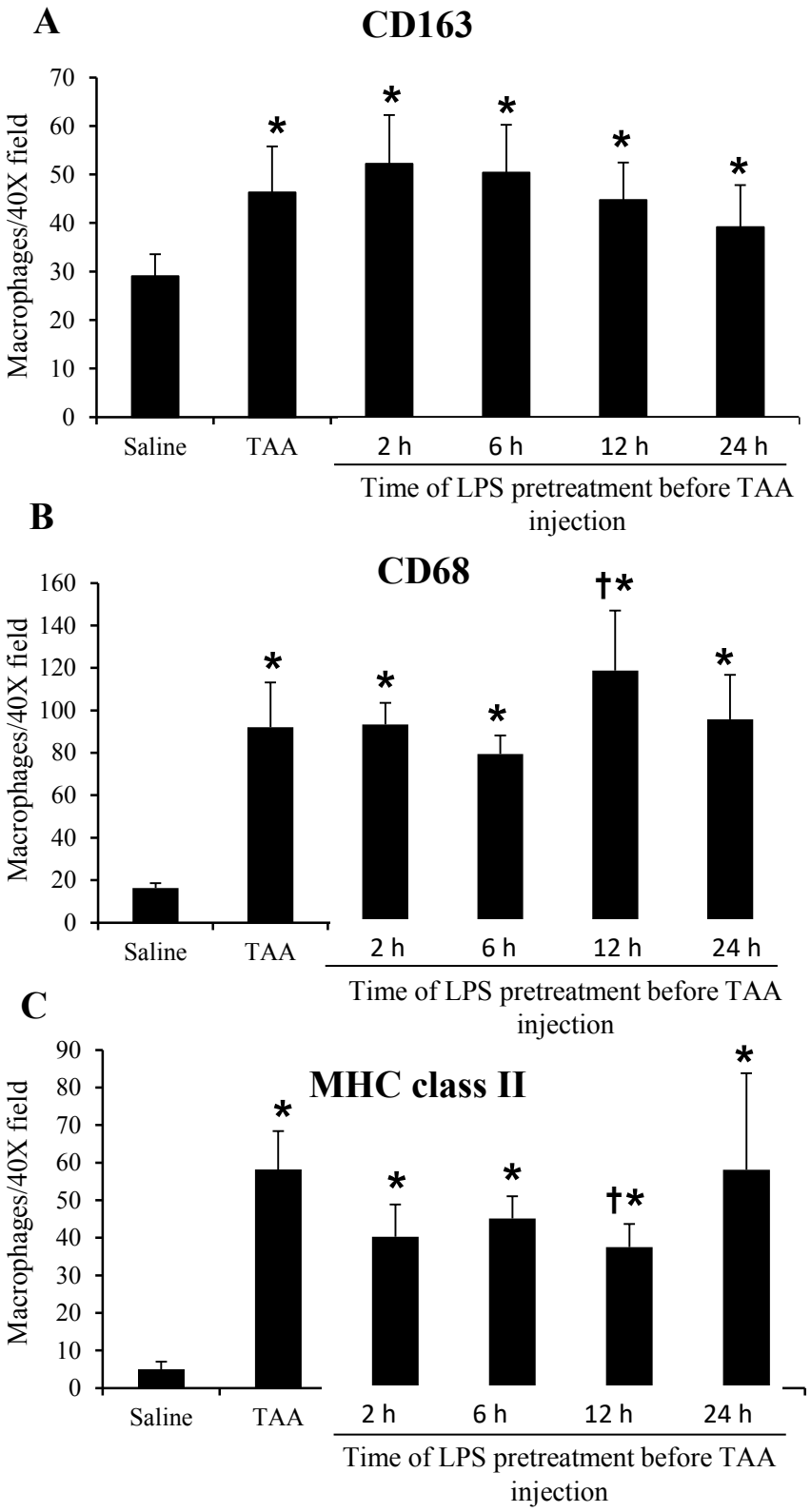
A
CD163
Macrophages/40X field
70
60
50
40
30
20
10
0
Saline
TAA
2 h
6 h
12 h
24 h
Time of LPS pretreatment before TAA injection
B
CD68
Macrophages/40X field
160
140
120
100
80
60
40
20
0
Saline
TAA
2 h
6 h
12 h
24 h
Time of LPS pretreatment before TAA injection
C
MHC class II
Macrophages/40X field
90
80
70
60
50
40
30
20
10
0
Saline
TAA
2 h
6 h
12 h
24 h
Time of LPS pretreatment before TAA injection

Fig. 3

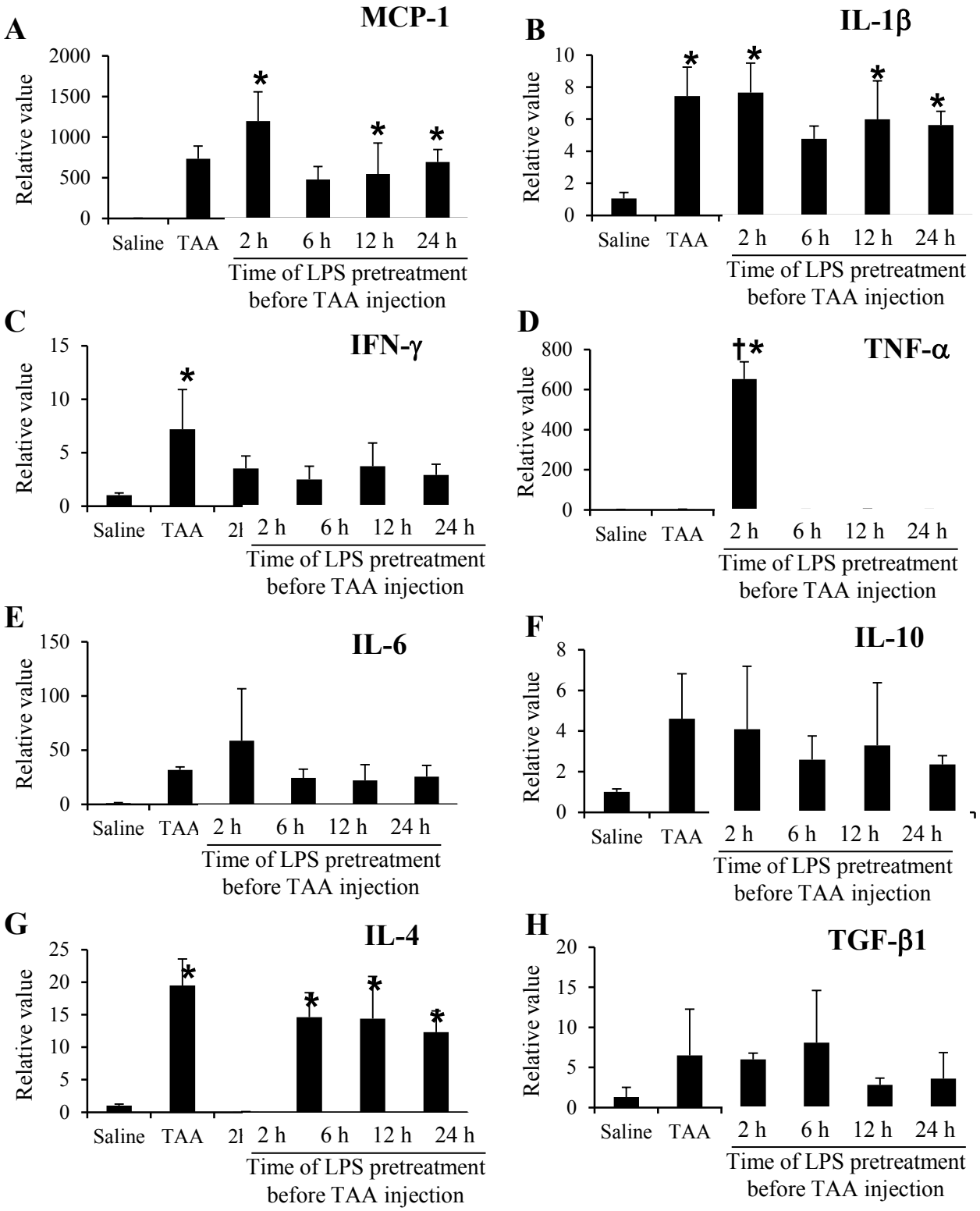
A
MCP-1
Relative value
2000
1500
1000
500
0
Saline
TAA
2 h
6 h
12 h
24 h
Time of LPS pretreatment before TAA injection
B
IL-1β
Relative value
10
8
6
4
2
0
Saline
TAA
2 h
6 h
12 h
24 h
Time of LPS pretreatment before TAA injection
C
IFN-γ
Relative value
15
10
5
0
Saline
TAA
2 h
6 h
12 h
24 h
Time of LPS pretreatment before TAA injection
D
TNF-α
Relative value
800
600
400
200
0
Saline
TAA
2 h
6 h
12 h
24 h
Time of LPS pretreatment before TAA injection
E
IL-6
Relative value
150
100
50
0
Saline
TAA
2 h
6 h
12 h
24 h
Time of LPS pretreatment before TAA injection
F
IL-10
Relative value
8
6
4
2
0
Saline
TAA
2 h
6 h
12 h
24 h
Time of LPS pretreatment before TAA injection
G
IL-4
Relative value
25
20
15
10
5
0
Saline
TAA
2 h
6 h
12 h
24 h
Time of LPS pretreatment before TAA injection
H
TGF-β1
Relative value
20
15
10
5
0
Saline
TAA
2 h
6 h
12 h
24 h
Time of LPS pretreatment before TAA injection

Fig. 4

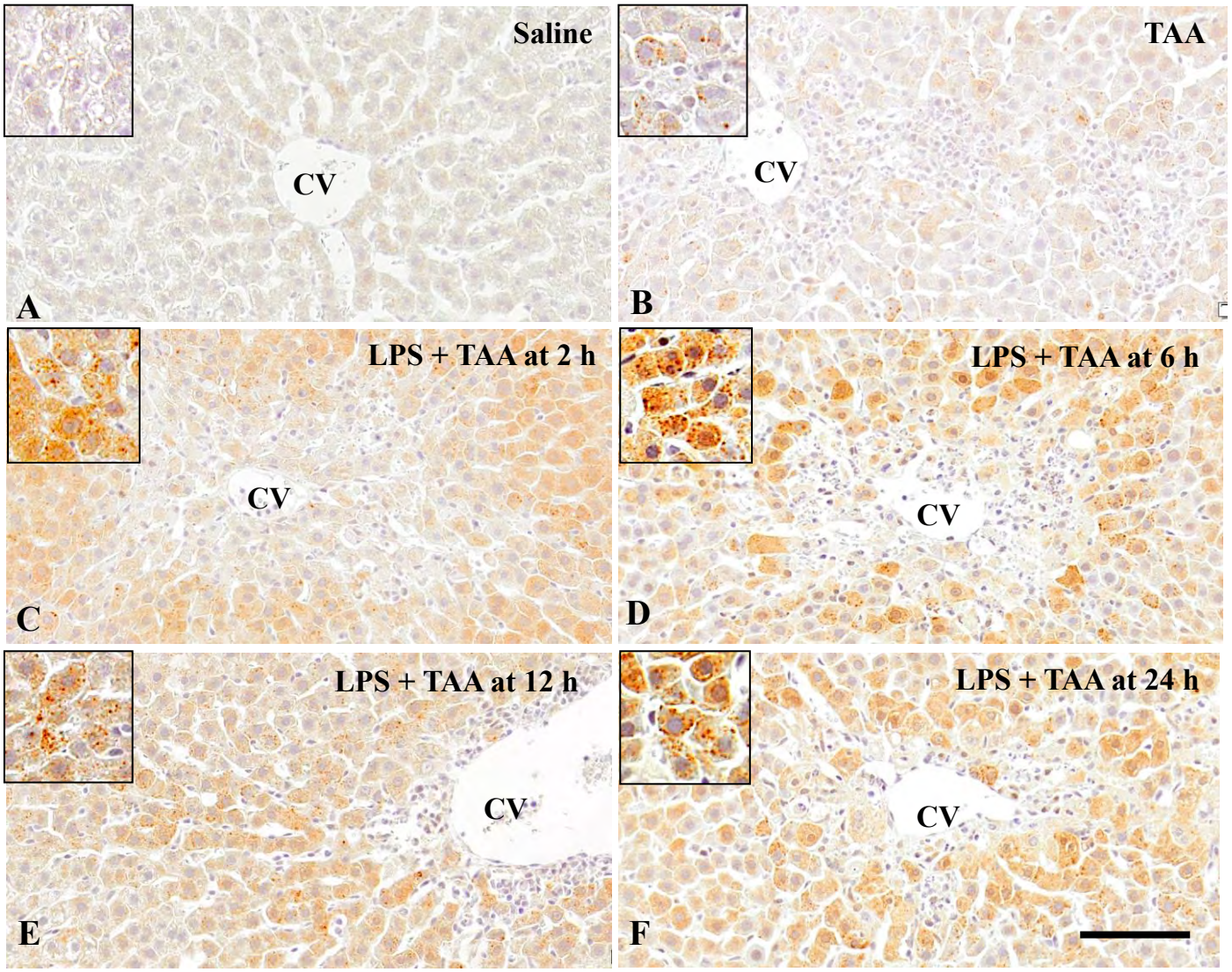
Saline
CV
A
TAA
CV
B
LPS + TAA at 2 h
CV
C
LPS + TAA at 6 h
CV
D
LPS + TAA at 12 h
CV
E
LPS + TAA at 24 h
CV
F
LC3B-labeled dots/ hepatocyte
0
2
4
6
8
10
12
*
†*
†*
†*
†*
Saline
TAA
2 h
6 h
12 h
24 h
Time of LPS pretreatment
Before TAA injection
G

Fig. 5

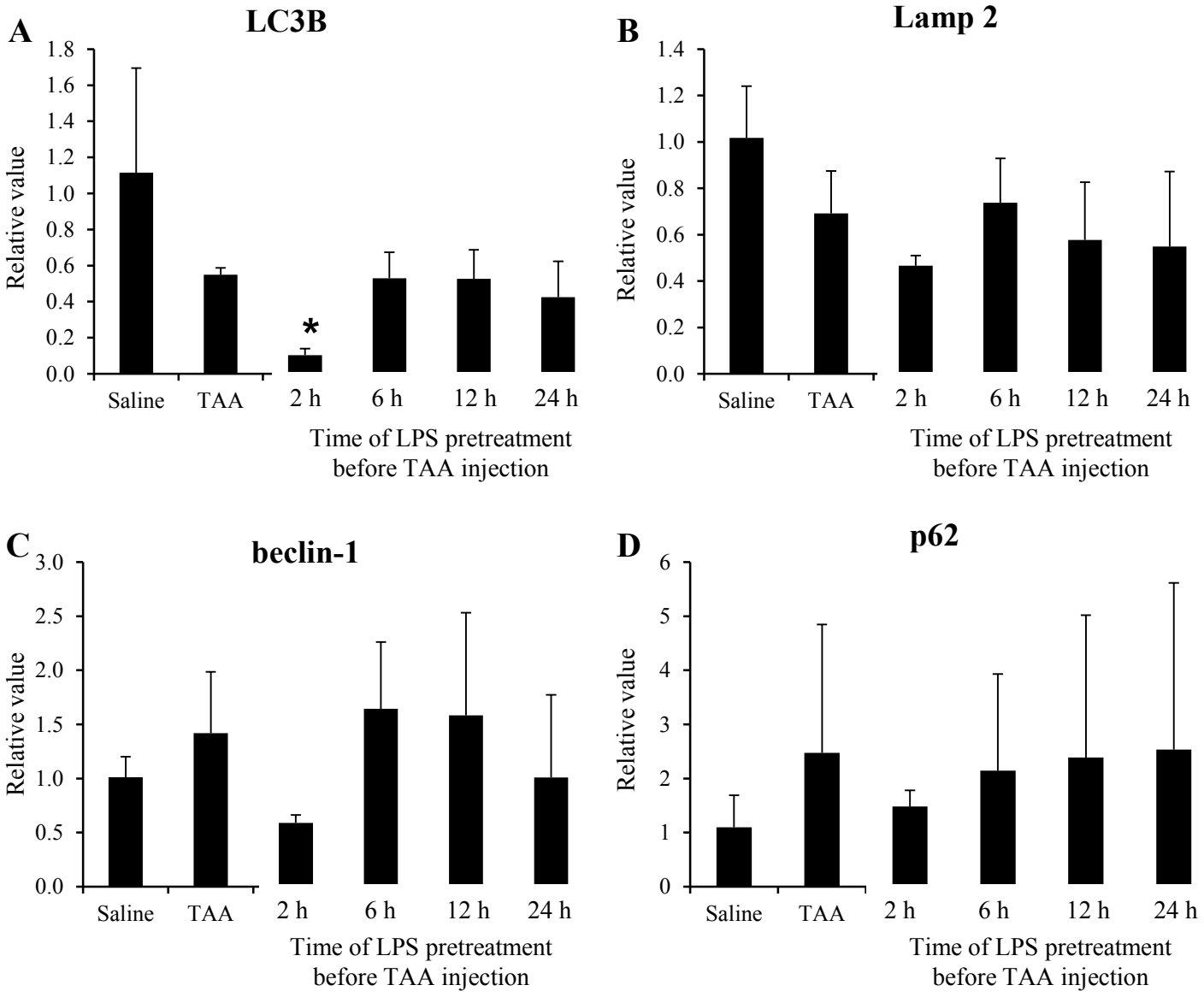
A
LC3B
Relative value
1.8
1.6
1.4
1.2
1.0
0.8
0.6
0.4
0.2
0.0
*
Saline
TAA
2 h
6 h
12 h
24 h
Time of LPS pretreatment
before TAA injection
B
Lamp 2
Relative value
1.4
1.2
1.0
0.8
0.6
0.4
0.2
0.0
Saline
TAA
2 h
6 h
12 h
24 h
Time of LPS pretreatment
before TAA injection
C
beclin-1
Relative value
3.0
2.5
2.0
1.5
1.0
0.5
0.0
Saline
TAA
2 h
6 h
12 h
24 h
Time of LPS pretreatment
before TAA injection
D
p62
Relative value
6
5
4
3
2
1
0
Saline
TAA
2 h
6 h
12 h
24 h
Time of LPS pretreatment
before TAA injection

Fig. 6

Section II

LPS-mediated cytoprotection in LPS-pretreated rat liver lesions induced by TAA in terms of hepatic macrophages and autophagy

Introduction

Thioacetamide (TAA) is a thiono-sulfur containing compound, which has been originally used as a plant fungicide. Due to its necrogenic (Fujisawa et al., 2011) and carcinogenic (Rommer et al., 2014; Gervasi et al., 1989) properties, TAA is commonly used as animal models for acute liver injury, liver fibrosis and cirrhosis. After administration, TAA is bioactivated in the liver by cytochrome P450 (CYP450) and flavin-containing mono-oxygenase systems to sulfine (sufoxide) and sulfene (sulfone) metabolites, of which activated metabolites cause centrilobular coagulation necrosis in the liver (Ide et al., 2005).

Macrophages are an essential component of innate immunity and are central in regulating the pathogenesis of acute and chronic liver injury. Activated macrophages play major roles in the pathogenesis of TAA-induced liver injury (Golbar et al., 2016; Wijesundera et al., 2014b; Wojcik et al., 2012). In particular, the divergent types of macrophages, which can be identified by specific molecules such as CD68, CD163, CD204, MHC class II, Iba-1 and Galectin-3 (Gal-3) in immunohistochemistry, may participate in the hepatic injury induced by TAA (Golbar et al., 2016; Wijesundera et al., 2014b; Wojcik et al., 2012). These macrophages are derived from bone marrow-originated blood monocytes, histiocytes and dendritic cells. These macrophages also produce and release potent inflammatory mediators, thereby participating in liver injury. Because of the

high plasticity and flexibility (Sica and Mantovani, 2012), macrophages are a focusing point in chemically-induced hepatotoxicity.

Beside macrophages, autophagy is also an important component of innate immunity. Like macrophages, autophagy is another vital candidate, who contributes to the pathogenesis of chemically-induced liver injury. Autophagy is a catabolic lysosomal degradation process that degrades cytoplasmic materials including misfolded proteins, dysfunctional organelles and invading pathogens (Ishida and Nagata, 2009; Komatsu et al., 2005; Nakagawa et al., 2004); these orchestrated pathway is crucial for development, differentiation, homeostasis, and survival of cells. Autophagy in liver can be activated by various liver diseases (Ueno and Komatsu, 2017). Therefore, autophagy is considered a targeting issue for research in liver diseases.

In liver, hepatic macrophages and autophagy may be activated by low dose of lipopolysaccharide (LPS). In Section I of Chapter 3, the author showed that the low dose of LPS (0.1 mg/kg body weight) can protect against TAA-induced acute liver injury; particularly, LPS pretreatment at 12 h and 24 h before TAA injection was the most effective to reduce the hepatic lesions. In Section II of Chapter 3, the author conducted further study to clarify the possible underling molecular mechanisms of LPS-mediated cytoprotection in TAA-induced acute liver injury in rats using LPS-pretreated rats at 2 h or 24 h.

Materials and methods

Animals and experimental procedures

Sixty-four 5-week-old male F344 rats were obtained from Charles River Laboratories Japan (Hino, Shiga, Japan). Rats were maintained in a room under controlled environment at 21±3°C with a 12 h light-dark cycle, and fed a standard rodent chow (DC-8, CLEA Japan, Tokyo, Japan) and tap water *ad libitum*. After one-week acclimatization, rats were randomly divided into two groups: LPS-pretreated group at 2 h and LPS-pretreated group at 24 h. Sixteen rats from each group were injected intraperitoneally once with LPS

(0.1 mg/kg body weight; *Escherechia coli* 055:B5; Sigma-Aldrich, St Louis, MO, USA) at 2 h or 24 h before TAA injection and the remaining sixteen rats received physiological saline instead of LPS. TAA dissolved in saline (100 mg/kg body weight; Wako Pure Chemicals, Osaka, Japan) was injected to thirty two rats (16 rats in LPS + TAA and 16 rats in saline + TAA) 2 h after LPS administration (LPS-pretreated group at 2 h), whereas TAA injection was also done in thirty two rats (16 rats in LPS + TAA and 16 rats in saline + TAA) 24 h after LPS administration (LPS-pretreated group at 24 h). Four rats were sacrificed on day 0, 1, 2 and 3 after TAA injection under deep isoflurane anesthesia. Blood samples were collected from abdominal aorta at necropsy and separated sera were subjected to biochemical assay for aspartate transaminase (AST), alanine transaminase (ALT), alkaline phosphatase (ALP) and total bilirubin (T. Bil) by SRL Inc. (Tokyo, Japan). The animal experiments were conducted under the institutional guidelines approved by the ethical committee of Osaka Prefecture University for the Care and Use of Experimental Animals.

Histopathology and immunohistochemistry

Liver tissues from the left lateral lobe were collected and immediately fixed in 10% neutral buffered formalin (NBF) and periodate-lysine-paraformaldehyde (PLP) solution processed by PLP-AMeX (acetone, methyl benzoate and xylene) method (Pervin et al., 2016). NBF-fixed tissues were dehydrated and embedded in paraffin and sectioned at 3-4 μm in thickness. The deparaffinized sections were stained with hematoxylin and eosin (HE) for histopathological examination. TAA-induced lesions were analyzed morphologically using a virtual slide scanner (VS-120, Olympus, Tokyo, Japan).

Tissue sections fixed in PLP were used in immunohistochemistry with mouse monoclonal antibodies specific for CD163 (clone ED2, 1:300, AbD Serotec, Oxford, UK), CD68 (clone ED1, 1:500, AbD Serotec, Oxford, UK), MHC class II (clone OX6, 1:1000, AbD Serotec, Oxford, UK) and rabbit polyclonal antibody specific for LC3B (1:2000, Sigma-Aldrich Co., MO, USA). After deparaffinization, sections to be labelled for CD68, MHC class II and LC3B were pretreated by microwaving for 20 min in citrate buffer (pH

6.0) and CD163 were pretreated by Proteinase K (100 μg/ml) for 10 min at room temperature for antigen retrieval. Then, the tissue sections were stained by Histostainer (Histofine, Nichirei Bioscience Inc., Tokyo, Japan). Briefly, sections were incubated with 5% skimmed milk for 10 min, followed by 1 h incubation with primary antibodies. After treatment with 3% H_2O_2 for 15 min, horseradish peroxidase-conjugated secondary antibody (Histofine simple stain MAX PO®; Nichirei Inc., Tokyo, Japan) was applied for 30 min. Then, they were incubated with 3, 3'-diaminobenzidine (DAB) (Nichirei Inc., Tokyo, Japan) for 5 min. Sections were counterstained with hematoxylin for 1 min. For negative controls, tissue sections were treated with mouse or rabbit non-immunized serum instead of the primary antibody. Cells expressing CD163, CD68 and MHC class II were counted per 40X field in randomly selected five areas in the perivenular areas of the liver. Cytoplasmic LC3B-positive granules within hepatocytes were counted in at least 100 hepatocytes in randomly selected five different perivenular or periportal areas of the liver.

Terminal deoxyribonucleotide transferase (TdT)-mediated deoxyuridine triphosphate nick end labeling (TUNEL)

A standard *in situ* TUNEL method (Appop Tag® Peroxidase In situ Apoptosis Detection Kit, Millipore, Bedford, USA) was used for detection of DNA fragmentation in the apoptotic cells according to manufacturer's instructions. NBF-fixed and deparaffinized tissue sections were retrieved with Proteinase K (100 μg/ml) for 20 min, and then, with 3% H_2O_2 for 20 min to inactivate endogenous peroxidases. Afterwards, the sections were incubated with TdT enzyme and digoxigenin DNA labeling mixture in TdT reaction buffer for 60 min at 37°C. Then, the sections were treated with horseradish peroxidase-conjugated anti-digoxigenin for 60 min at room temperature. The sections were visualized with DAB (Vector Laboratories). Negative control sections were incubated with distilled water instead of TdT enzyme. The number of TUNEL-positive hepatocytes was counted per 40X field and compared with total number of hepatocytes.

Real time reverse transcriptase-polymerase chain reaction (RT-PCR)

Liver samples from the left median lobe were immediately immersed in RNAlater^{TM} (Qiagen GmbH, Hilden, Germany) overnight at 4^{o}C and stored at −80^{o}C until use. Total RNA was extracted from liver tissues by using an SV total RNA isolation system (Promega, Madison, WI, USA) according to the manufacturer's instructions. Two and half μg of total extracted RNA was reverse-transcribed with Superscript VILO reverse transcriptase (Life Technologies, CA, USA). Real time PCR was performed using TaqMan gene expression assays (Life Technologies, Carlsbad, CA, USA) in a PikoReal Real-Time 96 PCR System (Thermo Scientific, CA, Massachusetts, USA). The TaqMan probes specific for the cytokines used were as follows (Assay IDs): monocyte chemoattractant protein-1 (MCP-1), Rn00580555_m1; interleukin-1β (IL-1β), Rn00580432_m1; interferon-γ (IFN-γ), Rn00594078_m1; tumor necrosis factor-α (TNF-α), Rn01525859_g1; transforming growth factor-β1 (TGF-β1), Rn00572010_m1; interleukin-4 (IL-4), Rn01456866_m1; interleukin-6 (IL-6), Rn01410330_m1; interleukin-10 (IL-10), Rn00563409_m1; microtubule associated protein 1 light chain 3 beta (LC3B), Rn02132764_s1; beclin 1, Rn00586976_n1; sequestosome 1 (Sqstm1/p62), Rn00709977_m1; lysosomal associated membrane protein 2 (Lamp 2), Rn00567053_m1; and eukaryotic 18S rRNA (18s rRNA), Hs99999901_s1. The mRNA expression was normalized against expression of the 18s rRNA mRNA as the internal control. The data were analyzed using the comparative C_t method ($^{\Delta\Delta}C_t$ method).

Statistical evaluation

Obtained data were expressed as mean ± standard deviation (SD). Statistical analysis was performed using Tukey-Kramer test. Significance was considered at $P < 0.05$.

Results

Histopathology of LPS-pretreated TAA-induced rat livers

In LPS-pretreated group at 2 h, normal histology of liver was seen on day 0 in saline + TAA and LPS + TAA rats (Fig. 1A, B). The TAA-induced liver lesions began to start on day 1 in saline + TAA and LPS + TAA rats, comprising centrilobular hepatocyte degeneration/necrosis and being accompanied with mononuclear cell infiltrates (Fig. 1C, D). The histological changes on day 2 became more intensive in saline + TAA rats than those in LPS + TAA rats (Fig. 1E, F). In addition, the pathological score showed that LPS pretreatment did not show difference in histopathologic lesions on days 1 and 2 between LPS + TAA and saline + TAA rats (Fig. 1I); inflammatory cells in the centrilobular hepatic lesions in both groups were mainly macrophages, as demonstrated below by immunohistochemistry using different macrophage markers. The hepatic lesions began to heal on day 3 in both groups (Fig. 1 G, H).

In LPS-pretreated group at 24 h, no histopathological lesions were seen in livers on day 0 in saline + TAA and LPS + TAA rats (Fig. 2A, B). On day 1, there were extensive coagulation necrosis of hepatocytes and inflammatory cell infiltrates mainly in the centrilobular regions in saline + TAA rats (Fig. 2C). However, the centrilobular lesions were markedly smaller in size in LPS + TAA rats than in saline + TAA rats with statistical significant difference (Fig. 2D, I). On day 2, the histological changes became more intensive in saline + TAA rats (Fig. 2E), whereas these lesions decreased with hepatocyte regeneration in LPS + TAA rats (Fig. 2F). In saline + TAA rats, on day 3, the hepatic lesions started to recover, being replaced by regenerating hepatocytes, whereas the centrilobular lesions completely disappeared in LPS + TAA rats on day 3 (Fig. 2G, H). Collectively, in LPS + TAA rats, centrilobular lesions induced by TAA were smaller and the recovery was earlier.

Serum enzyme activities in LPS-pretreated TAA-induced liver injury

In LPS-pretreated group at 2 h, the values of AST, ALT and ALP showed an abrupt increase on day 1 after TAA injection both in LPS + TAA and saline + TAA rats with a statistically significance (Fig. 3A-C). ALP value still remained significantly increased up to day 2 in both groups. In addition, the value of AST was significantly decreased on day 1

in LPS + TAA rats in comparison with saline + TAA rats (Fig. 3A). The value of T. Bil was significantly elevated on day 2 in LPS + TAA rats, with no difference from saline + TAA rats (Fig. 3D).

In LPS-pretreated group at 24 h, the values of AST, ALT and ALP showed a significant increase on day 1 following TAA injection in LPS + TAA and saline + TAA rats (Fig. 3E-G). Additionally, T. Bil value was increased significantly both in LPS + TAA and saline + TAA rats on day 1 and remained increased up to day 2 in saline + TAA rats, indicating prolonged liver lesions in saline + TAA rats (Fig. 3H). Interestingly, on day 1, between the groups, the values of AST, ALT and ALP and T. Bil were significantly decreased in LPS + TAA rats in comparison with those in saline + TAA rats (Fig. 3E-H).

Apoptosis in LPS-pretreated TAA-induced liver injury

Apoptotic cells, demonstrable with TUNEL method, were absent in livers on day 0 in saline + TAA and LPS + TAA rats (Figs. 4A, B and 5A, B). In LPS-pretreated group at 2 h and 24 h, a large number of apoptotic hepatocytes were seen within or around the necrotic areas on day 1 and apoptotic cells were decreased on days 2 and 3 (Figs. 4C-H and 5C-F) in saline + TAA and LPS + TAA rats. In LPS-pretreated group at 2 h, the number of apoptotic cells was significantly increased on days 1 and 2 in saline + TAA rats and on day 1 in LPS + TAA rats. In addition, the number of apoptotic cells were significantly decreased on day 1 in LPS + TAA rats in compared with that in saline + TAA rats (Fig. 4I). In LPS-pretreated group at 24 h, apoptotic cells were significantly increased on day 1 in LPS + TAA and saline + TAA rats, although the number was significantly lower in LPS + TAA rats than that of saline + TAA rats (Fig. 5G).

The kinetics of hepatic macrophages in LPS-pretreated TAA-induced liver injury

In LPS-pretreated group at 2 h, $CD163^+$, $CD68^+$ and MHC class II^+ macrophages were seen on day 0 in LPS + TAA and saline + TAA rats (Fig. 6A-C). Following TAA injection, $CD163^+$ macrophages were significantly increased on days 2 and 3 in LPS + TAA and saline + TAA rats, without any statistical difference between these groups (Fig.

6A). There was a significant increase in the number of $CD68^+$ macrophages on days 1 to 3 in LPS + TAA and saline + TAA rats, with a peak on day 2, and the number was greater in LPS + TAA rats than that in saline + TAA rats on day 2 (Fig. 6B). MHC class II^+ macrophages were markedly increased on days 1 and 2 after TAA injection, and the LPS pretreatment did not show difference between these groups (Fig. 6C).

In LPS-pretreated group at 24 h, the numbers of $CD163^+$, $CD68^+$ and MHC class II^+ macrophages were significantly increased on days 1 to 3 in LPS + TAA and saline + TAA rats (Fig. 6D-F). However, $CD163^+$, $CD68^+$ and MHC class II^+ macrophages were significantly decreased on day 2 in LPS + TAA rats than those in saline + TAA rats, of which the decrease continued up to day 3 for MHC class II^+ macrophages (Fig. 6D-F).

Expression of mRNAs in LPS-pretreated TAA-induced liver injury

In LPS-pretreated group at 2 h, increased expression of MCP-1, IL-1β, IL-4, IL-6, IL-10, TNF-α, IFN-γ and TGF-β1 and were seen on day 1 in LPS + TAA and saline + TAA rats, but these factors did not show statistical difference between these groups (Fig. 7A-H). Only MCP-1 expression showed a significant elevation on day 1 in LPS + TAA and saline + TAA rats (Fig. 7A).

On the other hand, in LPS-pretreated group at 24 h, the expression of MCP-1, IL-1β, IL-6, IL-10, IFN-γ, TNF-α, TGF-β1 and IL-4 were markedly increased on day 1 in LPS + TAA and saline + TAA rats (Fig. 7I-P). Interestingly, MCP-1 (Fig. 7I), IL-1β (Fig. 7J) and IL-4 (Fig. 7K) mRNA levels were significantly lower in LPS + TAA rats than these in saline + TAA rats. Additionally, a tendency to be decreased was seen in IL-6, IL-10, IFN-γ, TNF-α, and TGF-β1 mRNA levels in LPS + TAA rats as compared with those in saline + TAA rats (Fig. 7L-P).

Autophagy and autophagy-related genes in LPS-pretreated TAA-induced liver injury

In LPS-pretreated groups at 2 h and 24 h, LC3B-positive cytoplasmic granules/dots in hepatocytes were seen at basal level on day 0 in saline + TAA rats (Figs. 8A and 9A),

whereas these findings were greater on day 0 in LPS + TAA rats (Figs. 8B and 9B) with significant difference in LPS-pretreated LPS + TAA rats at 24 h (Fig. 9I), indicating that LPS injection induced autophagy. Following TAA injection, the expression of LC3B in hepatocytes were increased both in LPS + TAA and saline + TAA rats on days 1 to 3 (Figs. 8C-H and 9C-H), which were localized mainly around necrotic areas. LC3B-labeled cytoplasmic granules of hepatocytes were significantly increased on day 1 or days 0 and 2 in LPS + TAA rats of LPS-pretreated group at 2 h (Fig. 8I) and 24 h (Fig. 9I), respectively as compared with those in saline + TAA rats.

In LPS-pretreated groups at 2 h and 24 h, autophagy-related genes such as LC3B, Lamp 2, beclin 1 and p62 did not show significant change (Fig. 10A-H). However, in LPS-pretreated group at 24 h, the LC3B (Fig. 10E) and Lamp 2 (Fig. 10F) mRNAs was significantly decreased in saline + TAA rats on day 2 in comparison with those in rats on day 0, but difference was not seen as compared with those of LPS + TAA rats.

Discussion

LPS is the bacterial endotoxin and constituent of the outer membrane of cell walls of gram-negative bacteria. Under normal condition, a small amount of LPS can periodically be taken up into the liver through the portal venous system and then, scavengered by Kupffer cells. Therefore, LPS is implicated in the pathology of liver injury. In the present study, the author focused on the activation of hepatic macrophages and autophagy in LPS-induced protection against hepatotoxicity of TAA.

Alteration of TAA-induced hepatic lesions by LPS pretreatment

TAA-induced liver lesions in rats are characteristically seen in the centrilobular areas, comprising degeneration/necrosis of hepatocytes and mononuclear cell infiltrations. The lesions started on day 1 after TAA administration, and become more pronounced with inflammatory cell reaction (mainly by macrophages) on days 2 and 3. Afterwards, the lesions gradually decreased and completely recovered onwards (Golbar et al., 2016; Wijesundera et al., 2014b; Wojcik et al., 2012). In the present study, following TAA

injection (100 mg/kg body weight) hepatic lesions were seen as reported previously (Golbar et al., 2016; Wijesundera et al., 2014b; Wojcik et al., 2012). It is reported that LPS pretreatment before TAA administration can alleviate liver injury in rats, whereas post-treatment of LPS deteriorates the toxicity of TAA (Park et al., 2013; Chen et al., 2007). In the present study, TAA-induced hepatic lesions in LPS-pretreated rats at 2 h did not change at significant level, whereas LPS-pretreated rats at 24 h showed smaller liver lesions with statistically significance, indicating hepatoprotection against TAA injury.

Apoptosis is implicated in degeneration and reduction of inflammation (Mangan et al., 1993). In this study, the number of apoptotic cells was significantly decreased on day 1 in LPS + TAA rats of LPS-pretreated groups at 2 h and 24 h, indicating that TAA-induced hepatic lesions are attenuated by LPS pretreatment with reduced number of apoptosis; particularly, LPS pretreatment at 24 h showed better attenuation of hepatic lesions. AST, ALT, ALP and T. Bil levels provide indexes of hepatocyte integrity and bile metabolism (Giannini et al., 2005). Increased values in these indexes reflect hepatic dysfunction or liver damage. In LPS-pretreated group at 2 h, AST level was significantly lower on day 1 after TAA injection in LPS + TAA rats, with other hepatic enzymes such as ALT, ALP and T. Bil were not changed in comparison with those of saline + TAA rats, indicating a very low level of hepatoprotection in TAA-induced liver injury. On the contrary, LPS pretreatment at 24 h showed significantly lower levels of AST, ALT, ALP and T. Bil on day 1 after TAA injection in LPS + TAA rats compared with those of saline + TAA rats, suggesting that LPS pretreatment at 24 h is better for the hepatoprotection against TAA injury (Park et al., 2013; Chen et al., 2007). Similarly, LPS pretreatment at 24 h showed hepatoprotective role against acetaminophen and carbon tetrachloride toxicity (Liu et al., 2000).

Mechanism of hepatoprotection in TAA-induced hepatic lesions by LPS pretreatment

In pathological lesions, based on the functional roles, macrophages are classified as classically activated (M1) and alternatively activated (M2) macrophages. In response to activating stimuli, M1 macrophages are predominant, initially leading to inflammatory

reactions with tissue destruction, while M2 macrophages are activated later to resolve inflammatory responses (Wijesundera et al., 2014b). In TAA-induced acute liver injury, M1 macrophages (mainly $CD68^+$) and M1 macrophage-related factors (IL-1β, IFN-γ, TNF-α and IL-6) took part in the early lesion development (tissue damage), whereas M2 macrophages (mainly $CD163^+$) and M2 macrophage-related factors (IL-10 and TGF-β1) contributed to fibrosis and subsequent healing (Wijesundera et al., 2014a). In this study, the similar results were seen as described previously (Wijesundera et al., 2014b; Ide et al., 2005). However, on day 2, the numbers of $CD68^+$ $CD163^+$ and MHC class II^+ macrophages were significantly less in LPS + TAA rats than those in saline + TAA rats, particularly at 24 h of LPS-pretreated group. Although LPS acts as a potent hepatic macrophage activator including Kupffer cells, the reason behind decreased number of hepatic macrophages in LPS-pretreated TAA injury at 24 h remains to the investigated.

The hepatotoxicity of LPS depends mainly on the production and release of inflammatory mediators. The author analyzed expressions of cytokines and chemokines, because hepatic macrophages are a major source of inflammatory mediators. MCP-1 is a member of the chemokine family, acting as a highly potent chemotactic factor for blood-monocytes and resident macrophages (Zamara et al., 2007; Sakai et al., 2006). IL-1β induces the pro-inflammatory factors such as nitric oxide synthetase 2 and cyclooxygenase 2. IL-6 is a possible factor for induction and activation of M1 macrophages (Martinez, 2011; Pello et al., 2011). TNF-α and IFN-γ both are important proinflammatory cytokines and have roles on tissue destruction. On the other hand, IL-4, IL-10 and TGF-β1 act as anti-inflammatory factors, which may be produced by M2 macrophages in inflammation (Wijesundera et al., 2014a; Sica et al., 2013; Njoku et al., 2009). In the present study, both M1 and M2 macrophage-related cytokines are increased after TAA injection regardless of LPS pretreatment. Interestingly, in LPS-pretreated group at 24 h, a significantly lower level of MCP-1, IL-1β and IL-4 was observed in LPS + TAA rats as compared with that in saline + TAA rats, which might be related with the decreased hepatic injury. It is reported that autophagy plays an anti-inflammatory effect through the down regulation of proinflammatory cytokines such as IL-1β and IL-18 (Sun et al., 2017; Ilyas et al., 2016;

Lodder et al., 2015). In fact, as mentioned below, the autophagy was activated in LPS-pretreated TAA-injected rats.

Besides macrophages, autophagy is another vital candidate and contributes to pathogenesis for liver injury. Autophagy formation is an attempt by cells to limit the spread of subcellular damage by walling off the damage areas (Hendy and Grasso, 1972). Autophagy inhibits inflammation by down regulating of caspase 1-dependent inflammasome cleavage of IL-1β (Lodder et al., 2015) and macrophage autophagy may be required to suppress the M1 macrophage polarization (Liu et al., 2015). Autophagy exerts anti-apoptotic effect on hepatocytes and contributes to liver regeneration (Shi et al., 2015). In the present study, autophagy was distinctly increased in LPS-pretreated rats, and hepatocytes with LC3B-labeld autophagy granules were localized around the necrotic areas. Moreover, the number of apoptotic cells was significantly reduced in LPS-pretreated TAA-injected rats. These findings indicating that LPS-activated autophagy may participate in hepatoprotection to TAA-induced hepatic lesions.

In conclusion, the present study showed that LPS pretreatment could protect the TAA-induced hepatotoxicity. Particularly, LPS pretreatment at 24 h can protect against the toxicity of TAA, but LPS pretreatment at 2 h did not show such levels. These findings indicated that LPS pretreatment needs at least 24 h for preparing the microenvironments for the protection against the TAA-induced liver injury. The microenvironments could be established via LPS-stimulated hepatic macrophages or regulatory cytokines and LPS-activated autophagy. Therefore, the activation of hepatic macrophages and autophagy could be considered a therapeutic approach against hepatic complications induced by chemicals.

Summary

Hepatic macrophages and autophagy both are essential components in innate immunity, participating in the inflammation. Here, the author investigated cytoprotective roles of hepatic macrophages and autophagy in TAA-induced acute liver injury under lipopolysaccharide (LPS) pretreatment. Male F344 rats were pretreated with LPS (0.1 mg/kg body weight intraperotoneally) or saline at 2 h or 24 h before TAA injection (100 mg/kg body weight intraperotoneally). Histopathologically, LPS pretreatment at 2 h did not reduce the hepatic lesions, whereas the pretreatment at 24 h markedly attenuated hepatic injury, along with reduced apoptosis and decreased serum hepatic enzyme levels. The macrophages reacting to CD163, CD68 and MHC class II were significantly increased after TAA administration, regardless of LPS pretreatment at 2 h or 24 h. Interestingly, MCP-1, IL-1β and IL-4 were significantly decreased on day 1 in LPS-pretreated TAA-injured livers at 24 h, whereas, these factors did not change in LPS-pretreated TAA-injured livers at 2 h. The autophagy, demonstrable with LC3B immunohistochemistry, was markedly increased in LPS pretreatment at 24 h. These findings indicated that LPS pretreatment needs at least 24 h for preparing the microenvironments for protection against TAA-induced liver injury. Both activated macrophages and autophagy may contribute to hepatoprotective mechanisms.

Figure legends

Fig. 1. A-H: Histopathology of livers in saline + TAA and LPS + TAA rats in LPS pretreatment at 2 h. In both groups, the hepatic architecture is normal on day 0 (A, B), the centrilobular necrosis is seen in days 1 and 2 (C-F) and the lesions are decreased on day 3 (G, H). I. Quantative analysis of necrotic size in saline + TAA (□) and LPS + TAA (■) rats. Tukey's test; *, P <0.05, significantly different from day 0 in saline + TAA and LPS + TAA rats. Dotted lines indicate the necrotic area. d: day, CV: central vein. Bar = 100 μm.

Fig. 2. A-H: Histopathology of livers in saline + TAA and LPS + TAA rats in LPS pretreatment at 24 h. The hepatic architecture is normal in rats of both groups on day 0 (A, B). The centrilobular necrosis is seen in saline + TAA rats on days 1 (C) and 2 (E), which is reduced in LPS + TAA rats (D, F). The lesions disappeared on day 3 in both groups (G, H). I. Quantative analysis of necrotic size in saline + TAA (□) and LPS + TAA (■) rats. Tukey's test; *, P <0.05, significantly different from day 0 in saline + TAA and LPS + TAA rats; †, P <0.05, significantly different between saline + TAA and LPS + TAA rats at respective examination points. Dotted lines indicate the necrotic area. d: day, CV: central vein. Bar = 100 μm.

Fig. 3. A-H: Blood biochemical analyses. Aspartate transaminase (AST) (A), alanine transaminase (ALT) (B), alkaline phosphatase (ALP) (C) and total bilirubin (T. bil) (D) in LPS pretreatment at 2 h and AST (E), ALT (F), ALP (G) and T. Bil (H) in LPS pretreatment at 24 h. Tukey's test; *, P <0.05, significantly different from day 0 in saline + TAA (□) and LPS + TAA (■) rats; †, P <0.05, significantly different between saline + TAA and LPS + TAA rats at respective examination points. d: day.

Fig. 4. A-H: The TUNEL staining (for apoptosis) of livers in saline + TAA and LPS + TAA rats in LPS pretreatment at 2 h. I. Quantative analysis of number of apoptotic cells in saline + TAA (□) and LPS + TAA (■) rats. Tukey's test; *, P <0.05,

significantly different from day 0 in saline + TAA and LPS + TAA rats; †, P <0.05, significantly different between saline + TAA and LPS + TAA rats at respective examination points. d: day, CV: central vein. Bar = 100 μm.

Fig. 5. A-F: The TUNEL staining (for apoptosis) of livers in saline + TAA and LPS + TAA rats in LPS pretreatment at 24 h. G. Quantative analysis of number of apoptotic cells in saline + TAA (□) and LPS + TAA (■) rats. Tukey's test; *, P <0.05, significantly different from day 0 in saline + TAA and LPS + TAA rats; †, P <0.05, significantly different between saline + TAA and LPS + TAA rats at respective examination points. d: day, CV: central vein. Bar = 100 μm.

Fig. 6. The kinetics of macrophages reacting to CD163 (A), CD68 (B) and MHC class II (C) in LPS pretreatment at 2 h, and CD163 (D), CD68 (E) and MHC class II (F) in LPS pretreatment at 24 h in the liver of saline + TAA (□) and LPS + TAA (■) rats. Tukey's test; *, P <0.05, significantly different from day 0 in saline + TAA and LPS + TAA rats; †, P <0.05, significantly different between saline + TAA and LPS + TAA rats at respective examination points. d: day.

Fig. 7. A-P: mRNA expressions for inflammatory-related factors in the liver of saline + TAA (□) and LPS + TAA (■) rats in LPS pretreatment at 2 h and 24 h. Tukey's test; *, P <0.05, significantly different from day 0 in saline + TAA and LPS + TAA rats; †, P <0.05, significantly different between saline + TAA and LPS + TAA rats at respective examination points. d: day.

Fig. 8. A-H: LC3B immunohistochemistry of livers in saline + TAA and LPS + TAA rats in LPS pretreatment at 2 h. The basal level of LC3B expression is seen in both groups on day 0 (A, B). The expression of LC3B is increased in saline + TAA in days 1 (C) and 2 (E) and the expression level is more prominent in LPS + TAA rats (D, F). Inset shows LC3B-positive cells (arrow) in higher magnification. The expression returns to basal level on day 3 in both groups (G, H). I. Quantative analysis of LC3B-labeled dots/hepatocytes in saline + TAA (□) and LPS + TAA

(■) rats. Tukey's test; *, P <0.05, significantly different from day 0 in saline + TAA and LPS + TAA rats; †, P <0.05, significantly different between saline + TAA and LPS + TAA rats at respective examination points. d: day, CV: central vein. Bar = 100 μm.

Fig. 9. A-H: LC3B immunohistochemistry of livers in saline + TAA and LPS + TAA rats in LPS pretreatment at 24 h. The basal level of LC3B expression is seen in both groups on day 0 (A, B). The expression of LC3B is increased in saline + TAA on days 1 (C) and 2 (E) and the expression level is more prominent in LPS + TAA rats (D, F). Inset shows LC3B-positive cells (arrow) in higher magnification. The expression returns to basal level on day 3 in both groups (G, H). I. Quantative analysis of LC3B-labeled dots/hepatocytes in saline + TAA (□) and LPS + TAA (■) rats. Tukey's test; *, P <0.05, significantly different from day 0 in saline + TAA and LPS + TAA rats; †, P <0.05, significantly different between saline + TAA and LPS + TAA rats at respective examination points. d: day, CV: central vein. Bar = 100 μm.

Fig. 10. A-H: mRNA expressions for autophagy-related genes in LPS pretreatment at 2 h and 24 h. LC3B (A), Lamp 2 (B), beclin 1 (C), p62 (D) mRNAs do not show any change in LPS pretreatment at 2 h. LC3B (E) and Lamp 2 (F) are decreased in saline + TAA, but do not in LPS + TAA rats in LPS pretreatment at 24 h. Beclin 1 (G) and p62 (H) remain unchanged in both groups. Tukey's test; *, P <0.05, significantly different from day 0 in saline + TAA (□) and LPS + TAA (■) rats. d: day.

LPS pretreatment at 2 h

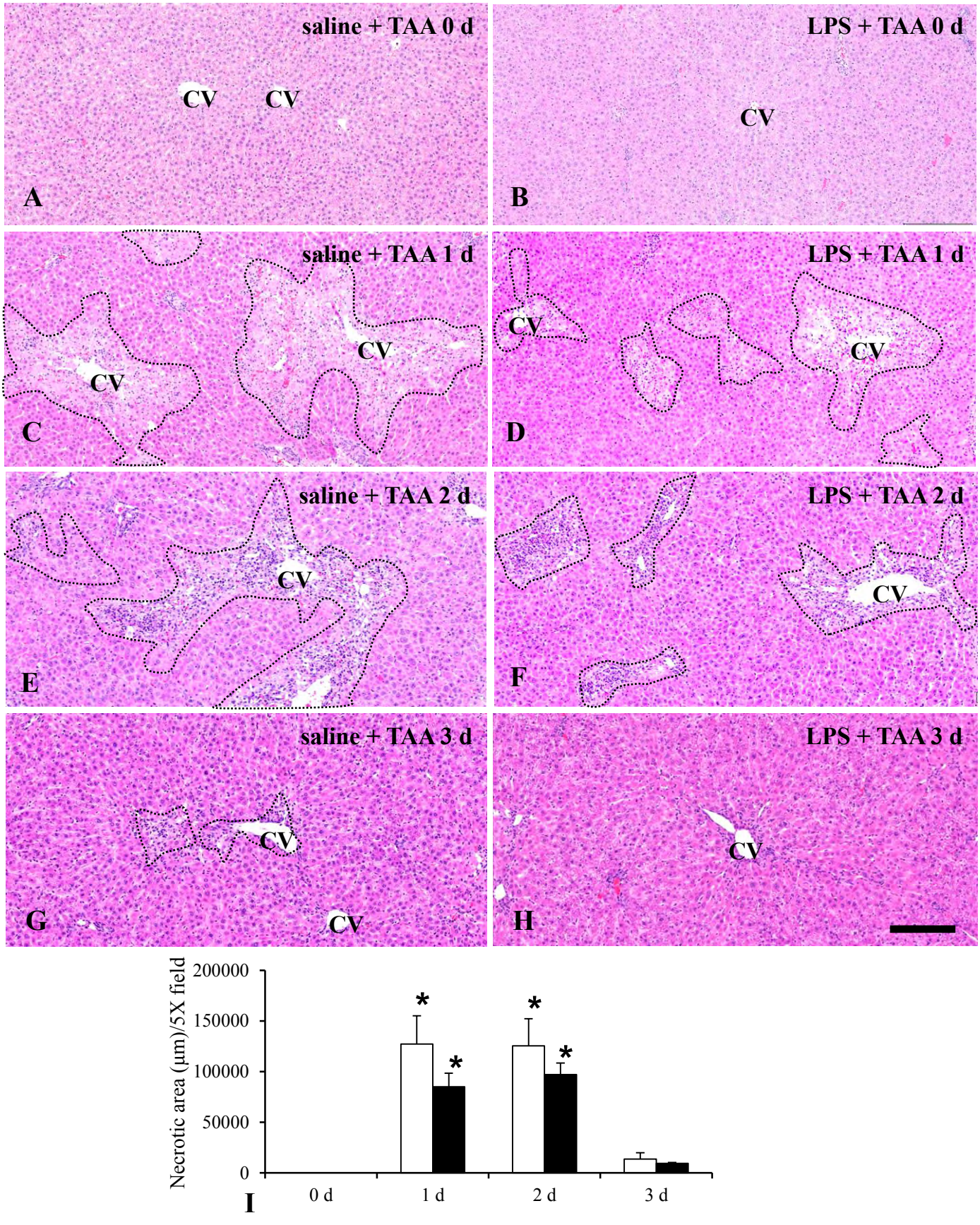

Fig. 1

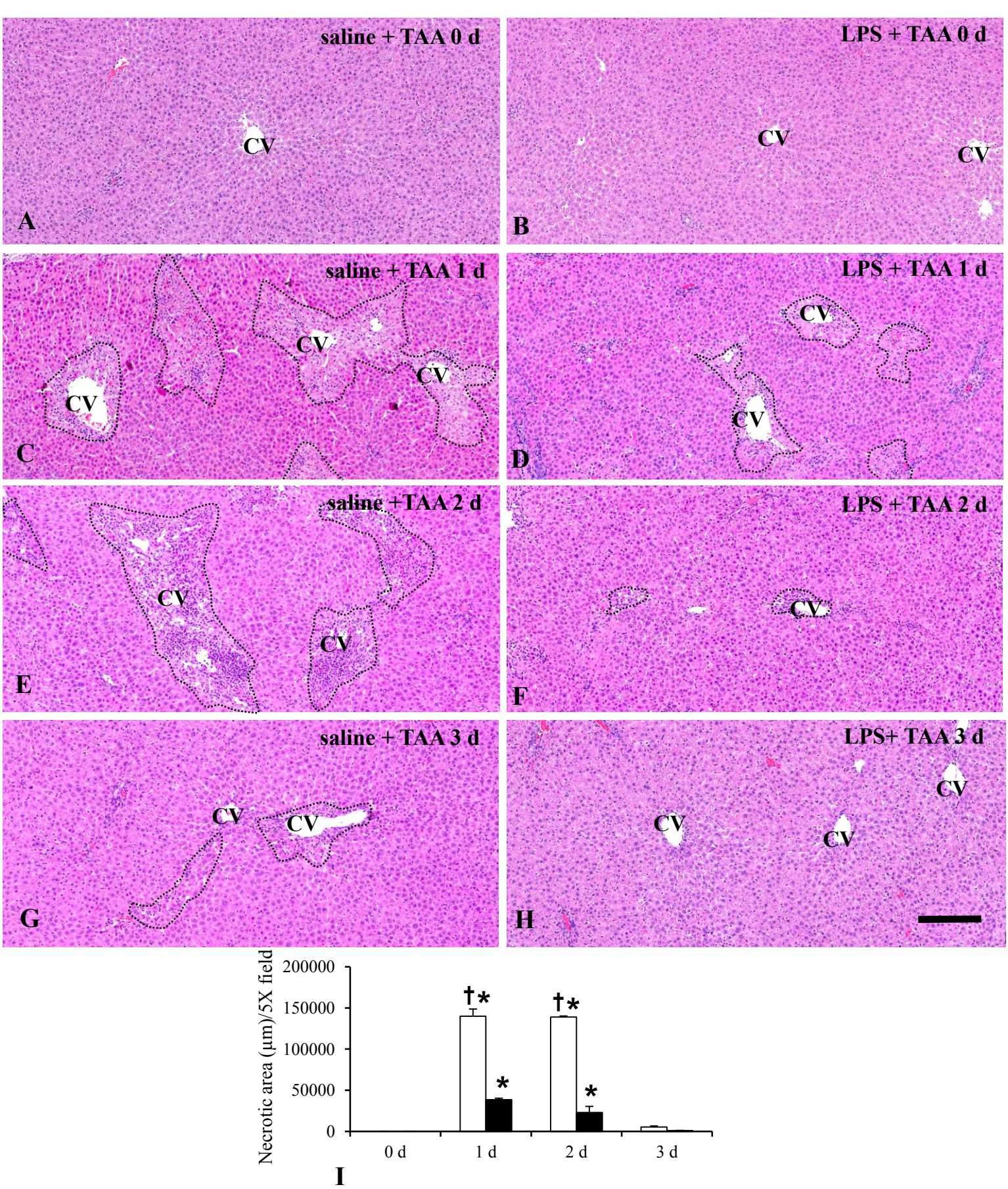
LPS pretreatment at 24 h
saline + TAA 0 d
LPS + TAA 0 d
saline + TAA 1 d
LPS + TAA 1 d
saline +TAA 2 d
LPS + TAA 2 d
saline + TAA 3 d
LPS+ TAA 3 d
CV
A
B
C
D
E
F
G
H
Necrotic area (μm)/5X field
200000
150000
100000
50000
0
†*
*
0 d
1 d
2 d
3 d
I

Fig. 2

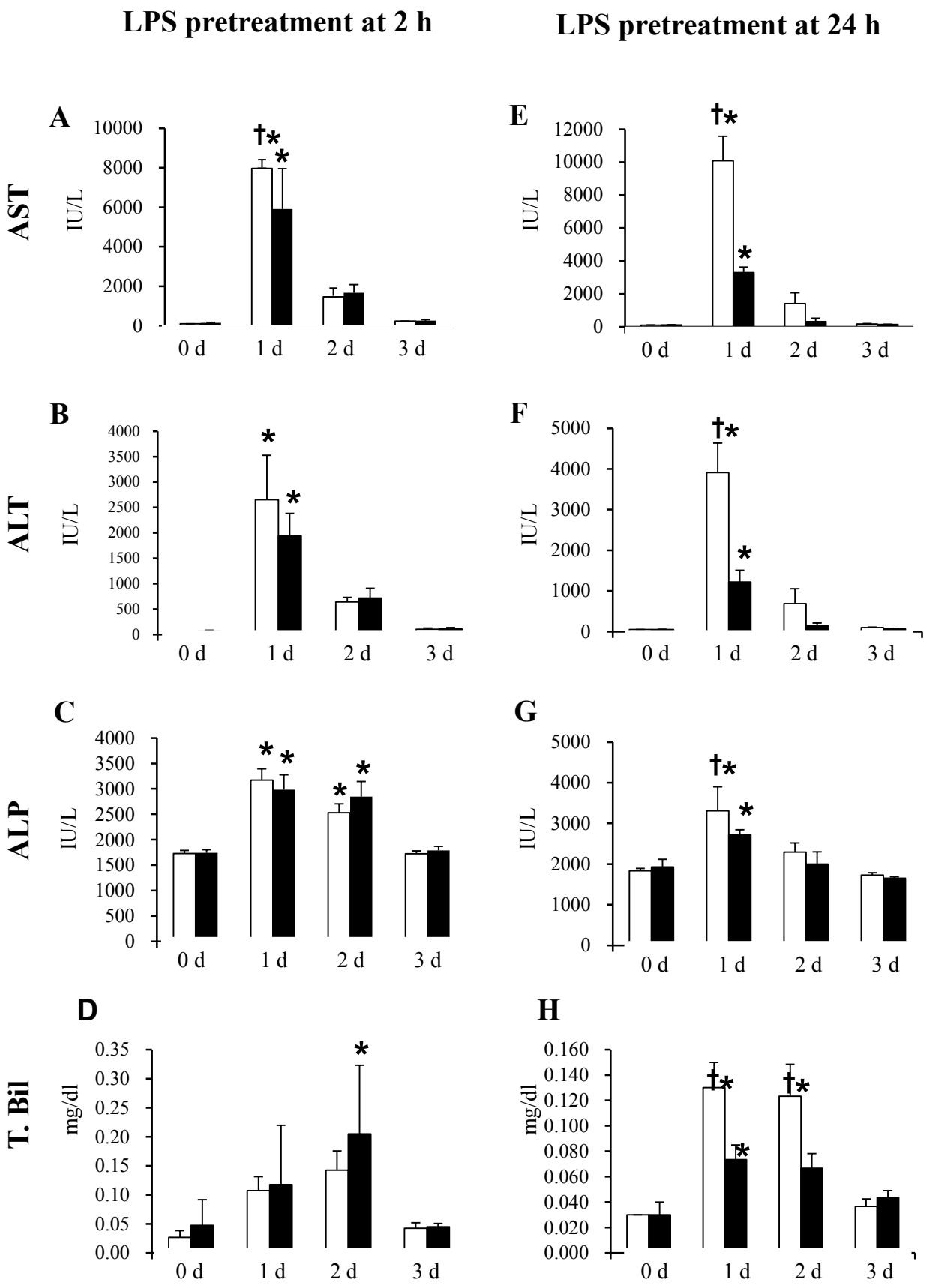
LPS pretreatment at 2 h
LPS pretreatment at 24 h
A
E
B
F
C
G
D
H
AST
ALT
ALP
T. Bil
IU/L
mg/dl
0 d
1 d
2 d
3 d
†*
*

Fig. 3

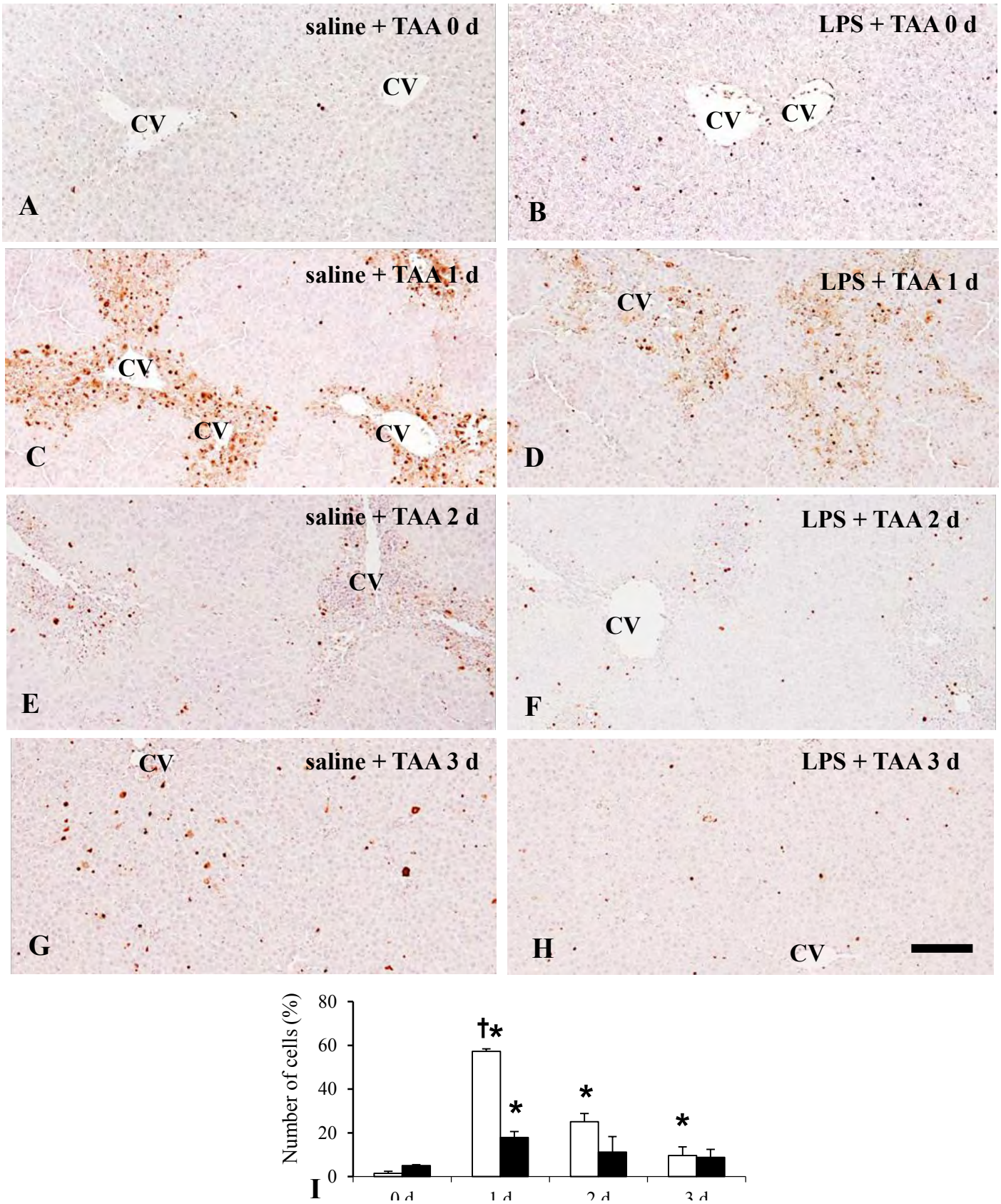
LPS pretreatment at 2 h
saline + TAA 0 d
LPS + TAA 0 d
saline + TAA 1 d
LPS + TAA 1 d
saline + TAA 2 d
LPS + TAA 2 d
saline + TAA 3 d
LPS + TAA 3 d
CV
A
B
C
D
E
F
G
H
Number of cells (%)
80
60
40
20
0
†*
*
*
*
0 d
1 d
2 d
3 d
I

Fig. 4

LPS pretreatment at 24 h

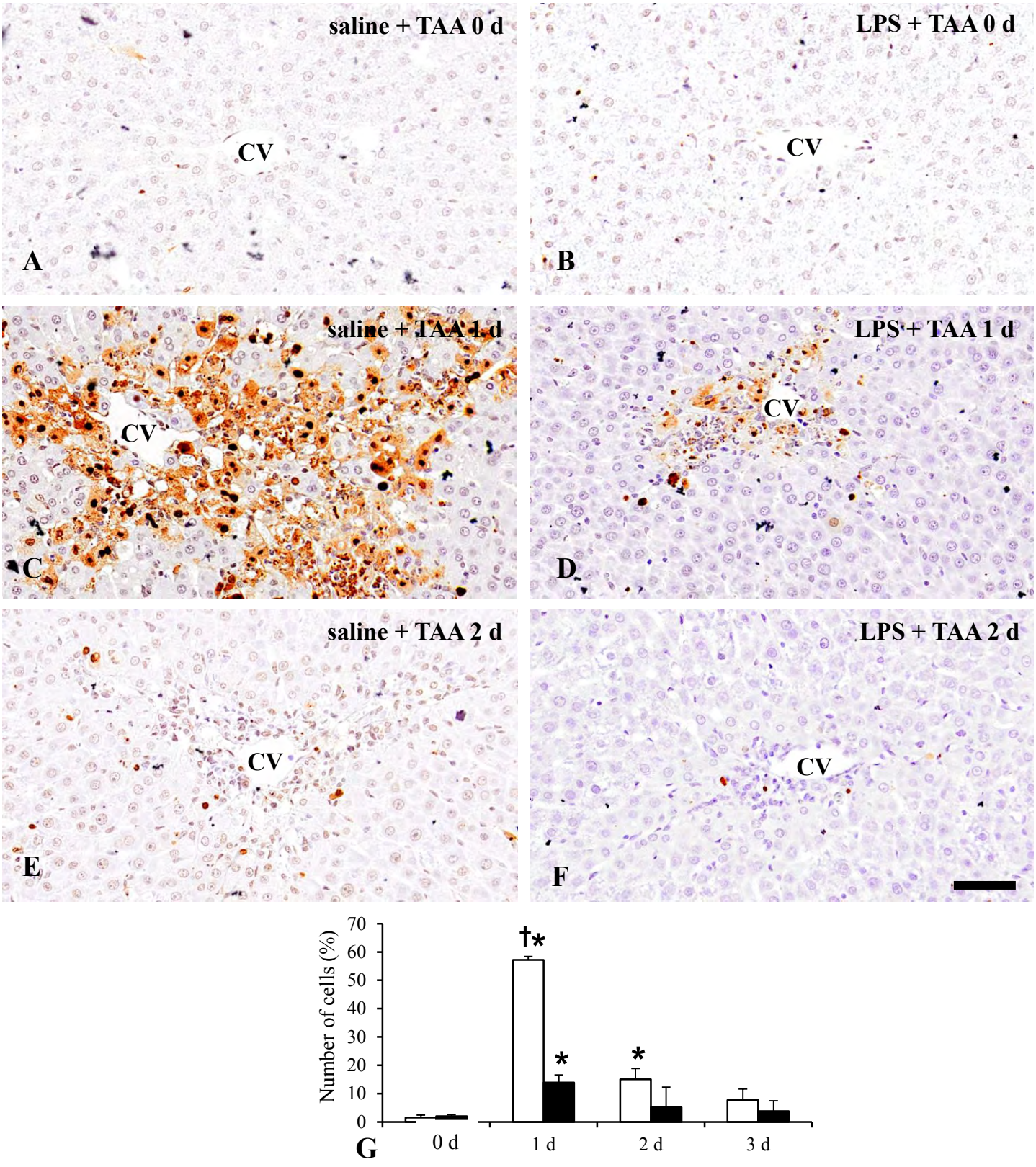

Fig. 5

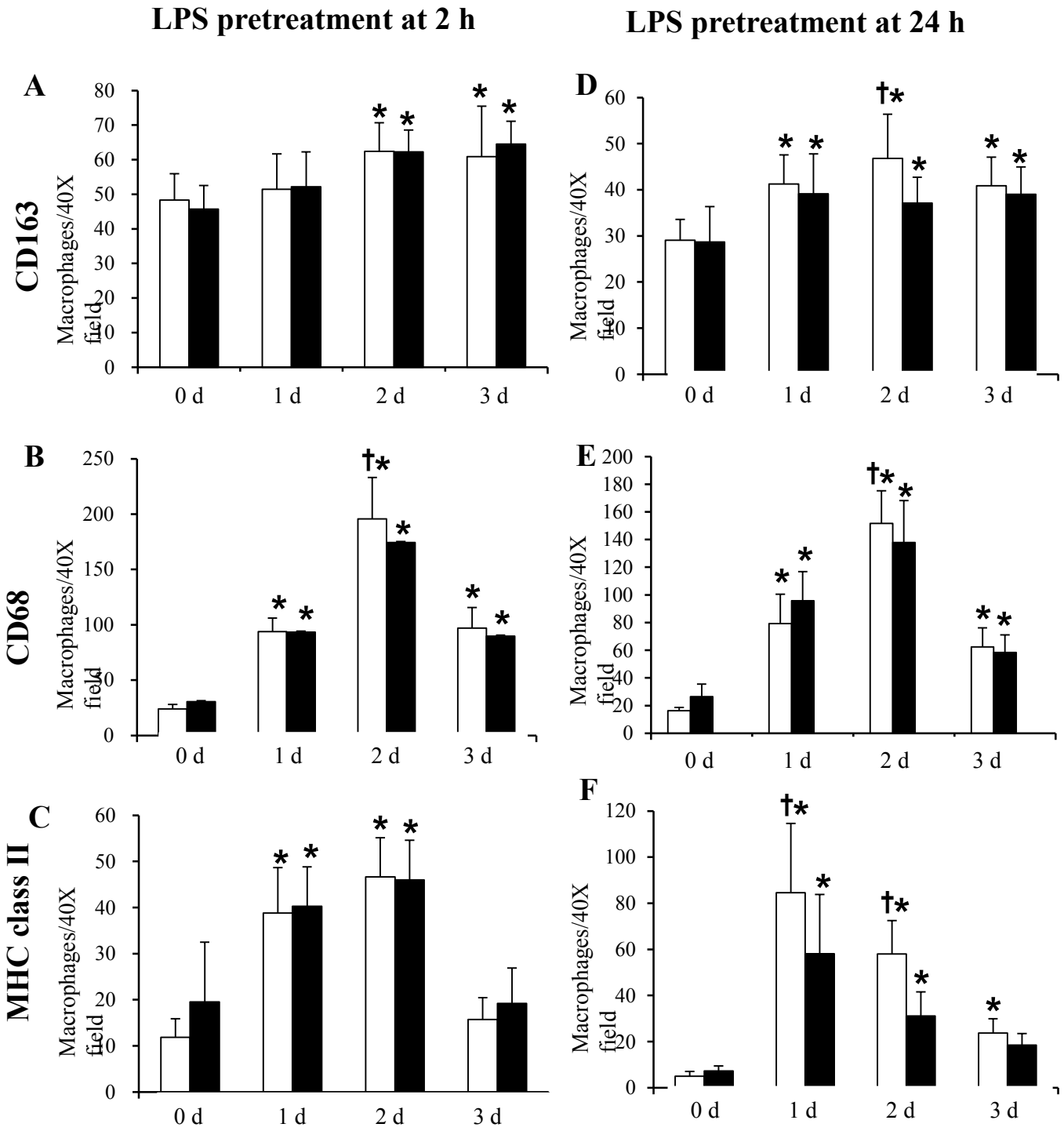
LPS pretreatment at 2 h
LPS pretreatment at 24 h
A
D
CD163
B
E
CD68
C
F
MHC class II
Macrophages/40X field
0 d
1 d
2 d
3 d
*
†*

Fig. 6

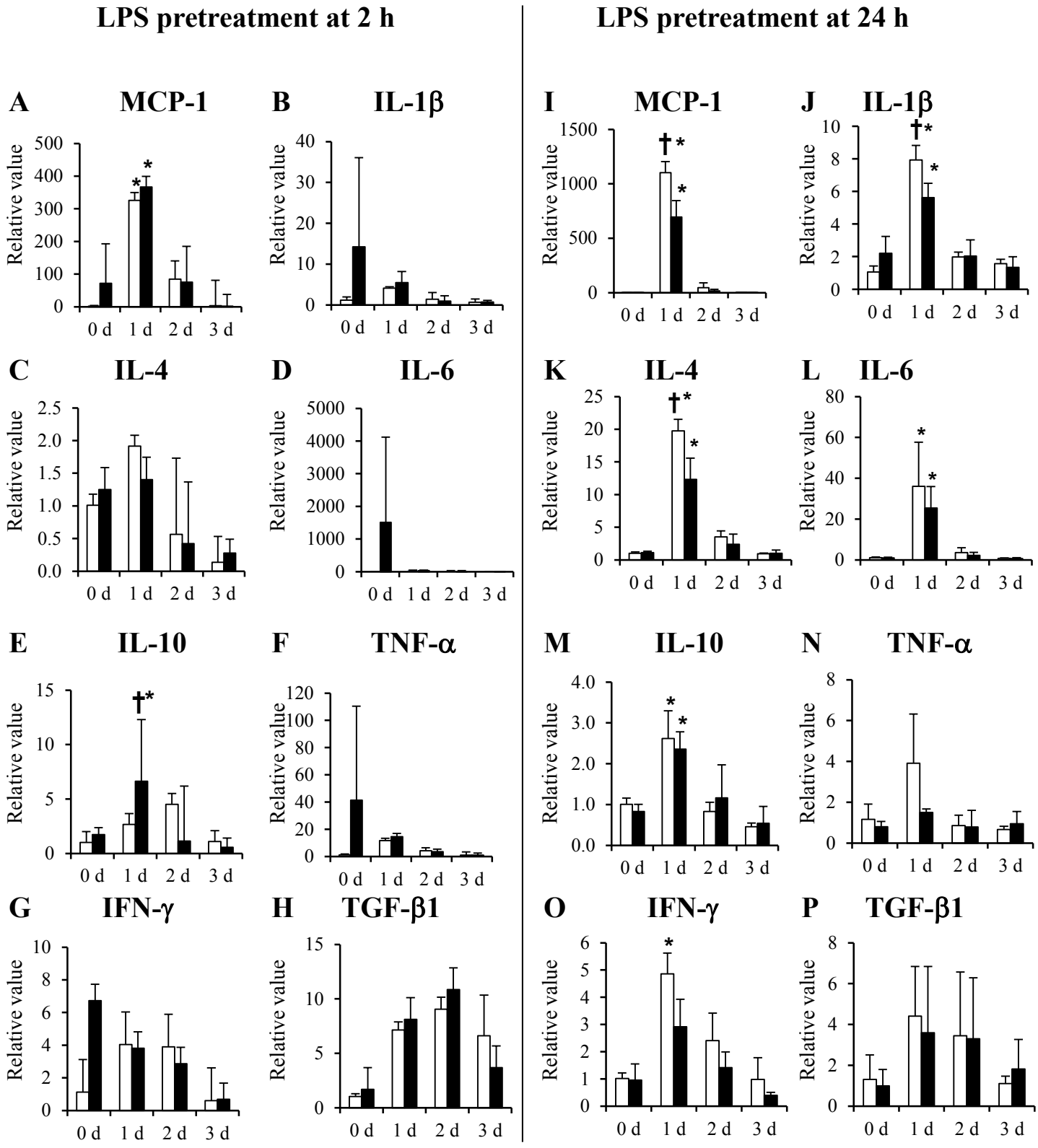
LPS pretreatment at 2 h
LPS pretreatment at 24 h
A MCP-1
B IL-1β
C IL-4
D IL-6
E IL-10
F TNF-α
G IFN-γ
H TGF-β1
I MCP-1
J IL-1β
K IL-4
L IL-6
M IL-10
N TNF-α
O IFN-γ
P TGF-β1
Relative value
0 d
1 d
2 d
3 d
*
†*

Fig. 7

LPS pretreatment at 2 h

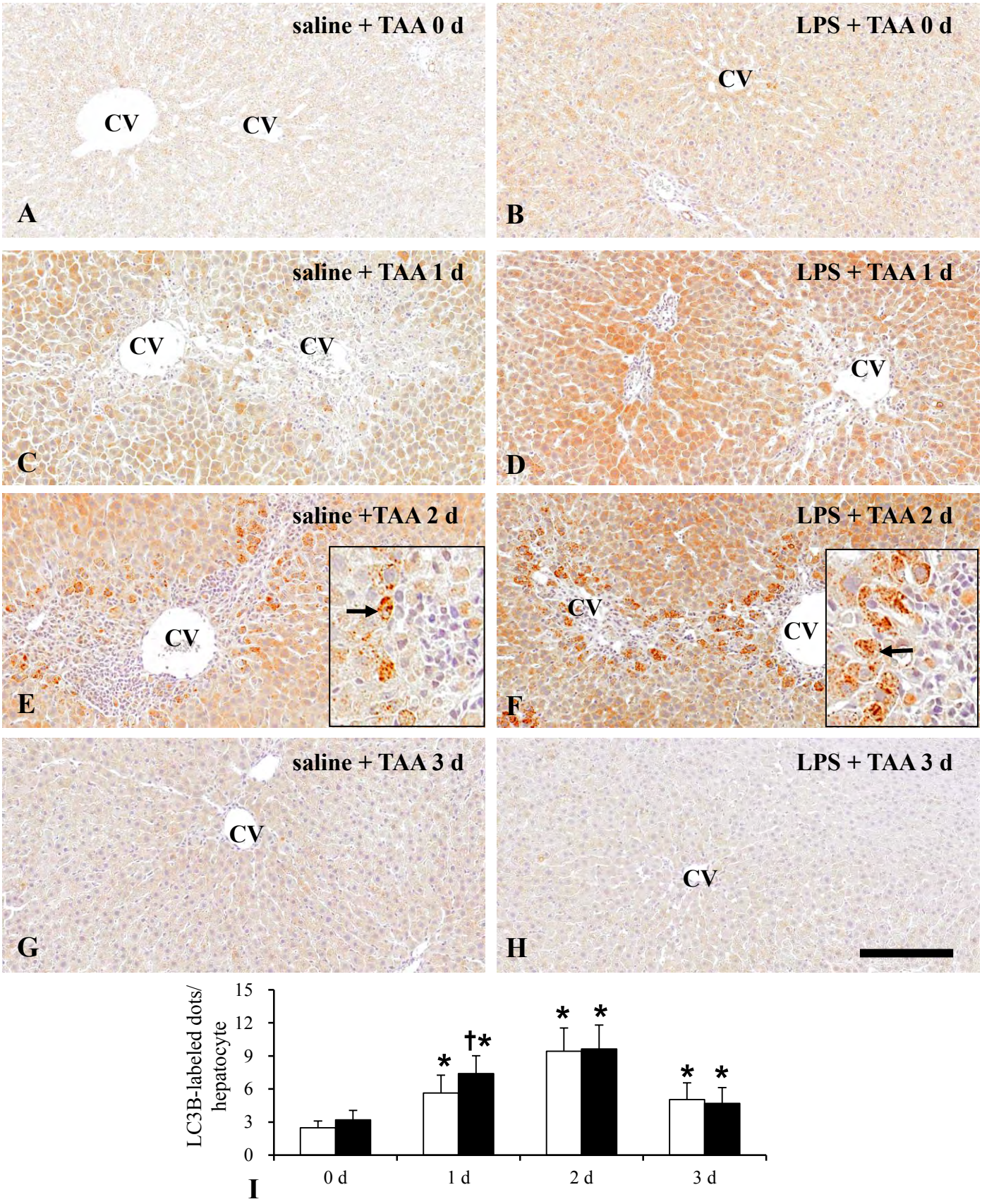

Fig. 8

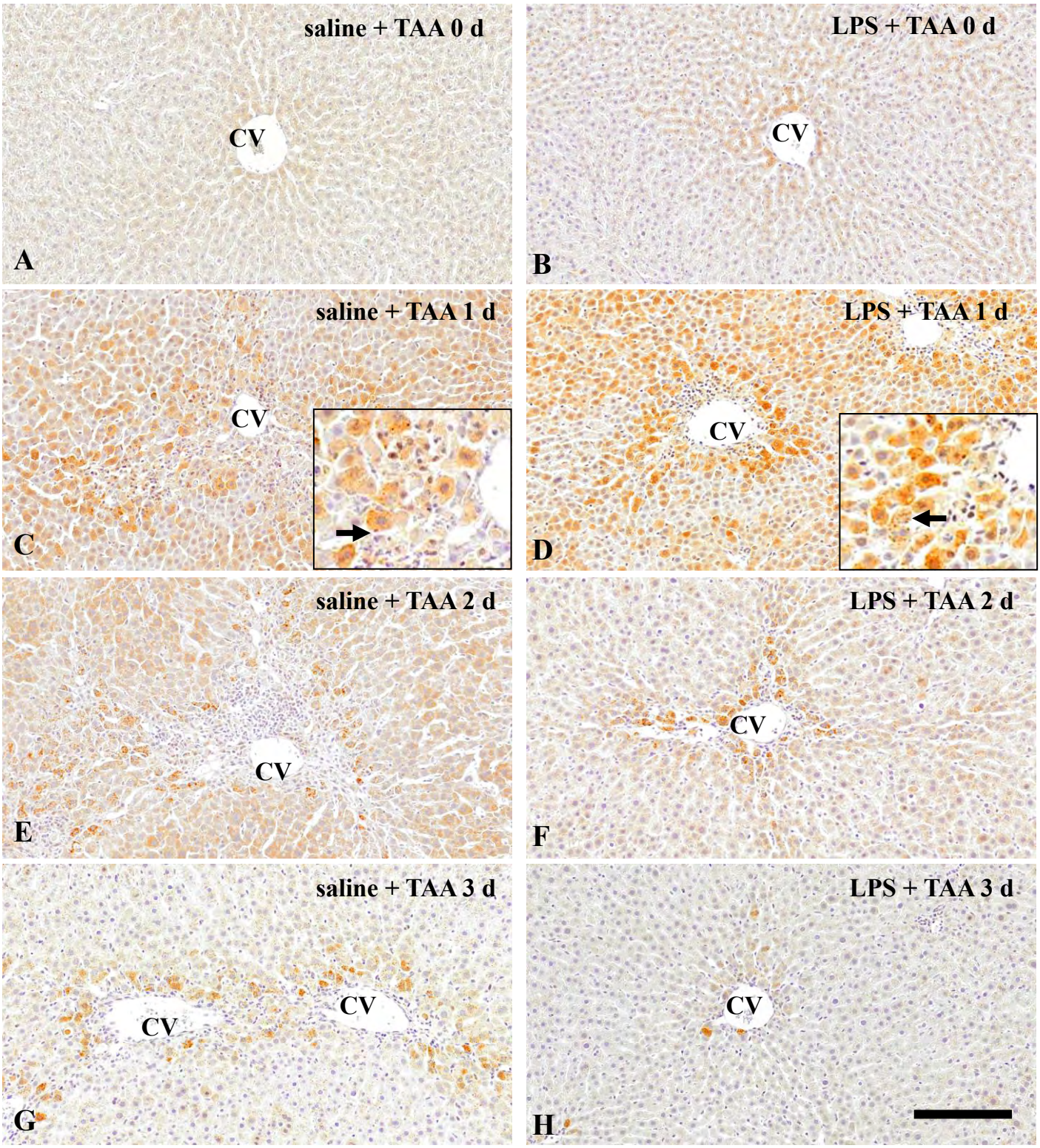
saline + TAA 0 d
CV
A
LPS + TAA 0 d
CV
B
saline + TAA 1 d
CV
C
LPS + TAA 1 d
CV
D
saline + TAA 2 d
CV
E
LPS + TAA 2 d
CV
F
saline + TAA 3 d
CV
CV
G
LPS + TAA 3 d
CV
H

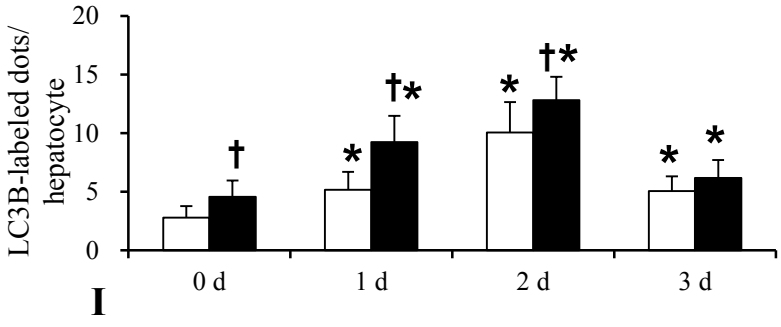
LC3B-labeled dots/ hepatocyte
20
15
10
5
0
†
*
†*
*
†*
*
*
0 d
1 d
2 d
3 d
I

Fig. 9

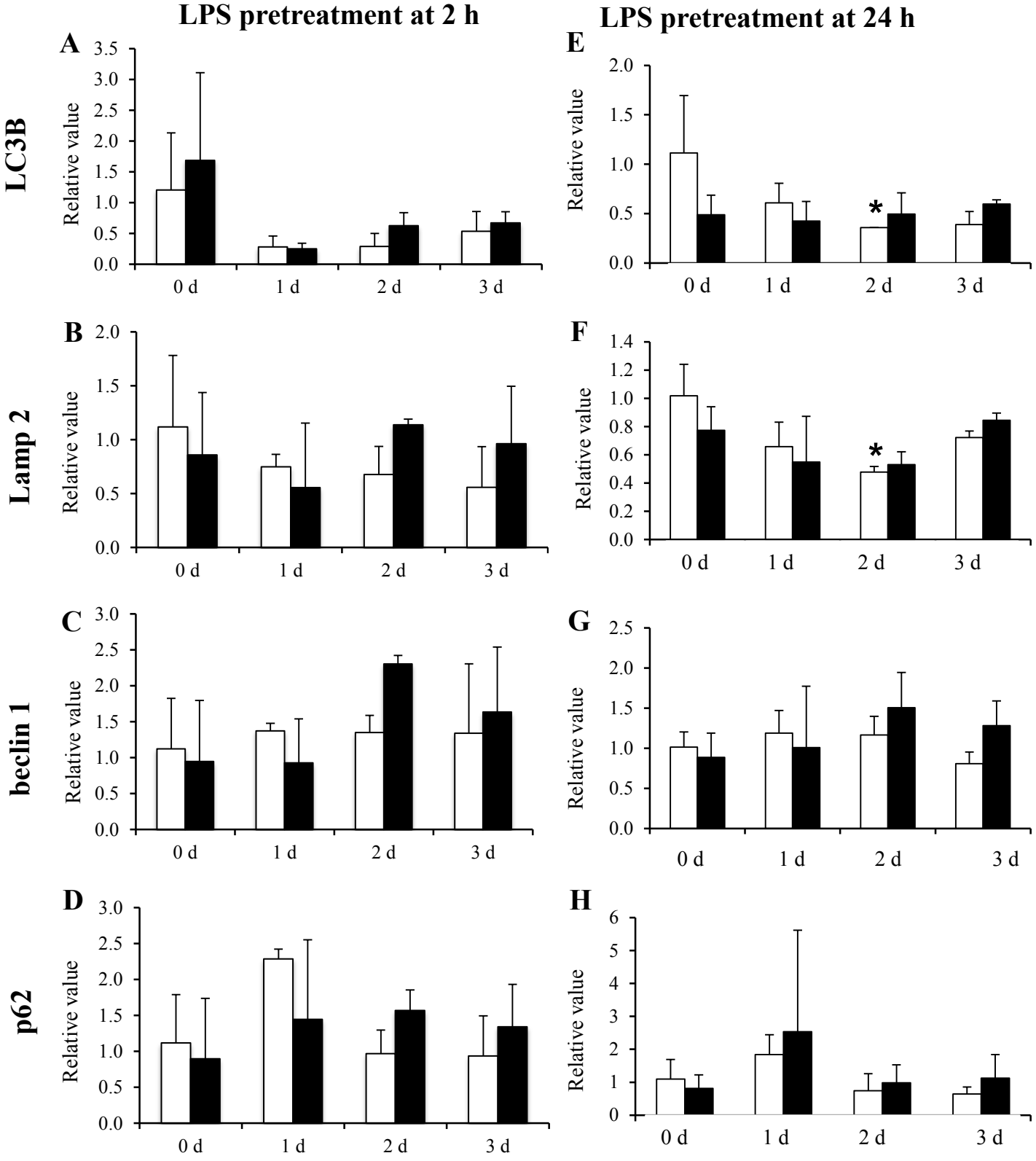
LPS pretreatment at 2 h
LPS pretreatment at 24 h
LC3B
Lamp 2
beclin 1
p62
A
B
C
D
E
F
G
H
Relative value
0 d
1 d
2 d
3 d
*

Fig. 10

Conclusions

In a series of studies, the author investigated the functional properties of hepatic macrophages and autophagy in relation to liver homeostasis and hepatotoxicity. The functional properties were mainly histopathologically analyzed using rats under low dose of lipopolysaccharide (LPS) or clodronate (CLD) treatment. Based on the obtained findings, the following conclusions are drawn (Scheme 1);

1. Empty liposomes activated hepatic macrophages with different immunophenotypes (mainly, CD68, CD163 and MHC class II), without histopathological changes. (Chapter 1, Section I).
2. CLD injection successfully depleted hepatic macrophages with different immunophenotypes in rat livers. Particularly, $CD163^{+}$ Kupffer cells were the most susceptible to CLD. (Chapter 1, Section II).
3. Low dose of LPS (0.1 mg/kg body weight) treatment activated hepatic macrophages without liver lesions. Furthermore, the LPS administration effected liver microenvironments via the increased production of inflammatory mediators. (Chapter 2, Section I).
4. Low dose of LPS treatment induced autophagy in hepatocytes and non-parenchymal cells such as hepatic macrophages and hepatic stellate cells (HSCs). Additionally, LPS-activated hepatic macrophages influenced autophagy functions in liver. (Chapter 2, Section II).
5. LPS pretreatment protected development of thioacetamide (TAA)-induced acute liver lesions depending on time points before TAA injection. Particularly, LPS pretreatment at 24 h greatly protected TAA-induced hepatotoxicity, whereas LPS pretreatment at 2 h did not show such levels. (Chapter 3).
6. Hepatic macrophages with different immunopohenotypes and activated autophagy might participate in the protective phenomenon against TAA-induced hepatotoxicity. (Chapter 3).
7. Therefore, the present findings would provide useful information on the properties of hepatic macrophages and autophagy in liver homeostasis and hepatotoxicity, leading to possible insights underlying effective therapeutic strategies against liver lesions.

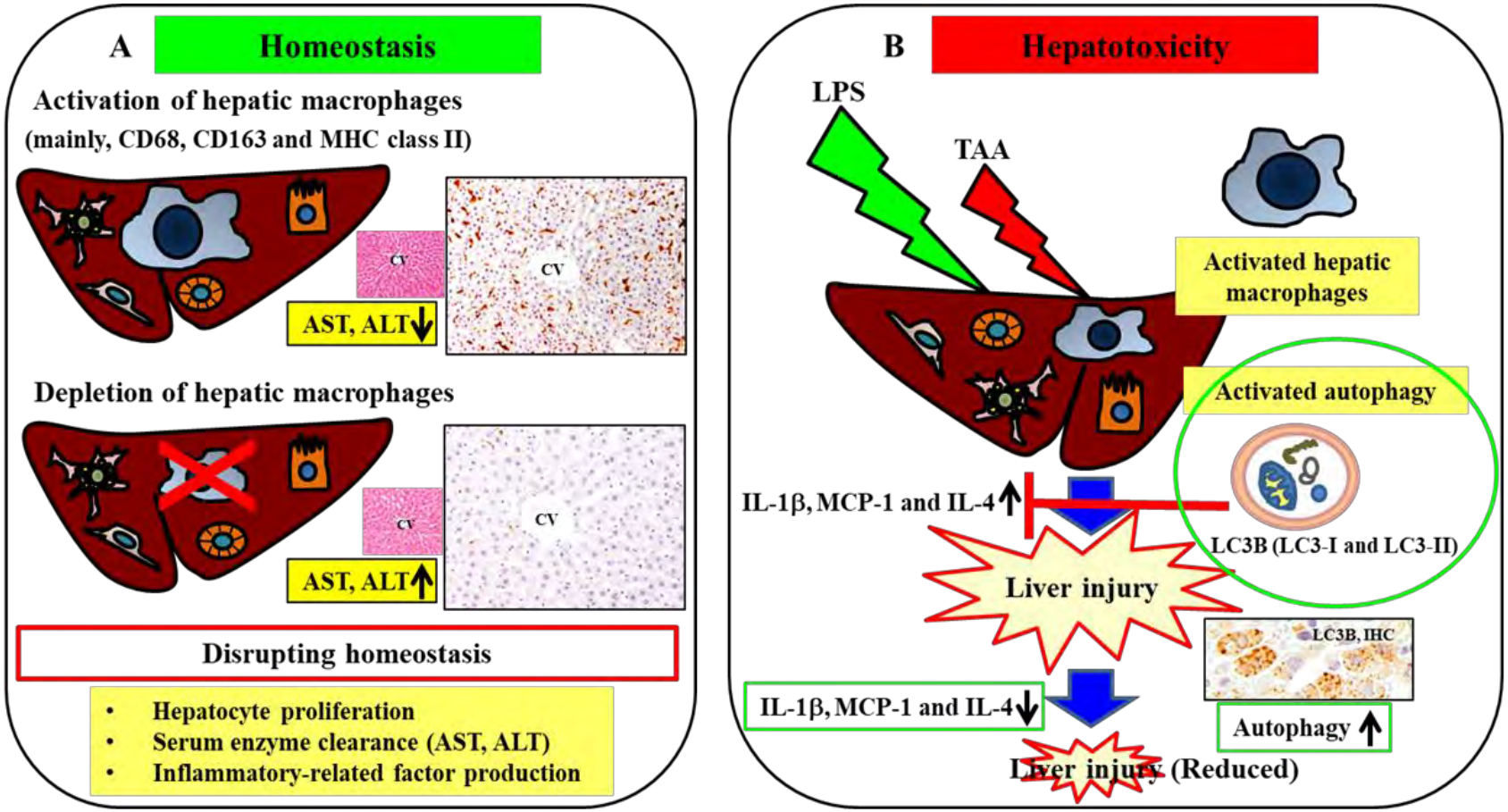

Scheme 1: Functional properties of hepatic macrophages and autophagy in liver homeostasis (A) and hepatotoxicity (B). A: In normal condition, hepatic macrophages play an important role in the maintenance of liver homeostasis. Either activation or depletion of hepatic macrophages results in disruption of liver homeostasis via influencing on hepatocyte proliferation, serum enzyme clearance and inflammatory-related factor production. B: In TAA-induced hepatotoxicity, the activated hepatic macrophages enhance liver tissue damage by producing the cytotoxic factors such as MCP-1, IL-1β and IL-4. On the contrary, the LPS pretreatment before TAA administration reduces the hepatic lesions; that is because LPS administration at low dose acts as hepatic macrophage activator and potent inducer of autophagy in the liver and the LPS-activated autophagy may participate in hepatoprotection against TAA-induce hepatic lesions by the downregulating of MCP-1, IL-1β and IL-4.

CV: central vein, AST: aspartate transaminase, ALT: alanine transaminase, TAA: thioacetamide, LPS: lipopolysaccharide, LC3B: microtubule-associated protein 1 light chain 3 beta, IHC: immunohistochemistry.

References

Allison AC. Macrophage activation and nonspecific immunity. *Int Rev Exp Pathol* 1978;18:303.

Amir M, Zhao E, Fontana L, Rosenberg H, Tanaka K, Gao G, et al. Inhibition of hepatocyte autophagy increases tumor necrosis factor-dependent liver injury by promoting caspase-8 activation. *Cell Death Differ* 2013;20:878-87.

Anand PK, Tait SW, Lamkanfi M, Amer AO, Nunez G, Pagès G, et al. TLR-2 and RIP-2 pathways mediate autophagy of Listeria monocytogenes via extracellular signal-regulated kinase (ERK) activation. *J Biol Chem* 2011;286:42981-91.

Apostolova N, Gomez-Sucerquia LJ, Gortat A, Blas-Garcia A, Esplugues JV. Compromising mitochondrial function with the antiretroviral drug efavirenz induces cell survival-promoting autophagy. *Hepatology* 2011;54:1009-19.

Bakker J, Sanders A, Van Rooijen N. Effects of liposome-encapsulated drugs on macrophages: comparative activity of the diamidine 4',6-diamidino-2-phenylindole and the phenanthridinium salts ethidium bromide and propidium iodide. *Biochim Biophys Acta* 1998;1373:93-100.

Barondes SH, Cooper DN, Gitt MA, Leffler H. Galectins. Structure and function of a large family of animal lectins. *J Biol Chem* 1994;269:20807-10.

Bautista M, Gomez del Rio MA, Benedi J, Sanchez-Reus MI, Morales-Gonzalez JA, Tellez-Lopez AM, et al. Effect of dichloromethylene diphosphonate on liver regeneration following thioacetamide-induced necrosis in rats. *World J Hepatol* 2013;5:379-86.

Beljaars L, Schippers M, Reker-Smit C, Martinez FO, Helming L, Poelstra K, et al. Hepatic localization of macrophage phenotypes during fibrogenesis and resolution of fibrosis in mice and humans. *Front Immunol* 2014;5:430.

Bouhlel MA, Derudas B, Rigamonti E, Dièvart R, Brozek J, Haulon S, et al. PPAR-γ activation primes human monocytes into alternative M2 macrophages with anti-inflammatory properties. *Cell Metab* 2007;6:137-43.

Calabrese EJ, Mehendale HM. A review of the role of tissue repair as an adaptive strategy: why low doses are often non-toxic and why high doses can be fatal. *Food Chem Toxicol* 1996;34:301-11.

Cecchini MG, Dominguez MG, Mocci S, Wetterwald A, Felix R, Fleisch H, et al. Role of colony stimulating factor-1 in the establishment and regulation of tissue macrophages during postnatal development of the mouse. *Development* 1994;120:1357-72.

Chen C, Deng M, Sun Q, Loughran P, Billiar TR, Scott MJ. Lipopolysaccharide stimulates p62-dependent autophagy-like aggregate clearance in hepatocytes. *Biomed Res Int* 2014;267350.

Chen CT, Chu CJ, Wang TF, Lu RH, Lee FY, Chang FY, et al. Evidence against a role for endotoxin in the hepatic encephalopathy of rats with thioacetamide-induced fulminant hepatic failure. *J Gastroenterol Hepatol* 2005;20:450-5.

Chen HN, Fan S, Weng CF. Down-regulation of TGFβ1 and leptin ameliorates thioacetamide-induced liver injury in lipopolysaccharide-primed rats. *J Endotoxin Res* 2007;13:176-88.

Cullen JM, Faiola B, Melich DH, Peterson RA, Jordan HL, Kimbrough CL, et al. Effects of Kupffer cell depletion on acute alpha-naphthylisothiocyanate-induced liver toxicity in male mice. *Toxicol Pathol* 2013;41:7-17.

Cursio R, Colosetti P, Codogno P, Cuervo AM, Shen HM. The role of autophagy in liver diseases: mechanisms and potential therapeutic targets. *Biomed Res Int* 2015;480508.

Dai XM, Ryan GR, Hapel AJ, Dominguez MG, Russell RG, Kapp S, et al. Targeted disruption of the mouse colony stimulating factor-1 receptor gene results in

osteopetrosis, mononuclear phagocyte deficiency, increased primitive progenitor cell frequencies, and reproductive defects. *Blood* 2002;99:111-20.

Damoiseaux JG, Dopp EA, Calame W, Chao D, MacPherson GG, Dijkstra CD. Rat macrophage lysosomal membrane antigen recognized by monoclonal antibody ED1. *Immunology* 1994;83:140-7.

Davison NL, Gamblin AL, Layrolle P, Yuan H, de Bruijn JD, Barrère-de Groot F. Liposomal clodronate inhibition of osteoclastogenesis and osteoinduction by submicrostructured beta-tricalcium phosphate. *Biomaterials* 2014;35:5088-97.

Debnath J, Baehrecke EH, Kroemer G. Does autophagy contribute to cell death? *Autophagy* 2005;1:66-74.

Ding WX, Li M, Chen X, Ni HM, Lin CW, Gao W, et al. Autophagy reduces acute ethanol-induced hepatotoxicity and steatosis in mice. *Gastroenterology* 2010;139:1740-52.

Dong S, Hughes RC. Macrophages surface glycoproteins binding to galectin 3 (Mac 2 antigen). *Glycoconj* J 1997;14:267-74.

Duffield JS, Forbes SJ, Constandinou CM, Clay S, Partolina M, Vuthoori S, et al. Selective depletion of macrophages reveals distinct, opposing roles during liver injury and repair. *J Clin Invest* 2005;115:56-65.

Fabriek BO, Dijkstra CD, Van den Berg TK. The macrophage scavenger receptor CD163. *Immunobiology* 2005;210:153-60.

Fainboim L, Cherñavsky A, Paladino N, Flores AC, Arruvito L. Cytokines and chronic liver disease. *Cytokine Growth Factor Rev* 2007;18:143-57.

Fleisch H. Bisphosphonates: a new class of drugs in diseases of bone and calcium metabolism. *Recent Results Cancer Res* 1989;116:1-28.

Freudenberg MA, Galanos C. Induction of tolerance to lipopolysaccharide (LPS)-D galactosamine lethality by pretreatment with LPS is mediated by macrophages. *Infect Immun* 1988;56:1352-57.

Fujisawa K, Miyoshi T, Tonomura Y, Izawa T, Kuwamura M, Torii M, et al. Relationship of heat shock protein 25 with reactive macrophages in thioacetamide-induced rat liver injury. *Exp Toxicol Pathol* 2011;63:599-605.

Ganey PE, Roth RA. Concurrent inflammation as a determinant of susceptibility to toxicity from xenobiotic agents. *Toxicology* 2001;169:195-208.

Gervasi PG, Longo V, Marzano M, Saviozzi M, Malvaldi G. Chronic liver injury by thioacetamide and promotion of hepatic carcinogenesis. *J Cancer Res Clin Oncol* 1989;115:29-35.

Giannini EG, Testa R, Savarino V. Liver enzyme alteration: a guide for clinicians, *CMAJ*, 2005;172:367-79.

Godoy P, Hewitt NJ, Albrecht U, Andersen ME, Ansari N, Bhattacharya S, et al. Recent advances in 2D and 3D *in vitro* systems using primary hepatocytes, alternative hepatocyte sources and non-parenchymal liver cells and their use in investigating mechanisms of hepatotoxicity, cell signaling and ADME. *Arch Toxicol* 2013;87:1315-530.

Golbar HM, Izawa T, Ichikawa C, Tanaka M, Juniantito V, Sawamoto O, et al. Slowly progressive cholangiofibrosis induced in rats by α-naphthylisothiocyanate (ANIT), with particular references to characteristics of macrophages and myofibroblasts. *Exp Toxicol Pathol* 2013;65:825-35.

Golbar HM, Izawa T, Murai F, Kuwamura M, Yamate J. Immunohistochemical analyses of the kinetics and distribution of macrophages, hepatic stellate cells and bile duct epithelia in the developing rat liver. *Exp Toxicol Pathol* 2012;64:1-8.

Golbar HM, Izawa T, Wijesundera KK, Bondoc A, Tennakoon AH, Kuwamura M, et al. Depletion of hepatic macrophages aggravates liver lesion induced in rats by thioacetamide (TAA). *Toxicol Pathol* 2016;44:246-58.

Golbar HM, Izawa T, Yano R, Ichikawa C, Sawamoto O, Kuwamura M, et al. Immunohistochemical characterization of macrophages and myofibroblasts in α-naphthylisothiocyanate (ANIT)-induced bile duct injury and subsequent fibrogenesis in rats. *Toxicol Pathol* 2011;39:795-808.

Gordon S. Alternative activation of macrophages. *Nat Rev Immunol* 2003;3:23-35.

Greaves DR, Gough PJ, Gordon S. Recent progress in defining the role of scavenger receptors in lipid transport, atherosclerosis and host defence. *Curr Opin Lipidol* 1998;9:425-32.

Hafenrichter DG, Roland CR, Mangino MJ, Flye MW. The Kupffer cell in endotoxin tolerance: mechanism of protection against lethal endotoxemia. *Shock* 1994;2:251-56.

Haralanova-Ilieva B, Ramadori G, Armbrust T. Expression of osteoactivin in rat and human liver and isolated rat liver. *J Hepatol* 2005;42:565-72.

Hayden RS, Vollrath M, Kaplan DL. Effects of clodronate and alendronate on osteoclast and osteoblast co-cultures on silk-hydroxyapatite films. *Acta Biomater* 2014;10:486-93.

Hendy R, Grasso P. Autophagy in acute liver damage produced in the rat by dimethylnitrosamine. *Chem Biol Interact* 1972;5:401-13.

Hernandez-Gea V, Ghiassi-Nejad Z, Rozenfeld R, Gordon R, Fiel MI, Yue Z, et al. Autophagy releases lipid that promotes fibrogenesis by activated hepatic stellate cells in mice and in human tissues. *Gastroenterology* 2012;142:938-46.

Hewett JA, Roth RA. Hepatic and extrahepatic pathobiology of bacterial lipopolysaccharides. *Pharmacol Rev* 1993;45:382-11.

Hofheinz RD, Gnad-Vogt SU, Beyer U, Hochhaus A. Liposomal encapsulated anti-cancer drugs. *Anticancer Drugs* 2005;16:691-707.

Hung TM, Yuan RH, Huang WP, Chen YH, Lin YC, Lin CW, et al. Increased autophagy markers are associated with ductular reaction during the development of cirrhosis. *Am J Pathol* 2015;185:2454-67.

Ide M, Kuwamura M, Kotani T, Sawamoto O, Yamate J. Effects of gadolinium chloride (GdCl3) on the appearance of macrophage populations and fibrogenesis in the thioacetamide induced rat hepatic lesions. *J Comp Pathol* 2005;133:92-102.

Ide M, Yamate J, Machida Y, Nakanishi M, Kuwamura M, Kotani T, et al. Emergence of different macrophage populations in hepatic fibrosis following thioacetamide-induced acute hepatocyte injury in rats. *J Comp Pathol* 2003;128:41-51.

Ilyas G, Zhao E, Liu K, Lin Y, Tesfa L, Tanaka KE, et al. Macrophage autophagy limits acute toxic liver injury in mice through down regulation of interleukin-1β. *J Hepatol* 2016;64:118-27.

Ishida Y, Nagata K. Autophagy eliminates a specific species of misfolded procollagen and plays a protective role in cell survival against ER stress. *Autophagy* 2009;5:1217-9.

Ishihara K, Hirano T. Molecular basis of the cell specificity of cytokine action. *Biochim Biophys Acta* 2002;1592:281-96.

Ishikawa M, Tanno K, Sasaki M, Takayanagi Y, Sasaki K. Antidotal effect of lipopolysaccharide against acetaminophen-induced mortality in mice. *Pharmacol Toxicol* 1990;67:387-91.

Izawa T, Horiuchi T, Atarashi M, Kuwamura M, Yamate J. Anti-fibrotic role of miR-214 in thioacetamide-induced liver cirrhosis in rats. *Toxicol Pathol* 2015;43:844-51.

Ju C, Reilly TP, Bourdi M, Radonovich MF, Brady JN, George JW, et al. Protective role of Kupffer cells in acetaminophen-induced hepatic injury in mice. *Chem Res Toxicol* 2002;15:1504-13.

Ju C, Tacke F. Hepatic macrophages in homeostasis and liver diseases: from pathogenesis to novel therapeutic strategies. *Cell Mol Immunol* 2016;13:316-27.

King JS, Veltman DM, Insall RH. The induction of autophagy by mechanical stress. *Autophagy* 2011;7:1490-9.

Komatsu M, Waguri S, Ueno T, Iwata J, Murata S, Tanida I, et al. Impairment of starvation-induced and constitutive autophagy in Atg 7-deficient mice. *J Cell Biol* 2005;169:425-34.

La Flamme AC, Kharkrang M, Stone S, Mirmoeini S, Chuluundorj D, Kyle R. Type II-activated murine macrophages produce IL-4. *PLoS One* 2012;7:e46989.

Laskin DL, Sunil VR, Gardner CR, Laskin, JD. Macrophages and tissue injury: agents of defense or destruction? *Annu Rev Pharmacol Toxicol* 2011; 51:267-88.

Laskin DL. Nonparenchymal cells and hepatotoxicity. *Semin Liver Dis* 1990;10:293-304.

Leon P, Redmond HP, Shou J, Daly JM. Interleukin-1 and its relationship to endotoxin tolerance. *Arch Surg* 1992;127:146-51.

Liu J, Sendelbach LE, Parkinson A, Klaassen CD. Endotoxin pretreatment protects against the hepatotoxicity of acetaminophen and carbon tetrachloride: role of cytochrome P450 suppression. *Toxicology* 2000;147:167-76.

Liu K, Zhao E, Ilyas G, Lalazar G, Lin Y, Haseeb M, et al. Impaired macrophage autophagy increases the immune response in obese mice by promoting proinflammatory macrophage polarization. *Autophagy* 2015;11:271-84.

Lodder J, Denaës T, Chobert MN, Wan J, El-Benna J, Pawlotsky JM, et al. Macrophage autophagy protects against liver fibrosis in mice. *Autophagy* 2015;11:1280-92.

Madrigal-Matute J, Cuervo MA. Regulation of liver metabolism by autophagy. *Gastroenterology* 2016;150:328-39.

Mangan DF, Mergenhagen SE, Wahl SM. Apoptosis in human monocytes: possible role in chronic inflammatory diseases. *J Periodontol* 1993;64:461-6.

Mantovani A, Sozzani S, Locati M, Allavena P, Antonio S. Macrophage polarization: Tumor-associated macrophages as a paradigm for polarized M2 mononuclear phagocytes. *Trends Immunol* 2002;23:549-55.

Martinez FO, Gordon S. The M1 and M2 paradigm of macrophage activation: Time for reassessment. *F1000Prime Reports* 2014;6-13.

Martinez FO, Sica A, Mantovani A, Locati M. Macrophage activation and polarization. *Front Biosci* 2008;13:453-61.

Martinez FO. Regulators of macrophage activation. *Eur J Immunol* 2011;41:1531-4.

Means TK, Golenbock DT, Fenton MJ. The biology of Toll-like receptor. *Cytokine Growth Factor Rev* 2000;11:219-32.

Meghari S, Berruyer C, Lepidi H, Galland F, Naquet P, Mege JL. Vanin-1 controls granuloma formation and macrophage polarization in Coxiella burnetii infection. *Eur J Immunol* 2007;37:24-32.

Meijer C, Wiezer MJ, Diehl AM, Yang SO, Schouten HJ, Meijer S, et al. Kupffer cell depletion by Cl_2MDP-liposomes alters hepatic cytokine expression and delays liver regeneration after partial hepatectomy. *Liver* 2000;20:66-77.

Mizushima N, Yoshimori T, Levine B. Methods in mammalian autophagy research. *Cell* 2010;140:313-26.

Mori Y, Izawa T, Takenaka S, Kuwamura M, Yamate J. Participation of functionally different macrophage populations and monocyte chemoattractant protein-1 in early stages of thioacetamide-induced rat hepatic injury. *Toxicol Pathol* 2009;37:463-73.

Mosser DM, Edwards JP. Exploring the full spectrum of macrophage activation. *Nat Rev Immunol* 2008;8:958-69.

Nakagawa I, Amano A, Mizushima N, Yamamoto A, Yamaguchi H, Kamimoto T, et al. Autophagy defends cells against invading group A Streptococcus. *Science* 2004;306:1037-40.

Ni HM, Williams JA, Yang H, Shi YH, Fan J, Ding WX. Targeting autophagy for the treatment of liver diseases. *Pharmacol Res* 2012;66:463-74.

Njoku DB, Li Z, Washington ND, Mellerson JL, Talor MV, Sharma R, et al. Suppressive and pro-inflammatory roles for IL-4 in the pathogenesis of experimental drug-induced liver injury. *Eur J Immunol* 2009;39:1652-63.

Novak ML, Koh TJ. Macrophage phenotypes during tissue repair. *J Leukoc Biol* 2013;93:875-81.

Ohsawa K, Imai Y, Kanazawa H, Sasaki Y, Kohsaka S. Involvement of Iba-1 in membrane ruffling and phagocytosis of macrophages/microglia. *J Cell Sci* 2000;113:3073-84.

Ohsumi Y. Molecular dissection of autophagy: two ubiquitin-like systems. *Nat Rev Mol Cell Biol* 2001;2:211-6

Park J, Kim E, Yang J, Lee H, Hong SH, Lee S, et al. Lipopolysaccharide alleviates liver injury induced by thioacetamide in rats. *J Prev Vet Med* 2013;37:146-51.

Patel NR, Bole M, Chen C, Hardin CC, Kho AT, Mih J, et al. Cell Elasticity Determines Macrophage Function. *PLoS One* 2012;7:e41024.

Pellicoro A, Ramachandran P, Iredale JP. Reversibility of liver fibrosis. *Fibrogenesis Tissue Repair* 2012;5:S26.

Pello OM, Silvestre C, De Pizzol M, Andrés V. A glimpse on the phenomenon of macrophage polarization during atherosclerosis. *Immunobiology* 2011;216:1172-6.

Perrigoue JG, Saenz SA, Siracusa MC, Allenspach EJ, Taylor BC, Giacomin PR, et al. MHC class II-dependent basophil-CD4^{+} T-cell interactions promote Th2 cytokine-dependent immunity. *Nat Immunol* 2009;10:697-705.

Pervin M, Golbar HM, Bondoc A, Izawa T, Kuwamura M, Yamate J. Immunophenotypical characterization and influence on liver homeostasis of depleting and repopulating hepatic macrophages in rats injected with clodronate. *Exp Toxicol Pathol* 2016;68:113-24.

Polfliet MM, Fabriek BO, Daniels WP, Dijkstra CD, Van den Berg TK. The rat macrophage scavenger receptor CD163: expression, regulation and role in inflammatory mediator production. *Immunobiology* 2006;211:419-25.

Radi ZA, Koza-Taylor PH, Bell RR, Obert LA, Runnels HA, Beebe JS, et al. Increased serum enzyme levels associated with Kupffer cell reduction with no signs of hepatic or skeletal muscle injury. *Am J Pathol* 2011;179:240-7.

Ramaiah SK, Apte U, Mehendale HM. Cytochrome P4502E1 induction increases thioacetamide liver injury in diet-restricted rats. *Drug Metab Dispos* 2001;29:1088-95.

Robinson MW, Harmon C, O'Farrelly C. Liver immunology and its role in inflammation and homeostasis. *Cell Mol Immunol* 2016;13:267-76.

Romer M, Eichner J, Metzger U, Templin MF, Plummer S, Ellinger-Ziegelbauer H, et al. Cross-platform toxicogenomics for the prediction of non-genotoxic hepatocarcinogenesis in rat. *PLoS One* 2014;9:e97640.

Roth RA, Harkema JR, Pestka JP, Ganey PE. Is exposure to bacterial endotoxin a determinant of susceptibility to intoxication from xenobiotic agents? *Toxicol Appl Pharmacol* 1997;147:300-11.

Sakai N, Wada T, Furuichi K, Shimizu K, Kokubo S, Hara A, et al. MCP-1/CCR2-dependent loop for fibrogenesis in human peripheral CD-14 positive monocytes. *J Leukoc Biol* 2006;79:555-63.

Sasaki Y, Ohsawa K, Kanazawa H, Kohsaka S, Imai Y. Iba-1 is an actin-cross-linking protein in macrophages/microglia. *Biochem Biophys Res Commun* 2001;286:292-7.

Schumann J, Wolf , Pahl A, Brune K, Papadopoulos T, Van Rooijen N, et al. Importance of Kupffer cells for T-cell dependent liver injury in mice. *Am J Pathol* 2000;157:1671-83.

Schwabe RF, Seki E, Brenner DA. Toll-like receptor signaling in the liver. *Gastroenterology* 2006;130:1886-900.

Seki E, De MS, Osterreicher CH, Kluwe J, Osawa Y, Brenner DA et al. TLR-4 enhances TGF-β signaling and hepatic fibrosis. *Nat Med* 2007;13:1324-1332

Shi S, Tan P, Yan B, Gao R, Zhao J, Wang J, et al. ER stress and autophagy are involved in the apoptosis induced by cisplatin in human lung cancer cells. *Oncol Rep* 2016;35: 2606-14.

Sica A, Invernizzi P, Mantovani A. Macrophage plasticity and polarization in liver homeostasis and pathology. *Hepatology* 2013;59:2035-43.

Sica A, Mantovani A. Macrophage plasticity and polarization: *In vivo* veritas. *J Clin Invest* 2012;122:787-95.

Smit MJ, Duursma AM, Joop M, Bouma W, Gruber JM. Receptor-mediated endocytosis of lactate dehydrogenase M, by liver macrophages: a mechanism for elimination of enzymes from plasma. *J Biol Chem* 1987;262:13020-6.

Soehnlein O, Lindbom L. Phagocyte partnership during the onset and resolution of inflammation. *Nat Rev Immunol* 2010;10:427-39.

Sporrer D, Weber M, Wanninger J, Weigert J, Neumeier M, Stögbauer F, et al. Adiponectin downregulates CD163 whose cellular and soluble forms are elevated in obesity. *Eur J Clin Invest* 2009;39:671-9.

Stein M, Keshav S, Harris N, Gordon S. Interleukin-4 potently enhances murine macrophage mannose receptor activity: a marker of alternative immunologic macrophage activation. *J Exp Med* 1992;176:287-92.

Sturm E, Havinga R, Baller JFW, Wolters H, Van Rooijen N, Kamps JAAM, et al. Kupffer cell depletion with liposomal clodronate prevents suppression of Ntcp expression in endotoxin-treated rats. *J Hepatol* 2005;42:102-9.

Suda T, McCaarthy K, Vu Q, McCormack J, Schneeberger EE. Dendritic cell precursors are enriched in the vascular compartments of lung. *Am J Respir Cell Mol Biol* 1998;19:728-37.

Sun Q, Loughran P, Shapiro R, Shrivastava IH, Antoine DJ, Li T, et al. Redox-dependent regulation of hepatocyte absent in melanoma 2 inflammasome activation in sterile liver injury in mice. *Hepatology* 2017; 65:253-68

Tacke F, Zimmermann HW. Macrophage heterogeneity in liver injury and fibrosis. *J Hepatol* 2014;60:1090-6.

Takahashi K, Naito M, Takeya M. Development and heterogeneity of macrophages and their related cells through their differentiation pathways. *Pathol Int* 1996;46:473-85.

Tomokiyo R, Jinnouchi K, Honda M, Wada Y, Hanada N, Hiraoka T, et al. Production, characterization, and interspecies reactivities of monoclonal antibodies against human class-A macrophage scavenger receptors. *Atherosclerosis* 2002;161:123-32.

Ueno T, Komatsu M. Autophagy in the liver: functions in health and disease. *Nat Rev Gastroenterol Hepatol* 2017;14:170-84.

Unuma K, Aki T, Matsuda S, Funakoshi S, Yoshida K, Uemura K. Inducer of heme oxygenase-1 cobalt protoporphyrin accelerates autophagy and suppresses oxidative damages during lipopolysaccharide treatment in rat liver. *Hepatol Res* 2013;43:9-6.

Van Rooijen N, Hendrikx E. Liposomes for specific depletion of macrophages from organs and tissues. *Methods Mol Biol* 2010;605:189-203.

Van Rooijen N, Kors N, Ende MVD, Dijkstra CD. Depletion and repopulation of macrophages in spleen and liver of rat after intravenous treatment with liposome-encapsulated dichloromethylene diphosphonate. *Cell Tissue Res* 1990;260:215-22.

Van Rooijen N, Sanders A, Van den Berg TK. Apoptosis of macrophages induced by liposome-mediated intracellular delivery of clodronate and propamidine. *J Immunol Methods* 1996;193:93-9.

Van Rooijen N, Sanders A. Liposome mediated depletion of macrophages: mechanism of action, preparation of liposomes and applications. *J Immunol Methods* 1994;174:83-93.

Vodovotz Y, Liu S, McCloskey C, Shapiro R, Green A, Billiar TR. The hepatocyte as a microbial product-responsive cell. *J Endotoxin Res* 2001;7:365-73.

Wijesundera KK, Izawa T, Tennakoon AH, Murakami H, Golbar HM, Katou-Ichikawa C, et al. M1 and M2 macrophage polarization in rat liver cirrhosis induced by thioacetamide (TAA), focusing on Iba-1 and galectin-3. *Exp Mol Pathol* 2014a;96:382-92.

Wijesundera KK, Izawa T, Murakami H, Tennakoon AH, Golbar HM, Kato-Ichikawa C, et al. M1 and M2 macrophage polarization in thioacetamide (TAA)-induced rat liver lesions; a possible analysis for hepatopathology. *Histol Histopathol* 2014b;29:497-511.

Williams JF. Carbon tetrachloride hepatotoxicity in endotoxin tolerant and polymyxin-treated rats. *Int J Immunopharmacol* 1988;10:975-80.

Wojcik M, Ramadori P, Blaschke M, Sultan S, Khan S, Malik IA, et al. Immunodetection of cyclooxygenase-2 (COX-2) is restricted to tissue macrophages in normal rat liver and to recruited mononuclear phagocytes in liver injury and cholangiocarcinoma. *Histochem Cell Biol* 2012;137:217-33.

Wu D, Wang X, Zhou R, Yang L, Cederbaum AI. Alcohol steatosis and cytotoxicity: the role of cytochrome P4502E1 and autophagy. *Free Radic Biol Med* 2012;53:1346-57.

Xu CS, Jiang Y, Zhang LX, Chang CF, Wang GP, Shi RJ, et al. The role of Kupffer cells in rat liver regeneration revealed by cell-specific microarray analysis. *J Cell Biochem* 2012;113:229-37.

Xu Y, Jagannath C, Liu XD, Sharafkhaneh A, Kolodziejska KE, Eissa NT. Toll-like receptor-4 is a sensor for autophagy associated with innate immunity. *Immunity* 2007;27:135-44.

Yamamoto T, Naito M, Moriyama H, Umezu H, Matsuo H, Kiwada H, et al. Repopulation of murine Kupffer cells after intravenous administration of liposome encapsulated dichloromethylene diphosphonate. *Am J Pathol* 1996;149:1271-86.

Yamashiro S, Takeya M, Nishi T, Kuratsu J, Yoshimura T, Ushio Y, Takahashi K. Tumor-derived monocyte chemoattractant protein-1 induces intratumoral infiltration of monocyte-derived macrophage subpopulation in transplanted rat tumors. *Am J Pathol* 1994;145:856-67.

Yamate J, Izawa T, Kuwamura M. Histopathological analysis of rat hepatotoxicity based on macrophage functions: in particular, an analysis for thioacetamide-induced hepatic lesions. *Food Safety* 2016;3:61-73.

Yamate J, Yoshida H, Tsukamoto Y, Ide M, Kuwamura M, Ohashi F, et al. Distribution of cells immunopositive for AM-3K, a novel monoclonal antibody recognizing human macrophages, in normal and diseased tissues of dogs, cats, horses, cattle, pigs, and rabbits. *Vet Pathol* 2000;37:168-76.

Yee SB, Kinser S, Hill DA, Barton CC, Hotchkiss JA, Harkema JR, et al. Synergistic hepatotoxicity from coexposure to bacterial endotoxin and the pyrrolizidine alkaloid monocrotaline. *Toxicol Appl Pharmacol* 2000;166:173-85.

Yovchev MI, Xue Y, Shafritz DA, Locker J, Oerte M. Repopulation of the fibrotic/cirrhotic rat liver by transplanted hepatic stem/progenitor cells and mature hepatocytes. *Hepatology* 2014;59:284-95.

Yoza B, LaRue K, McCall C. Molecular mechanisms responsible for endotoxin tolerance. *Prog Clin Biol Res* 1998; 397:209-15.

Yuan H, Perry CN, Huang C, Iwai-Kanai E, Carreira RS, Glembotski CC, et al. LPS-induced autophagy is mediated by oxidative signaling in cardiomyocytes and is associated with cytoprotection. *Am J Physiol Heart Circ Physiol* 2009;296:470-9.

Zamara E, Galastri S, Aleffi S, Petrai I, Aragno M, Mastrocola R, et al. Prevention of severe toxic liver injury and oxidative stress in MCP-1-deficient mice. *J Hepatol* 2007;46:230-8.

Zhang Y, Morgan MJ, Chen K, Choksi S, Liu ZG. Induction of autophagy is essential for monocyte-macrophage differentiation. *Blood* 2012;119:2895-905.

Zhao L, Kaneko T, Okiji T, Takagi M, Suda H. Immunoelectron microscopic analysis of CD11c-positive dendritic cells in the periapical region of the periodontal ligament of rat molars. *J Endod* 2006;32:1164-7.

Zheng J, Yu S, Jiang Z, Shi C, Li J, Du X, et al. Microarray comparison of the gene expression profiles in the adult vs. embryonic day 14 rat liver. *Biomed Rep* 2014;2:664-70.

Zhu L, Xiang P, Guo K, Wang A, Lu J, Tay SS et al. Microglia/monocytes with NG2 expression have no phagocytic function in the cortex after LPS focal injection into the rat brain. *Glia* 2012;60:1417-26.

Zizzo G, Hilliard BA, Monestier M, Cohen PL. Efficient clearance of early apoptotic cells by human macrophages requires M2c polarization and MerTK induction. *J Immunol* 2012;189:3508-20.

Acknowledgements

Firstly, the author likes to express deeply her indebtedness to her supervisor Dr. Jyoji Yamate, Professor, Laboratory of Veterinary Pathology, Osaka Prefecture University for his scholastic guidance, sympathetic encouragement, valuable advice, active co-operation and support throughout her study period.

The author expresses cordial respect and sincere thanks to Dr. Yoichi Nakamura, Professor, Laboratory of Integrative Physiology, and Dr. Kikuya Sugiura, Professor, Laboratory of Advanced Pathobiology, Osaka Prefecture University, for their critical and constructive review of this thesis.

The author is indebted and thankful and would like to express heartfelt gratitude and regards to Dr. Mitsuru Kuwamura, Associate Professor, and Dr. Takeshi Izawa, Associate Professor, Laboratory of Veterinary Pathology, Osaka Prefecture University, for their valuable suggestion and generous technical support.

The author feels much pleasure to convey her thanks to the entire members of Laboratory of Veterinary Pathology for assistance and kind co-operation during the tenure of the study and living in Osaka, Japan.

The author is ever indebted to her parents, brothers, sisters, and accompany of her husband (Mohammad Rabiul Karim) and son (Rafsan Karim Rayan) who provide her careless inspiration and never stop pray for her.

The author gratefully acknowledges the kind co-operation and support of the International Office and Rinku student support office, Osaka Prefecture University.

The author appreciates the sacrifice of the animals used in this study.

Grateful acknowledgement is made to Grant-in Aid for scientific research from the Ministry of Education, Culture, Sports, Science and Technology (MEXT; Monbukagakusho) Scholarship (No. 132300) of Japan for grant and Bangladesh Agricultural University, Bangladesh for allowing her the deputation during this study period in Japan.

Above all, the author is grateful to Almighty Allah enable her to complete the research work and the thesis for PhD degree.